Urease: New Methods for Sensing and Prevention of Urease-Associated Pathogenicity

Heylen, Rachel

Award date:
2023

Awarding institution:
University of Bath

Urease: New Methods for Sensing and Prevention of Urease-Associated Pathogenicity

submitted by

Rachel A. Heylen

for the degree of Doctor of Philosophy

of the

University of Bath

Department of Chemistry

May 2023

Abstract

Urease is an enzyme associated with plants, bacteria, and fungi. It metabolises urea into ammonia, therefore producing a nitrogen source for organisms and altering the pH of their environment. Bacterial infections caused by urease-positive microorganisms have associated urease pathogenicity, for example *Proteus mirabilis*.

The research presented here examines potential new methods for sensing and preventing urease-associated pathogenicity. In Chapter 3 and Chapter 4 a diagnostic sensor to detect impending urinary catheter blockage was optimised and clinically tested in a pilot clinical trial. The diagnostic sensor provides a colorimetric indication that the urinary catheter is more likely to block. The optimised sensor provides an almost 7 h warning prior to blockage, as demonstrated using an *in vitro* model of a catheterised tract. Furthermore, the sensor is stable in healthy human urine and can be sterilised using ethylene oxide. A small-scale pilot study tested the potential utility of the sensor in donated urine from long-term catheter users. The sensor correctly predicted the two blockage events and successfully correlated turn-on with the use of bladder maintenance solutions. The microbial composition of the urine donated by the participants was additionally investigated and there was polymicrobial diversity amongst users suffering catheter-associated urinary tract infections.

In Chapter 5, a rational drug discovery technique was employed to identify new urease inhibitors. A targeted approach was developed, whereby published literature was used to develop an *in silico* screen. Ligands were computationally docked on to the crystal structure of urease, the results were filtered and three compounds tested further in *in vitro* assays. This approach identified *N, N'*-Bis(3-pyridinylmethyl)thiourea as a potent inhibitor to urease and when tested successfully extended the lifetime of a catheter and outperformed the only clinically licensed urease inhibitor: acetohydroxamic acid, when tested *in vitro*. In Chapter 6, *Nasturium officinale* extract was examined for its therapeutic benefits against urease. *N. officinale* is a semi-aquatic plant which contains multiple compounds believed to have therapeutic properties. The extract demonstrated a dual mechanistic approach to reducing urease pathogenicity. The research presented in this thesis has investigated urease pathogenicity, tested a device to detect its action which could be used by long-term catheter users and investigated various compounds, including a newly identified urease inhibitor and natural products were explored as potential future therapeutics.

Acknowledgements

Firstly I wish to thank my fantastic supervisors Prof. Toby Jenkins and Dr. Maisem Laabei. Thank you for all your support throughout my PhD, I appreciate the freedom you gave me to follow my own journey and complete my experiments - even when they turned out to not work! Thank you for all the pints, allowing me to visit various conferences, and start up different collaborations.

Secondly, to the brilliant researchers who worked alongside me and supported me through the last few years. Dr. Thet Naing, Dr. Bethany Patenall, Dr. Lauren Gwynne, Dr. George Williams, Dr. Jordan Gardiner, Toska Wonfor, Emily Owen, Emelie Alsheim, and Natasha Harwood. To my lovely MChem students who gave me the opportunity to explore new avenues of my research and have all contributed to this thesis: Max Branson, Nicola Cusick, and Tom White. I couldn't have got through all the laboratory experiments without your support and motivation!

Thank you for my fantastic friends and family. Jacob - despite having no idea what I do each day, your continued support and belief in me has made this research possible. You and Riley have been excellent, especially during this gruelling writing experience. Thank you for the drinks, friendship, and love over the last 4 years. I was so lucky in Bath to meet excellent friends and flatmates: Jaidene, Beth, and Alicia. Jaidene, thank you for keeping me company during my final year, always supporting my office chats and rants, and being an all round fabulous friend. Beth, the support you gave me in the lab was invaluable. It was great to have someone so experienced who I called a friend, thank you for reading every word of my thesis - I can't thank you enough! Alicia, it was so amazing to meet you in Bath. Thank you for being my running partner, listening to my ridiculous theories, and always being there for lots of wine; I can't wait for you to be my bridesmaid this year. Dr Fiona Sargison, thank you for supporting me throughout my PhD, knowing you were going through a similar experience and could relate made loads of difference. Even though you were far away in Edinburgh it was always good to know you were there for me. To my parents, Mum and Dad, thank you for your support and care throughout the process. Thanks to Mum for telling every patient with a urinary catheter about me; hearing about the catheter users did spur me on!

Declarations

This thesis is the result of my own work. It includes work done in collaboration which is specifically indicated in the text and here.

Section 3.3.1.3: the lozenges were drum-coated by Nina Hauschildt from Evonik, Germany. She carried out the coating procedure using Eudragit S100 polymer and the following quantity of coating assessment.

Section 4.3.1: set up and design of the pilot clinical trial was conducted with the assistance of the Clinical Team: Dr. Edward Jefferies, and Mrs Annette Morton (Royal United Hospitial, Bath). Study design, registration of the trial, completion of the Integrated Research Application System (IRAS) form, and submission to Research Ethics Committee (REC) was completed by Dr June Mercer-Chalmers and Prof. A. Toby. A. Jenkins (University of Bath). The study was sponsored by the University of Bath.

Section 5.3.1 was designed by Nicola Cusick as part of her chemistry Masters research project, which was supervised by Rachel Heylen.

Section 6.2.0.1 was done in collaboration with Watercress Research Ltd. Unit 24, Exeter SkyPark, Exeter, EX5 2GE, UK. The founders of Watercress Research: Dr Kyle Stewart and Prof. Paul Winyard, assisted in the research carried out. A list of compounds believed to be present in *N. officinale* was provided for the docking experiments and based on previous literature (Appendix 6.1).

Dissemination of Research

- **Oral presenter**: International Continence Society Conference, Sept 2022, Vienna.
- **Poster presenter**: Doctoral Research event, University of Bath, June 2022 - Runner-up prize winner.
- **Oral presenter**: Bolland Symposium, University of Bath, June 2022.
- **Oral presenter**: European Congress of Clinical Microbiology and Infectious Diseases, April 2022.
- **Poster presenter**: Bolland Symposium, University of Bath, September 2021.

- **Oral presenter**: Incontinence the Engineering Challenge XIII hosted by Institute of Mechanical Engineering, November 2021 (remote).
- **Poster presenter**: Incontinence the Engineering Challenge XII hosted by Institute of Mechanical Engineering - sponsored attendance, November 2019.

Publications

- **Heylen, R. A.,** Owen, E., Stewart, K., Winyard, P., Caballero-Lima, D., Cwikla, B., Jenkins, A. T. A. '*Nasturtium officinale* extract: natural urease inhibitors to treat urease-positive infections. Under review at Heliyon.
- **Heylen, R. A.,** Cusick, N., White, T., Owen, E., Patenall, B. L., Alm, M., Thomsen, P., Laabei, M., Jenkins, A. T. A. 'Rational design of new urease inhibitors to treat long-term urinary catheter blockage'. Pending submission.
- **Heylen, R. A.,** Mercer-Chalmers, J., Moreton, A., Urie, J., Jefferies, Edward., Patenall, B. L., Laabei, M., Jenkins, A. T. A. 'Pilot Clinical Trial using Donated Urine from Long-term Catheterised Patients to test the function of a Diagnostic Sensor in predicting Impending Urinary Catheter Blockage.' Under review at Journal of Clinical Urology. Preprinted in medRxiv. https://doi.org/10.1101/2022.10.25.22281351
- Gaur, N., Patenall, B. L., Ghimire, B., Thet, N. T., Gardiner, J. E., Le Doare, K. E., Ramage, G., Short, B., **Heylen, R. A.,** Williams, C., Short, R. D., Jenkins, A. T. A. 'Cold Atmospheric Plasma-Activated Composite Hydrogel for an Enhanced and On-Demand Delivery of Antimicrobials.' 2023; 15 (16): 19989–19996. ACS Applied Materials & Interfaces. https://doi.org/10.1021/acsami.3c01208
- Tsikriteas, Z. M., **Heylen, R. A.,** Jindal, S., Mancuso, E., Li, Z., Khanbareh, H. 'Additively Manufactured Ferroelectric Particulate Composites for Antimicrobial Applications.' 2023; 8 (7): 2202127. Advanced Material Technologies. https://doi.org/10.1002/admt.202202127
- Yan, K-C., Patenall, B. L., Gardiner, J. E., **Heylen, R. A.,** Thet, N., He, X-P., Sedgewick, A. C., James, T. D., Jenkins, A. T. A. 'TCF-based fluorescent probe for monitoring superoxide anion produced in bacteria under chloramphenicol- and heat-induced stress.' 2022 (58) 13103-13106. Chemical Communications. https://doi.org/10.1039/D2CC04662H

- **Heylen, R. A.,** Branson, M., Gwynne, G., Patenall, B. L., Hauschildt, N., Urie, J., Mercer-Chalmers, J., Thet, N. T., Laabei, M., Jenkins, A. T. A. 'Optimisation of a lozenge-based sensor for detecting impending blockage of urinary catheters.' 2022 (197) 113775. Biosensors and Bioelectronics. https://doi.org/10.1016/j.bios.2021.113775

- Milo, S., **Heylen, R. A.,**‡ Glancy, J., Williams, G. T., Patenall, B. L., Hathaway, H.J., Thet, N. T., Allinson, S. L., Laabi, M., Jenkins, A. T. A. 'A small-molecular inhibitor against *Proteus mirabilis* urease to treat catheter-associated urinary tract infections.' 2021 (11) 3726. Scientific Reports. https://doi.org/10.1038/s41598-021-83257-2

Contents

Acronymns and Abbreviations

2-MA	2-mercaptoacetamide
ADMET	Absorption, Distribution, Metabolism, Excretion, and Toxicity
AHA	Acetohydroxamic Acid
AU	Artificial Urine
Bis-TU	*N,N'*-Bis(3-pyridinylmethyl)thiourea
bp	base pair
CADD	Computer aided drug design
CAUTI	Catheter-associated Urinary Tract Infections
CBA	Columbia Blood Agar
CF	5(6)carboxyfluroescein
CFU/mL	Colony Forming Units/mL
CLED	Cysteine-Lactose-Electrolyte-Deficient
CRF	Case Report Form
DDS	Drug Delivery System
DMEM	Dulbecco's Eagle Medium complete
DMSO	Dimethyl sulfoxide
eCRF	Electronic Case Report Form
EDTA	Ethylenediaminetetraacetic acid
EMA	European Medical Agency
FDA	US Food and Drug Administration
GMP	Good Manufacturing Practice
HBA	Hydrogen-Bond Acceptors
HBD	Hydrogen-Bond Donors

HRA	Health Research Authority
HTS	High Throughput Screen
IAD	Incontinence Associated Dermatitis
IC_{50}	Inhibitory Concentration 50
ICIQ	International Consultation on Incontinence Questionnaire
IRAS	Integrated Research Application System
ISRCTN	International Standard Registered Clinical/soCial sTudy Number
ITCs	Isothiocyanates
LF	Lead Finder
LB	Luria-Bertani
MC	MaConkey
MEM	Minimum Essential Media
MH	Müeller Hinton
MHRA	Medicines and Healthcare products Regulatory Agency
MIC	Minimum Inhibitory Concentration
MTT	Methyl Tetrazolium
NBPT	*N*-(n-butyl) thiophosphoric triamide
NMR	Nuclear Magnetic Resonance
NHS	National Health Service
NICE	National Institute for Health and Care Excellence
PDB	Protein Data Bank
PBS	Phosphate Buffer Saline
PCR	Polymerase Chain Reaction
PE-ITC	phenethyl isothiocyanate

poly(HEMA-co-PEGMEA)	poly(2-hydroxyethyl methacrylate-co-poly(ethylene glycol) methyl ether acrylate)
poly(vinyl-alcohol)	PVA
REACH	Research Ethics Approved Committee for Health
REC	Research Ethics Committee
RMSD	Root Mean Squared Deviation
RUH	Royal United Hospital
SAR	Structural-Activity Relationships
SF	Sodium Fluorescein
TSB	Tryptone Soya Broth
UoBath	University of Bath
UTI	Urinary Tract Infections

List of Figures

List of Tables

Chapter 1

Introduction

1.1 The Clinical Problem: Catheter-associated Urinary Tract Infections (CAUTI)

One of the most common bacterial infections are Urinary Tract Infections (UTIs), there are ≈150-250 million cases globally per year.[1] UTIs are defined as an infection of the lower urinary tract or a combination of lower and upper urinary tract. A positive urinary tract bacterial inoculum of $>10^5$ colony forming units/mL (CFU/mL) is used to diagnose bacteriuria (bacteria within the urine).[2] Approximately 50% of women will develop a UTI compared to only 5% of men.[3] Recurrent UTIs are defined as: two uncomplicated infections within 6-months or three infections in a year, the chance a patient develops a second UTI in 6 months is 25%, within 12 months it's 46%.[4,5] Owing to the high occurrence and high recurrence of UTI infectious, there is an associated high morbidity and economic cost; in the USA the cost of UTI treatment is $1.6-3.5 billion per year.[1] UTIs pose a significant risk to people who are elderly owing to changes in the immune function, additional co-morbidities, and longer stays in hospital; which increase exposure to nosocomial infections.[2]

UTIs can either be uncomplicated or complicated; uncomplicated UTIs can be treated with one dosage of antibiotics or no treatment; these infections occur in otherwise healthy females. Women are more likely to suffer from UTIs owing to their shorter ureter and therefore have higher predisposition to the occurrence of bacterial infection.[6] A complicated UTI is any other UTI: those occurring in males, pregnant women, with atypical bacteria present, immune-compromised patients, persistent UTIs, and patients with ureteric stents or Foley catheters (CAUTI).[6]

1.1.1 Urinary Catheters

Historically, drainage of the bladder using urinary catheters has been reported as early as 1500 BC; where reeds, straws or bronze tubes were used to treat urinary retention.[7,8] In 1929, Edgar Ballenger and Dr Frederick Foley designed the Foley catheter (Fig. 1-1).[9] Today, the design has barely changed.[10] Catheters are a Class 2 medical device under the US Food and Drug Administration (FDA) and European Medical Agency (EMA) regulations, these are devices which are invasive to the body.[11,12] Intermittent catheterisation is used to treat urinary retention; often observed in patients suffering from spinal cord injuries, which have resulted in a neurogenic bladder.[13] It is also used to treat incontinence, and in this case is an indwelling catheter.[14] Indwelling catheters can either be short-term: <30 days, or long-term >30 days and up to 3 months.[15] All patients undergoing surgery will be fitted with catheters, and many patients in critical

care.[15] This study focuses of the use of long-term urinary catheters.

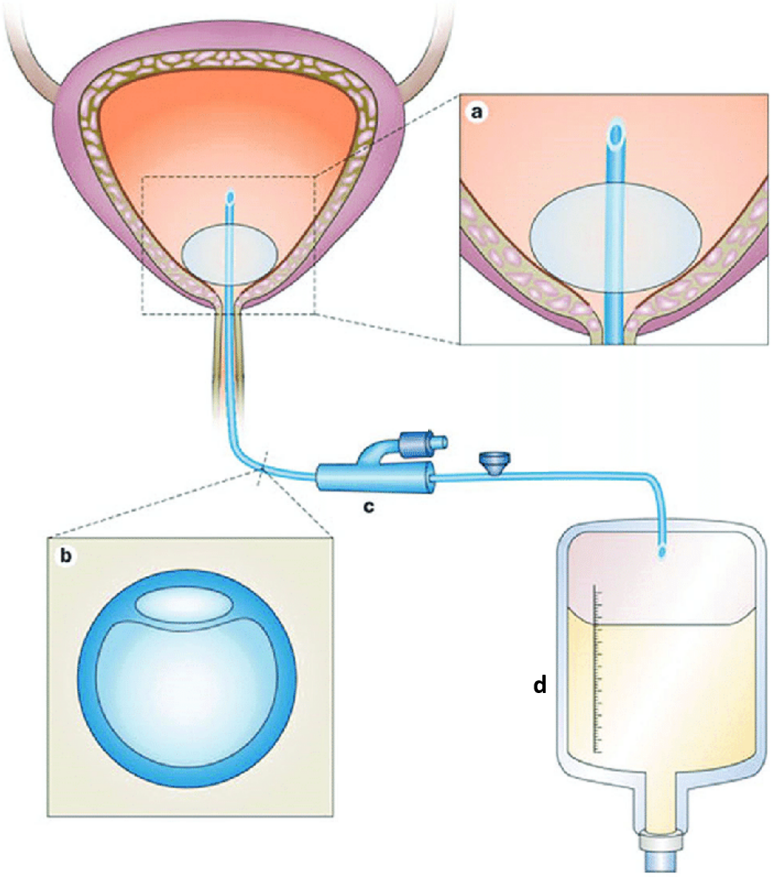

Figure 1-1: Diagram of the Foley catheter inserted into the bladder. (a) is the balloon of the catheter used to keep the catheter within the bladder and held tight against the base of the bladder to prevent leakage. (b) the lumen of the catheter, the wider lumen allows the urine to drain from the bladder to the drainage bag, the narrower lumen inflates the balloon of the catheter. (c) is the closed sterile system, where the catheter is connected to the drainage bag. (d) the drainage bag. Reprinted with permission from Journal of Materials Chemistry B, Royal Society of Chemistry.[16]

A survey of 66 European Hospitals found that 17.6% of in-patients had an indwelling catheter.[17] In the UK, 12.9% of patients in National Health Service (NHS) hospitals were catheterised.[18] Whilst in the UK Community, the prevalence of catheter use was 10.8% within the District Nurse caseloads, and in nursing homes 5% of residents have long-term indwelling catheters.[19,15] Each year ∼96 million catheters are sold worldwide.[20] Consequently, the urinary catheter is the most common prosthetic device.[21]

Catheters can be inserted by two methods: urethral insertion where the catheter goes up the urethra and into the bladder, or supra-pubic where the catheter is surgically inserted through the abdominal wall into the bladder.[8] In the UK, the majority of long-

term catheter users have a urethral insertion, 60% vs 40% however, amongst women supra-pubic insertion is more common.[22] To keep a catheter in place the balloon is inflated, normally with 10 mL of saline. The balloon is then pulled down to the base of the bladder and creates a seal to prevent incontinence (Fig. 1-1).[8] All long-term indwelling catheters are made from silicone or silicone-coated latex; there is variation in the size, type, and coatings on catheters and for long-term patients generally they will trial various manufacturers until they find a catheter that works well for them.[23]

1.1.2 Catheter-Associated Urinary Tract Infections (CAUTI)

CAUTI are UTIs specifically associated with the presence of a catheter. The presence of a catheter leads to an increase in bacteriuria.[24] The increase in bacteriuria occurs because the catheter prevents the natural filling and voiding of the bladder, this natural process is effective at emptying the bladder. When a catheter is fitted the bladder is constantly emptying, and around the balloon, below the lumen, a pool of residual urine remains (Fig. 1-1).[21] This pool provides a continuously refreshed nutrient source for bacteria.[21] CAUTI are the most common nosocomial infection.[1] CAUTIs accounted for for 47 717 excess bed days in NHS hospitals during 2016-2017 and cost the NHS between £1.5-2.25 billion per year to treat and manage.[25,8]

Contamination of the bladder often comes from the patient's microbiome, generally through faecal or skin contamination.[10] However, in hospital settings cross-contamination between hospital staff or asymptomatic patients can lead to outbreaks.[26] Once colonised the bacteria are difficult to treat; they demonstrate antimicrobial abilities and often form biofilms on the catheter surface or the wall of the bladder (Section 1.1.2.2).[27] Within hospitals the difficulty of treatment is heightened, owing to 60-80% of the patients already being treated with antimicrobial treatments (Section 1.5).[27] Contamination occurs because bacteria can migrate either along the extraluminal surface, ≈66%, or internally, ≈34% owing to disruption to the closed-loop sterile system.[28] CAUTI is time-dependent, catheters that are *in situ* for less than 3 days rarely cause bacteriuria whilst those in place for more than 28 are universally likely to have bacteriuria.[28] Chronic catheter users will always have bacteria within their urine.[24] Many of these long-term users might not have a symptomatic infection. An asymptomatic infection is defined as $\geq 10^5$ CFU/mL of ≥ 1 bacterial species with no UTI symptoms, however this is rarely tested for in the clinic. Symptomatic CAUTI is $\geq 10^3$ CFU/mL of ≥ 1 bacterial species with UTI symptoms.[29]

1.1.2.1 Bacteria causing CAUTI

Bacteria are defined into two separate groups: Gram-positive and Gram-negative, due to their different abilities to absorb crystal violet stain during Gram straining. Gram-positive bacteria have a thick outer cell wall, peptidoglycan layer and absorb Gram stain, whilst Gram-negative have a outer membrane and thinner petidoglycan layer (under the cell membrane).[30] Gram negative bacteria generally demonstrate a higher level of resistance to antibiotics because their outer membrane prevents antibiotic permeability. *Escherichia coli* (*E. coli*) is the most common microbe isolated from UTIs.[3] In CAUTI patients, the bacteria causing infection often varies. Patients with short-term catheterisation are likely to be infected with: *E. coli*, *Staphylococcus aureus* (*S. aureus*), *Enterococcus faecalis* (*E. faecalis*), and *Staphylococcus epidermis* (*S. epidermis*).[28,31] Whilst in long-term users species such as: *E. coli*, *Klebisella pneumoniae* (*K. pneumoniae*), *Pseudomonas aeruginosa* (*P. aeruginosa*), and *Proteus mirabilis* (*P. mirabilis*), are likely to be isolated.[32,33,34] Long-term catheter users are more likely to have polymicrobial infections compared to short-term users.[23]

1.1.2.2 Biofilms

A biofilm is defined as a community of bacterial cells which have attached to a surface, the cells are enclosed within a matrix which is made from extracellular polymeric substances (EPS)[35]. Planktonic (free-living) bacteria adhere to a surface, for example: urinary catheters and bladder walls; a microcolony of bacteria cells forms and the colony begins to produce EPS (Fig. 1-2).[36] EPS protects the bacteria against the host-immune system and also enables tolerance against antimicrobial agents.[37] Tolerance to antibiotics can occur via these three main mechanisms: (1) the inability of antimicrobial agents to penetrate the biofilm because of the EPS, if the majority of the biofilm has been removed persister cells can regenerate the biofilm. (2) Persister cells are metabolically dormant bacteria which are produced in a biofilm community, they are resistant to multiple drugs and are the cause of many re-infections post-antibiotic treatment.[38] (3) Concentration gradients of the antibiotics occur as they diffuse through the EPS, therefore the bacteria received the antibiotic at less than the minimum inhibition concentration (MIC)(the minimum concentration of antibiotic required to kill bacteria), they are not killed and can develop resistance characteristics.[39] CAUTI is difficult to treat owing to the formation of biofilms and as many long-term catheter users have polymicrobial infections, they also have polymicrobial biofilms.[23] It has been shown that common bacteria causing CAUTI: *E. faecalis* and *P. mirabilis* demonstrate polymeric interactions which promote the formation of both biofilms and enable enhanced

resistance to antimicrobials.[40] Additionally, a co-infection of *P. mirabilis* and *Providencia stuartii* has been shown to increase urease activity and therefore, cause greater pathogenesis.[41]

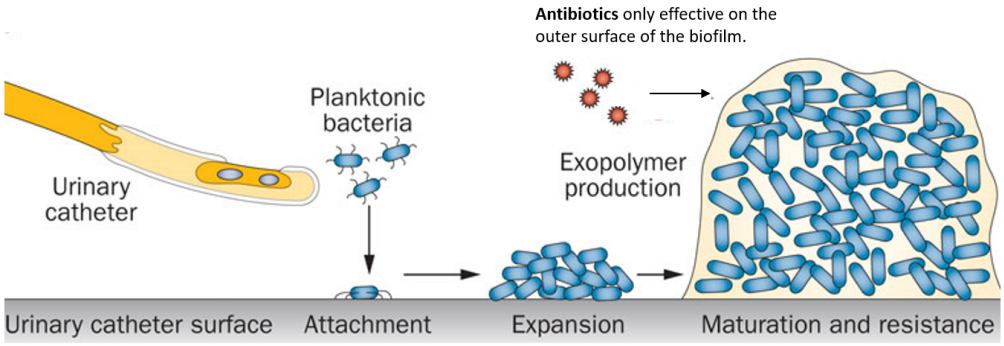

Figure 1-2: Formation of a biofilm created by uropathogenic bacteria on the surface of a urinary catheter. Initially, plantonic bacteria adhere to the surface of the catheter, the bacteria expand, and mature into a biofilm. Reprinted with permission from Nature Review Urology, Springer Nature.[1]

1.2 *Proteus mirabilis*

P. mirabilis is a Gram-negative, rod-shaped, urease-positive bacteria; named after the Greek God *Proteus*, a shape-shifting God.[42] This is because *Proteus spp.* are able to morphologically change shape from swimmer cells to swarming cells when placed on a solid surface (Section 1.2.3).[43] *P. mirabilis* is commonly associated with long-term catheter users, it is found in 40% of urine samples taken from long-term users.[24] *Proteus* is effective at forming biofilms (Section 1.1.2.2), studies had shown that *P. mirabilis* can produce extensive biofilms and can persist within the bladder for longer periods of time.[24,44] *P. mirabilis* is also the most common microbe isolated from bacteremia (bacteria found within the bloodstream) within nursing homes, and consequently it possess a significant mortality risk owing to the likelihood of developing septicaemia.[29,45]

1.2.1 Virulence Factor: Urease

Urease is found within *P. mirabilis*.[46] It is an metalloenzyme (EC 3.5.1.5) with a dinuclear nickel ion centre that metabolises urea to carbamic acid and molecule of ammonia which is then hydrolysed to carbon dioxide and another molecule of ammonia. (Fig. 1-3).[47,43] The hydrolysis of urea (not catalysed) has a half-life of approximately 3.6 years, the activity of urease increases the rate of reaction by 10^{14} times compared to the non-catalysed.[48] Multiple bacterial species, as well as some fungi and plants produce urease, mainly to provide a nitrogen source for growth and survival.[43,45] Urease

is found in bacteria isolated from CAUTI, for example: *S. aureus*, *P. mirabilis*, and *P. aeruginosa*.[49,50,51] However, other bacteria associated with CAUTI do not produce urease, for example: *E. coli* and *E. faecalis*.[49,52] For more information on structure of the urease enzyme see Section 1.7.

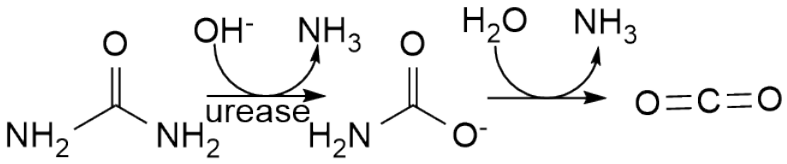

Figure 1-3: Urease catalyses urea to two molecules of ammonia. Scheme drawn using ChemDraw (PerkinElmer Informatics Inc, v. 19.0.1.28).

1.2.2 Crystalline Biofilms and Catheter Blockage

Urease activity produces ammonia which increases the pH within the bladder, this causes the precipitation of struvite ($MgNH_4PO_4 \cdot 6H_2O$) and apatite ($Ca_{10}(PO_4)_6(OH)_2$) salts.[50] Struvite and apatite are soluble salts from urine, at high pH they form crystal deposits on the catheter and within the bladder.[53] Biofilms form on the crystals and crystals from within biofilms from bacteria which have infected the bladder; this leads to extensive crystalline biofilm formation causing catheter blockage and the formation of bladder stones (Fig. 1-4).[50,54] Catheter blockage is dangerous for the patient; it causes a painful distention of the bladder leading to incontinence - leakage of urine from around the catheter.[55] Blockage causes the infected urine to travel up the ureter, or mobile bacteria can travel up the ureter, causing pyelonephritis and kidney stones.[45] Struvite kidney stones are hard to treat, if the stones are removed there is still a 40% chance patients will suffer recurrent stone formation, owing to fragments remaining after the operation.[56] Kidney and bladder stone formation enables the infection to remain within the bladder between catheter changes.[54,57] In a worst case scenario, catheter blockage causes urosepsis and thus leads to possible fatalities.[45] In conclusion, urease is a key virulence factor in catheter blockage and the resulting clinical consequences.[46,49]

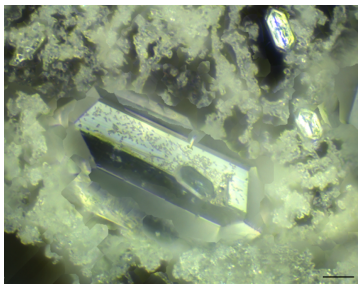

Figure 1-4: Large struvite crystal formed after 20 days on a silicone catheter surface, the catheter was exposed to *Proteus mirabilis*. The crystal is embedded in a diffuse crystalline material which is likely to be apatite. Magnification at x500, scale bar represents 20 μm. Image reprinted under the Creative Commons Attribution License.[58]

1.2.3 Virulence Factor: Motility

A unique feature of *Proteus spp.* bacteria is their ability to change their morphology and swarm, this is where they form a polyploid cell and travel as a unit over a solid surface (Fig. 1-5a).[59] After some time, the cells revert back to swimmer form, this creates the characteristic bulls-eye pattern observed on agar plates (Fig. 1-5b).[42] The swimmer cells have peritrichous flagella (flagella all over the surface) whilst the swarming cells have bundles of flagella (Fig. 1-5a).[43] Flagella are essential in swarming, there is an up-regulation in flagella genes prior to swarming.[60] However, the role of flagella in UTIs is contested; a double mutant study which knocked out the virulence factors: $\triangle$*hpmA* (haemolysin) and $\triangle$*flaA*(involved in the assembly of flagella); found that the double mutant was 100-fold lower in the urinary tract compared to wild-type and $\triangle$*hpmA* alone.[61] Conversely, a different study demonstrated that knock out of FlaA and FlaB (structural proteins in flagella) did not change the ability to cause an ascending UTI.[62] Generally, it is believed that flagella do have a role in establishing a UTI, none of these studies were conducted on a catheterised model; therefore, it is difficult to conclude on the function of flagella in CAUTI in *in vivo* models. Armbruster *et al.,* carried out transposon mutagenesis and identified flagella components: *fliF, fliI* and *flgC*, these components of the flagella are fitness factors in during CAUTI, establishment and infection.[63] Additionally, components of the virulence factor, urease, were also identified as fitness factors for causing CAUTI (*ureG* (single-species infection) and *ureRDCF* (polymicrobial infection)).

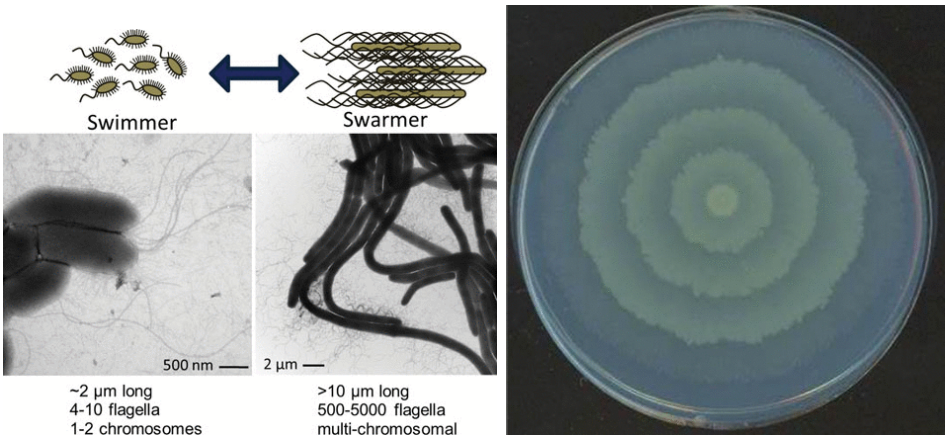

(a) Morphological switch from swimmer cells to swarming cells. Transmission electron micrograph showing the differences between swimmer and swarming states.

(b) Swarming characteristic bulls-eye pattern of *Proteus mirabilis*.

Figure 1-5: Physiological swarming of *Proteus spp.* Images reproduced with permission of Microbiology Spectrum.[43]

1.3 Diagnostics of CAUTI - Traditional Methods

Traditionally, UTIs are diagnosed using a urine dipstick and microbiological examination of a urine specimen. A urine dipstick tests for the presence of nitrites (associated with bacteria) and leukocytes (white blood cells).[64] A urine dipstick is not used for patients older than 65 years, as the presence of asymptomatic bacteriuria is common and antibiotic treatment, in these cases, is unlikely to be effective.[65] In a urine sample, a culture of bacteria $>10^3$-10^5 CFU/mL indicates positive infection, however this varies due to age and sex.[65] Additional symptoms include: dysuria (pain during urination), increased frequency and urgency to urinate, new/worsening delirium, fever, incontinence, suprapubic pain, and visible haematuria (blood in urine).[65]

The presence of asymptomatic CAUTI is common in long-term catheterised patients.[24] CAUTI is harder to diagnose because patients do not have dysuria or increased frequency owing to the presence of the catheter. In the UK, National Institute for Health and Care Excellence (NICE) have specific guidelines for antibiotic treatment and recommend catheter removal, and urine specimen culture (Table 1.3).[66] However, microbiological testing is rarely carried out on catheterised patients, owing to the high likelihood bacteria are present (communication from Dr Edward Jefferies, Urology Department, Royal United Hospital (RUH) Bath).

1.3.1 Lozenge Technology

The lozenge concept was invented and developed by Milo *et al.*[67] The lozenge is a hydrogel containing carboxyfluorescein (CF) which has been coated in a pH-sensitive polymer.[67] It is designed to detect impending catheter blockage, by responding to the pH increase within the drainage bag of the patient (Fig. 1-6). The pH sensitive polymer, Eudragit S100, was developed to breakdown at pH >7, it is used to coat tablets which require release of the drug within the colon.[68] Initially, Milo *et al.,* coated the catheter tip in the pH sensitive polymer and dye, thus allowing dye release into the bladder. This was re-engineered into a lozenge which sits within the drainage bag.[69] Visually patients can observe the colour change produced by the lozenge, when their urine increases thus indicating that their catheter could block and allowing clinical invention prior to the catheter blockage event.[67]

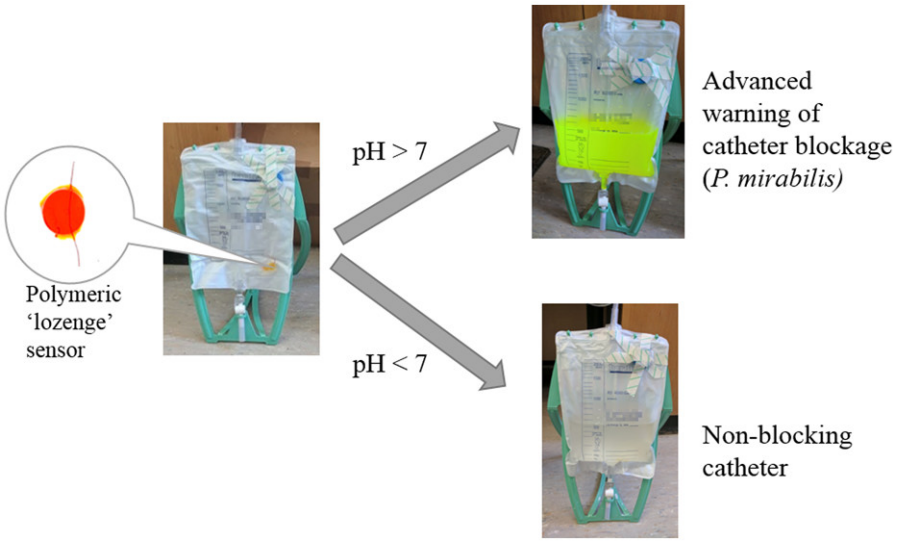

Figure 1-6: Schematic of the lozenge showing its fluorescence release in response to pH change. Reprinted with permission from Milo *et al.*[67] Copyright 2018 American Chemical Society.

1.3.2 Bromothymol Blue Diagnostic Sensor

Currently, there is no catheter blockage sensor in clinical use. However, previous research has been completed in this field. Stickler *et al.,* and Malic *et al.,* developed a bromothymol blue pH sensor, the first prototype was placed in the drainage bag and the second in the tubing between the catheter and the drainage bag, this gave an *in vitro* warning of 17-24 h before blockage (Fig. 1-7).[70,71] A clinical trial testing the sensor, demonstrated that it was successful at detecting urease-positive infection and catheter blockage.[72] However, the sensor gave a warning time of ≥18 days prior to

blockage, this was too much of an early warning and made it difficult for clinicians to decide whether to change the catheter or not. Additionally, there was a concern that urine could leak between the junctions and this would break the sterile closed-loop system potentially causing infection to occur.[72] Since the clinical trial was conducted on the bromothymol sensor in 2013, there have been no additional reports on the use of the sensor in the clinic.

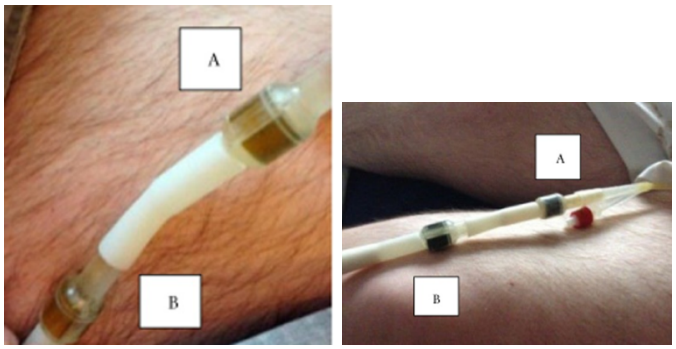

(a) Sensors upon insertion.

(b) Sensors with positive, turn-on, changed to blue-black.

Figure 1-7: Sensors for catheter blockage developed by Stickler *et al.*, and Malic *et al.* Reprinted with permission from John Wiley and Sons.[72]

1.4 Prevention of CAUTI

The best way to prevent CAUTI is not to prescribe an indwelling catheter.[24] Owing to the high likelihood that CAUTI will occur in long-term catheterised patients, avoidance of an indwelling catheter is the best policy.[28] However, intermittent catheterisation or incontinence treatments are not always viable alternatives; especially for patients suffering from urinary retention, post-operative urologic surgery, require hourly urine monitoring, or to aid the healing of pressure sores/incontinence-associated dermatitis (IAD).[15] For patients requiring catheterisation, aseptic insertion and maintenance of the closed-sterile loop system is essential.[24] The use of daily periurethral cleansing (in addition to routine cleaning) with saline, soap, or antiseptic does not show any benefit.[73]

1.4.1 Bladder Maintenance

Bladder maintenance can be carried out using either bladder irrigation, bladder washouts, or bladder installations. Table 1.1 describes the differences between each technique, generally the techniques are very similar and the correct terminology is not consistently used in the literature.[74] Bladder maintenance solutions often use just saline, however

there are other chemical based solutions available (Table 1.2). Citric based solutions are designed to buffer the high pH of the bladder, caused by urease activity and therefore, prevent catheter blockage and clear catheter encrustations.[75] A recent Cochrane review, examined the efficacy of bladder washout solutions and compared clinical trails testing different washout solutions; they concluded that there was no evidence that bladder washout solutions were able to reduce the rate of symptomatic CAUTI or affect the length of time the catheter was *in situ*.[76] Additionally, there were reports in some of the clinical trials of harmful effects from the washout solutions such as: blood in washout solution, changes in bladder spasms, and changes in blood pressure.[76]

Table 1.1: Terminology for Bladder Maintenance Therapies.

Therapy	Definition	Reference
Bladder irrigation	Irrigation of the bladder continuously using saline, using a three-way catheter.	77
Bladder washouts or catheter maintenance solutions	Flush the bladder to remove debris, carried out using a 60 mL syringe with saline and flushing the catheter and bladder until the debris are removed.	75
Bladder installations	A pre-packed reagent, 100 mL, is allowed to flow into the bladder under gravity, it is retained within the bladder for approximately 15 min then allowed to drain.	78

Table 1.2: Different maintenance solutions available to long-term catheterised patients, reproduced by permission from Wolters Kluwer Health, Inc., adapted by author.[75]

Solution	Description
Suby G	3.23% citric acid solution, pH 4.
Suby R	6% citric acid solution, pH 2.
Renacidin	Citric acid solution, pH 3.5-4.2.
Mandelic acid 1%	Acidic solution, pH 2.
Saline	Neutral solution.
Chlorhexidine 0.02%[1]	Antiseptic solution to reduce the growth of *E. coli* and *Klebsiella spp.*
Polyhexanide 0.02%	Antiseptic solution to reduce bacterial colonisation and biofilm growth.

[1] No longer in clinical use.

Bladder washout, 0.02% chlorohexidine, is a broad spectrum antiseptic, its use is has been discontinued in the clinic owing to reports it irritated the mucosal lining of the bladder.[79] Additional concerns about its use were reported by Dance *et al.,* where an outbreak of chlorhexidine and antibiotic-resistant *P. mirabilis* was detected and the only solution was to discontinue the use of chlorhexidine.[80,21] Recently, a new urotrainer (bladder maintenance solution) containing 0.02% polyhexanide (a second generation of chlorhexidine) was developed by Braun Medical Ltd. and was trialled in 2018, the trial demonstrated that no adverse events occurred when the urotrainer was used.[81] *In vitro* studies showed 0.02% polyhexanide was able to reduce bacterial counts when compared to saline washout solution.[82] It is too early to state whether 0.02% polyhexanide urotrainer is effective in the clinic, and whether it increases the likelihood of antibiotic resistance.

1.4.2 Catheter Engineering

Another common therapy for preventing CAUTI is the use of antimicrobial catheters, these are catheters which have been coated or impregnated with antimicrobials. Silver is commonly used as an antimicrobial material, Bard Pharmaceuticals Ltd. market a silver coated catheter which releases silver ions over time. Initial studies showed significant decrease in bacteriuria and reported a 45% reduction in CAUTI.[21,83] However, a larger study found no difference between a standard silicone catheter and a silver-coated catheter.[84] Various antimicrobials and antibiotics have been coated onto catheter surfaces including: nitrofurazone, minocycline, and rifampicin.[21,85] A 2004 Cochrane Review determined that for short-term catheterisation silver-coated catheters prevent UTIs, however, the clinical trials which were completed were of poor quality.[86] Studies have shown that silver coated catheters are ineffective against crystalline biofilms, produced by urease-positive bacteria such as *P. mirabilis* (Section 1.2.2).[87,88] Many of the studies into catheter coatings are conducted on patients with short-term catheterisation, few examine the effect on long-term users, or are just not effective in long-term use.[21]

Zhu *et al.,* has reviewed other coatings currently at the *in vitro* or initial clinical trail stage, these include: bactericidal enzymes, bacteriophage, antimicrobial peptides, carbon nanotubes and graphene oxide, polyethylene glycol, hydrogels, and polyzwitterions.[39] Challenges associated with developing catheter coatings include: preventing antibiotic resistance, maintaining patient safety, and ensuring efficacy in preventing CAUTI for long-term catheter users. Almost all long-term users use a silicone based catheter, whether they are coated in a hydrogel, or contain silver appears to be a

personal decision decided by trial and error.[8]

1.4.3 Alternative Methods to Prevent CAUTI

Various alternative methods have been suggested to prevent catheter blockage, two such methods involve increased fluid intake and the ingestion of citrate drinks. Encrustations and crystals form when the pH of the urine surpasses the nucleation pH (pH_n), this is when struvite and apatite crystals begin to form.[89] Patients who regularly experience catheter blockage are termed 'blockers'.[75] The difference between pH_n and voided pH (pH_v) indicates whether a patient is a blocker or non-blocker; blockers have a smaller difference between the pH_n-pH_v (closer to 0) whilst non-blockers have a difference greater than 1.[89,90] An *in vitro* experiment comparing the effect of concentrated and dilute urine (increasing fluid input) showed that for the concentrated urine blockage time occurred between 19-31 h, whilst with diluted urine blockage was 110-137 h; diluting the urine increased the pH_n and prevented the blockage event occurring.[91] The addition of 1.5 mg/mL of citrate to the *in vitro* model, increased the pH_n to above 8.3 and the models ran without blockage for 7 days.[91] A clinical trial comparing the effect of drinking lemon juice, potassium citrate, and increasing fluid intake showed that drinking lemon juice increased the difference between the pH_n-pH_v.[92] Although a small study with only 24 participants; the results presented a cheap, and safe alternative treatment to prevent catheter blockage.

The drinking of cranberry juice has often been associated as a treatment for UTIs, proanthocyanidins from cranberrys, prevent bacteria adhering to the inside of the bladder lining.[93] A large randomized, double-blind clinical trial (373 participants) tested the effect of cranberry supplementation on preventing reoccurring UTIs in women and found the total number of UTI events significantly reduced in the cranberry group.[94] The control compared cranberry juice vs a placebo that smelled and looked like cranberry juice but did not contain the active cranberry juice, therefore the researchers were able to control as much as possible for fluid intake. Cranberry supplementation appears to be a good preventative measure for uncomplicated UTIs, however it requires good compliance in drinking 240 mL of cranberry juice each day, and the results demonstrate a reduction in UTI events only for the group and not necessarily on an individual basis.[94] Testing of cranberry supplementation to prevent CAUTI or catheter blockage has only been conducted on a small 22 participant study; it demonstrated that cranberry supplementation prevented symptomatic CAUTI events and reduced the colony counts, although this study did not have a control group to allow direct comparisons.[95] In conclusion, increasing fluid intake and the consumption of cranberry and citrate drinks

could offer a safe preventative treatment to CAUTI and catheter blockage.

1.5 CAUTI Treatment

1.5.1 Antibiotic Treatment

When a catheter blocks it needs to be removed quickly to prevent the damaging clinical consequences (Section 1.2.2). Removal of an encrusted catheter is painful, can cause damage to the urethra, and is uncomfortable for the patients.[29] Guidelines can vary between country, but generally antibiotics are administered post blockage, an outline of antibiotics to treat CAUTI is shown in Table 1.3. Antibiotic resistance is a current and future challenge in the clinic, bacteria establish resistant mechanisms against antibiotics, which can be shared via horizontal gene transfer to other bacterial cells and different species.[96,97] UTIs are the top 4th infectious disease with associated deaths owing to resistance, ≈250 000 global deaths in 2019.[96] Healthcare providers are attempting to reduce resistance by generating guidelines and restrictions on antibiotics, especially broad-spectrum (Table 1.3). Antibiotics are heavily relied upon in the clinic to treat UTIs, therefore they are major contributors to the global use and resistance, and the current emergence of multi-drug resistant bacteria which pose a significant risk to patients.[27]

Historically, various antibiotics such as norfloxacin and trimethoprim-sulfamethaxazole have been used as prophylaxis for patients with long-term catheters. A Cochrane review examined various clinical trials testing the efficacy of using antibiotic prophylaxis vs antibiotic by microbiological indication, there was no significant benefit of using prophylaxis antibiotics to reduce symptomatic CAUTI.[98] In one of the studies using norfloxacin, a significant decrease in CAUTI was observed especially for Gram-negative bacteria, however, the authors observed an increase in resistant Gram-positive bacteria.[99] Authorities do not recommend the use of prophylaxis antibiotics to treat or prevent CAUTI.[29]

Table 1.3: NICE guidelines on antibiotic treatment for CAUTI, if the patient is over 16 years old and non-pregnant. Table is adapted from [66].

Antibiotic	**Dosage and course length**	**Antibiotic mechanism**	**Reference**
First choice oral antibiotics if no upper UTI symptoms			
Nitrofurantoin	100 mg modified-release twice a day for 7 days	Nitrofurantoin is rapidly absorbed and released into the urine, thus acting at site within the bladder. Bacteria metabolise nitrofurantoin into its active electrophilic intermediates, using nitroreductase enzymes, which interfere with ribosomal activity reducing protein synthesis. Although formation of resistant strains have been reported, these are much less prevalent compared to other antibiotics.	100,101
Trimethoprim - if low risk of resistance	200 mg twice a day for 7 days	Trimethoprim is a structural analogue of the pteridine portion of dihydrofolic acid which binds to dihydrofolate reductase. Therefore, trimethoprim is a competitive inhibitor. Resistance rates have been increasing against trimethoprim.	102,103
Amoxicillin - only if culture results available and susceptible	500 mg three times a day for 7 days	Amoxicillin is a beta-lactam antibiotic, which interrupts the crosslinks in the bacteria cell wall. Bacteria containing beta-lactamases confer resistance to beta-lactam antibiotics. *E. coli*, the most common pathogen causing UTI, often is resistant to amoxicillin.	104,105

Second choice oral antibiotics if no upper UTI symptoms			
Pivmecillinam (a penicillin)	400 mg initial dose then 200 mg three times a day for 7 days	Pivmecillinam is used to treat uncomplicated UTIs has been increasing owing to in resistant strains for other treatments. Pivmecillinam works well against Gram-negative bacteria, it is metabolised in the patient to it's active form: mecillinam. The exact mechanism is unknown, however it binds to the penicillin-binding protein 2 resulting in disruption to the bacterial cell wall.	106
First choice oral antibiotics if upper UTI symptoms			
Cefalexin	500 mg twice or three times a day (up to 1 to 1.5 g three or four times a day for severe infections) for 7 to 10 days	Cefalexin is also a beta lactam which interrupts the bacterial cell wall. It is particularly effective at disrupting the crosslinks between peptidoglycan. Cefalexin is more effective against Gram-positive bacteria compared to Gram-negative. Resistance has been reported against cefalexin, resistance is predominantely seen in Gram-negative strains of bacteria.	107,108
Co-amoxiclav - only if culture results available and susceptible	500/125 mg twice a day for 14 days	Co-amoxiclav is a combination therapy using amoxicillin and clavulanic acid antibiotics together. Amoxicillin is a beta-lactam antibiotic and clavulanic acid inhibits beta-lactamases. Use of co-amoxiclav can increase likelihood of being infected with co-amoxiclav resistant *E. coli*. Hence, guidelines suggest that culture results and susceptibility has been assessed.	104,109,110

Trimethoprim - only if culture results available.	200 mg twice a day for 14 days	See above	
Ciprofloxacin - consider safety issues	500 mg twice a day for 7 days	Ciprofloxacin is a fluoroquinolone, it inhibits the DNA gyrase. It appears more effective against Gram-negative bacteria compared to other fluoroquinolones. Analysis of resistance showed increased resistance over time, it is believed that some fluoroquinolones have been overused.	111,110
First choice intravenous antibiotics (if vomiting, unable to take oral antibiotics or severely unwell). Antibiotics may be combined if susceptibility or sepsis is a concern			
Co-amoxiclav - only in combination or if culture results available.	1.2 g three times a day	See above	
Cefuroxime	750 mg to 1.5 g three or four times a day	Cefuroxime is a cephalosporin, it inhibits transpeptidases and carboxypeptidases which are involved in cell wall synthesis. Cefuroxime is a broad spectrum antibiotic, effective against Gram-positive and Gram-negative bacteria, including those in the presence of beta-lactamases. Resistance has occurred especially in micro-organisms containing beta-lactamases, however it is still effective in higher concentrations.	112,113.

Ceftriaxone	1 to 2 g once a day	Ceftriaxone is also a cephalosporin antibiotic, effective against Gram-negative bacteria more so than other cephalosporins. The stability of ceftriaxone to beta-lactamase is similar to that of cefotaxime and cefuroxime.	114
Ciprofloxacin - consider safety issues	400 mg twice or three times a day	See above	
Gentamicin	Initially 5 to 7 mg/kg once a day, subsequent doses adjusted according to serum-gentamicin concentration	Gentamicin is an aminoglycosides antibiotic, it is a broad spectrum which is specifically effective against Gram-negative bacteria. Gentamicin has enhanced activity through application with other antibiotics, often beta-lactams. Aminoglycosides work by inhibiting protein synthesis by binding to the 16S ribosomal RNA.	115
Amikacin	Initially 15 mg/kg once a day, subsequent doses adjusted according to serum-amikacin concentration	Amikacin is also an aminoglycoside, it performs similarly to gentamicin and by the same mechanism.	115
Second choice intravenous antibiotics - consult local microbiologist			

1.5.2 Alternative Treatments

1.5.2.1 Acetohydroxamic acid (AHA)

Urease inhibitors can be used to treat CAUTI, the only licensed urease inhibitor is AHA (Fig. 1-8). AHA is prescribed to patients with a urease-positive infection, it is licensed in America under the name Lithostat, and in Kuwait and Spain as Uronefrex.[116,117,118] AHA is a competitive inhibitor which binds to the active site of urease.[119] Patients identified as catheter 'blockers' can be prescribed it, as well as patients suffering *Helicobacter pylori* (*H. pylori*, urease-positive) infection; *H. pylori* infects the stomach where it can cause stomach cancer and cirrhosis owing to high levels of ammonia.[117,120,121] However, AHA is currently rarely prescribed due to its high toxicity; it causes teratogenesis and hemolytic anemia.[116,122,123]

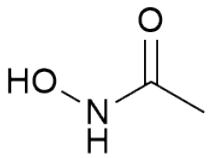

Figure 1-8: Acetohydroxamic acid, licensed urease inhibitor. Image drawn by ChemDraw (PerkinElmer Informatics Inc, v. 19.0.1.28).

1.5.2.2 Phage Therapy and Phage Enzymes

Bacteriophage, viruses that infect bacteria, offer an alternative to antibiotics to treat infectious diseases.[124] The benefit of phage therapy is that they are specific to the target bacteria, are difficult to develop resistance against and do not affect mammalian cells.[124] In the clinic they have only been used as last-resort therapies or in small clinical trials.[125] Phage can offer an alternative treatment as whole viruses or virulent components from the phage can be isolated as treatments. Rice *et al.,* identified a phage-derived depolymerase which is able to disrupt *P. mirabilis* biofilms.[126] The researchers identified a *Proteus* phage and characterised the genome to identify the enzyme depolymerase, which has efficacy against *Proteus* biofilms. Alternative treatments, involving phage could be a future medicine for CAUTI.

1.5.2.3 Anti-virulence Therapies

Anti-virulence therapies target a virulence factor from the bacteria. For example: mannosides are analogues of FimH receptors, FimH is an adhesin found on a type 1 pili in *E. coli*, it allows *E. coli* to invade host cells.[127] The type 1 pili are essential for *E. coli's* invasion and persistent infection in UTIs, as demonstrated in a mouse blad-

der model.[128] Orally delivered mannosides have been shown in *in vivo* mouse models to be effective against UTIs.[129,130] Anti-virulent therapies do not necessarily kill the bacteria, though this is an effective way of removing an infection, instead they disarm their virulence mechanisms which can reduce the pathogenicity of the infection.[131] In comparison to antibiotics, these therapies protect the gut commensal bacteria and do not confer the same resistant pressures associated with antibiotics.[129]

1.6 Drug Discovery

Drug discovery can start from two positions and take two different routes: (1) identification of a compound which has a desirable physiological effect, then understand the mechanism of action and the molecular target; (2) identification of a molecular target, identification of compounds which bind to the molecular target, and then understand the physiological effect.[132] Both routes have successfully yielded effective clinical drugs, in this project route 2 is used because there is already an understanding of the molecular target, urease (Section 1.7). An overview of the drug discovery process is shown in Figure 1-9. During the early drug discovery stage the following experiments take place: target validation, compound screening, secondary assays, *in vivo* analysis and the identification of a lead candidate.[133] Target validation involves an understanding of the disease, or the virulence factor associated with the subsequent pathology; in this case the target is the urease enzyme from urease-positive uropathogenic bacteria which cause CAUTI, lead to catheter blockage, and the subsequent serious clinical consequences such as: pyelonephritis and urosepsis (Section 1.2.2). Compounds screening traditionally involves large libraries of compounds tested against the target, often in the form of a high-throughput screen (HTS), this is an iterative process and classes of compounds are often re-synthesised with similar analogues to identify the most potent compound. Secondary assays (hit-to-lead followed by lead optimisation), compromises of *in vitro* and *ex vivo* experiments which test a selection of the best compounds to understand the mechanism of the their action. *In vivo* analysis involves testing the lead compounds in an animal model, often a mouse model; this is to examine the pharmacology, efficacy of the compound, and to test the toxicity. By the end of the *in vivo* studies a lead compound has been identified, this is taken forward for pre-clinical testing and registration for clinical trials. Drug discovery is a high risk, and expensive activity; if a lead compound is identified approximately only 1 in 15-25 candidates make it through human and animal safety testing, and during clinical trials 4-7% of drugs make it through to clinical use and registration.[134] The total cost of getting a drug to market is approximately $1.14 billion and on average takes 10-15 years according to

industry body: PhRMA.[134,135]

Figure 1-9: Outline of the main steps taken from the initial identification of a compound to regulatory approval and use in the clinic.

1.6.1 *In silico* techniques

The drug discovery process described in Section 1.6, is a general outline of the traditional approach, however, owing to advancements in methodology, alternative approaches are also in use. A particular example of this is the advancement in computational aided drug design (CADD), which is being used to replace the large HTS used at the start of the discovery process.[136] CADD can be used to rule out compounds at the initial stage without physically synthesising the compounds or performing the screen; there are two types of CADD: structural-based methods and ligand-based methods. Structural-based methods use the atomic structure of the target site e.g. a crystal structure of a protein, whilst the ligand-based involves comparing compounds to known existing drugs.[136] As the atomic structure of urease is known, the focus will be on structural-based methods, particularly on ligand-docking whereby a library of virtual compounds are computationally docked onto the protein and the strength of binding is predicted.[137] This approach can also use fragments of compounds called fragment-based drug design.[137] CADD can be used iteratively, a library of virtual compounds can be docked, assessed, and re-designed and the docking repeated. Other properties such as solubility or Lipinski's Rule of 5 can be investigated and the compounds again can be optimised and docked. Lipinski's Rule of 5 are empirical and based on the physiological properties of the majority of drugs, they relate to the ability of the drugs to be orally delivered: (1) calculated logP (lipophiliocity) is <5, (2) molecular weight is <500 Da, (3) <5 hydrogen-bond donors (HBD), (4) <10 hydrogen-bond acceptors (HBA).[138] Lipinski's Rule of 5 allows a good prediction of an oral bioavailability however, many clinical drugs which are efficacious do not follow these rules such as the antibiotic vancomycin. Target structures can also be computationally assessed to identify possible binding sites for ligands. CADD can be carried out at a molecular docking level, which has a lower computational cost, or at a quantum level; the quantum level allows the free-energy of binding to be predicted and can predict the mechanism of binding however, has a higher computational cost.[139] CADD is often used in the initial compound screen, although it can also be employed later on in the discovery process, such as

at the hit-to-lead stage, in the identification of structural-activity relationships (SAR), and examining adsorption, distribution, metabolism, excretion, and toxicity (ADMET) properties during the pre-clinical stage.

CADD has been used to screen for urease inhibitors which could bind to *H. pylori*, 5 million virtual compounds were screened.[140] Compounds were ranked by docking score, then interactions with key residues, and analysis of binding modes with comparison to AHA, the class of the compounds was identified and finally the ability to synthesise was assessed. From the 5 million screen, 8 compounds were synthesised and the best compound 5-benzylidene barbituric acid demonstrated an IC_{50} of 41.6 μM compared to 100 μM for hydroxyurea.[140] CADD offers a cost-effective and quick alternative to a HTS, however the results should be taken with caution; computational data should be compared to laboratory data or followed up with laboratory experiments and well-designed computational controls should used to check docking parameters.

1.6.2 *In vitro* experimentation

In vitro experimentation takes place after the initial screen, a HTS may involve an *in vitro* enzymatic activity assay but the following hit-to-lead phase requires a series of robust *in vitro* experiments. For virtual screens, this is the first opportunity to physically test the compounds out. Most assays involve the recombinant production of the target enzyme; either by production in a mammalian cell line or in bacteria.[133] The target enzymes are purified allowing biochemical determination of the compound selectivity and potency. The ligand dissociation constant, K_d, determines the tendency of the ligand (compound) to bind to the target enzyme, this allows the strength of binding to the receptor to be measured. Equation 1.1, shows how the K_d is measured.[132]

$$K_d = \frac{[R][L]}{[RL]} \tag{1.1}$$
$$[R] = concentration\ of\ receptor, [L] = concentration\ of\ ligand,$$
$$[RL] = concentration\ of\ receptor - ligand\ complex$$

For inhibitors which are reducing an enzyme's activity, the activity of the enzyme can be measured and an inhibitory concentration 50% (IC_{50}) determined. IC_{50} is the concentration of inhibitor (ligand) which reduces the activity of the enzyme by 50%. This determines the potency of the compound. Figure 1-10, shows how the IC_{50} is determined from an enzyme-inhibitor graph. The mechanism of inhibition is

important: competitive (binds to active site, prevents substrate from binding), non-competitive (binds to site other than active site, does not prevent substrate binding), uncompetitive (binds to the enzyme-substrate complex), or mixed.[132] These assays do not assess the ability of the compound to reach the target site; for targets which are intracellular, a cell-based assay is helpful in informing whether the compound can cross the cell membranes.[141]

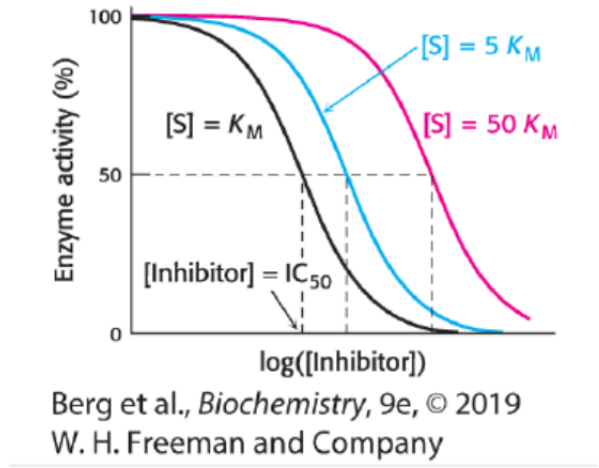

Figure 1-10: Graph of enzyme activity in presence of inhibitor showing competitive inhibition of the enzyme's activity. IC_{50} is the concentration at which the activity of the enzyme has been reduced by 50%. Competitive inhibition depends on the concentration of substrate present as the inhibitor must compete for the active site.

Continuously, throughout the drug discovery process the hit list is being decreased and optimised. During the *in vitro* stage initial toxicology cell-based assays are carried out such as the Methyl tetrazolium (MTT) assay which is used to assess cell viability in mammalian cells or a hemolysis assay, which measures whether the compound causes the lysis of erythrocytes.[142,143] Researchers often test the compounds on *in vitro* models which mimic the clinical problem, for example: the *in vitro* bladder model, a physiologically representative model of the catheterised tract (Section 2.2.3).[144]

1.6.3 Clinical Trials

Clinical trials are costly and time-consuming, in the UK trials involving medical devices or drugs must be approved by the Medicines and Healthcare products Regulatory Agency (MHRA), Health Research Authority (HRA), and the Research Ethics Committee (REC). Those testing an intervention not involving a drug or medical device requires approval by HRA and REC. Clinical trials have to be conducted for all drugs to gain a license from FDA, EMA, and MHRA. Currently, there is a growing requirement

for clinical trials to also be conducted for medical devices and new surgical techniques, where historically these were not conducted.[145] Clinical trials often need to be co-ordinated with NHS hospitals and prior to conducting a trial, various toxicity tests, including animal studies, and quality manufacture of the drug or medical device needs to be demonstrated (Good Manufacturing Practice (GMP)).

1.7 Urease - a Drug Target

Urease is a good anti-virulence target, as discussed in Section 1.2.1; urease is pivotal in causing catheter blockage and the associated clinical consequences. Urease is not present in mammalian cells, therefore treatments against it should not affect normal mammalian metabolism.[47] To design an effective anti-virulence treatment, researchers need to have a good understanding of the mechanism and function of urease. Urease is found in bacteria, plants and fungi; though the structure varies generally it is well-conserved at the active site, all major amino acids involved in the catalytic mechanism are 100% conserved (Fig. 1-11). A recent review of compounds which can inhibit urease determined that compounds can be designed against urease from one species but still demonstrate activity against urease form other species.

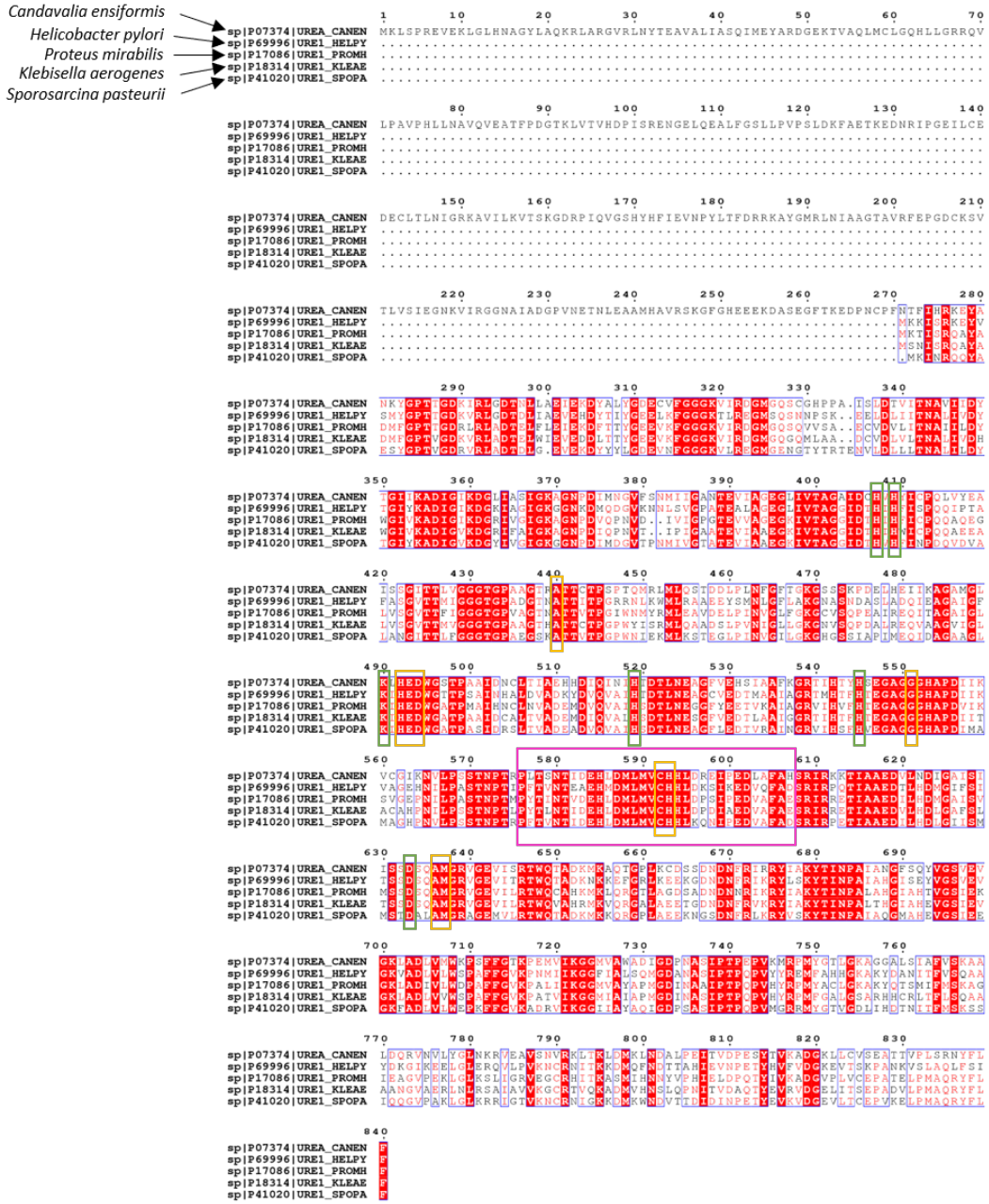

Figure 1-11: Amino acid sequence of urease from different species, aligned, and the conservation examined. α subunit of urease taken from: *Canavalia ensiformis* (plant), *Helicobacter pylori*, *Proteus mirabilis*, *Klebsiella aerogenes*, and *Sporosarcina pasteurii* (bacteria). Amino acids outlined in green boxes indicate conserved amino acids involved in coordinating the Ni ions found in the active site, yellow boxes indicate amino acids involved in the catalytic mechanism, and pink boxes indicate amino acids involved in the active site flap: helix-turn-helix motif. Red columns show completely conserved amino acids across all species. Sequences gathered from UniProt (entry numbers are next to sequences), and information on the amino acids involved in the mechanism are taken from Benini *et al.*[119] Alignment completed using Multalin and presented with ENDscript.[146,147]

Conservation at the amino acid level does not necessarily translate to the supramolecular level, as small changes in the amino acid sequence can alter the folding and 3D structure of an enzyme. There are differences in the supramolecular structure in urease; comparing the functional units: α, β, and γ, in *P. miraiblis* (and most bacteria) the formation is a trimer of trimers $(\alpha\beta\gamma)_3$ (Fig. 1-12 & 1-13).[148,149] α subunit contains the structural protein and the active site, β subunit is located on the outside of the trimer and contains a β-folding domain, and the γ subunit includes both an α-helix and β-fold.[150] *H. pylori* is an exception, it forms a heterodimer, $\alpha\beta$, which then associates to form a larger tetramer of trimers $((\alpha\beta)_3)_4$, a dodecameric structure that has a size of 1.1 MDa.[151,116] Whilst in plants and fungi, only a single subunit of α is observed (Fig. 1-13). Although there is variation in the supramolecular structures of urease, it is well conserved with bacterial species and therefore, urease is a good drug-target to treat various urease-positive infections.

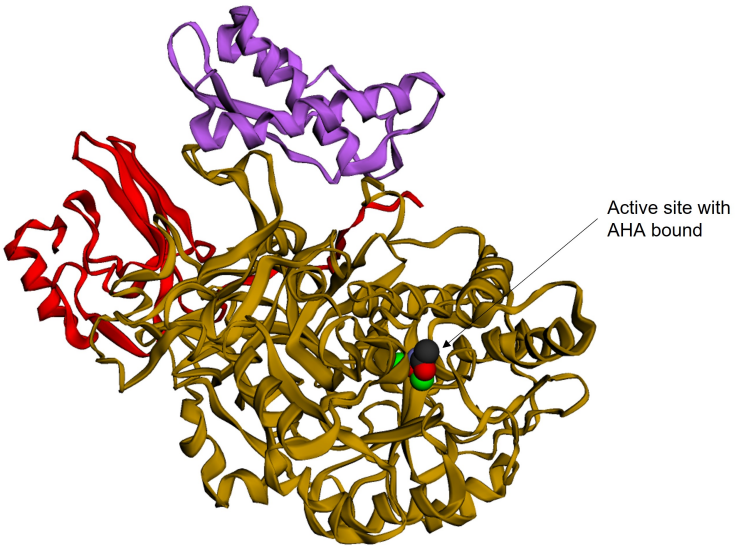

Figure 1-12: Crystal structure of urease from *Sporoscarcina pasteurii* (PDB = 4UPB) with acetohydroxamic acid bound in the active site. α subunit contains the active site and is coloured gold. β subunit is in red and the γ subunit in green.[119]

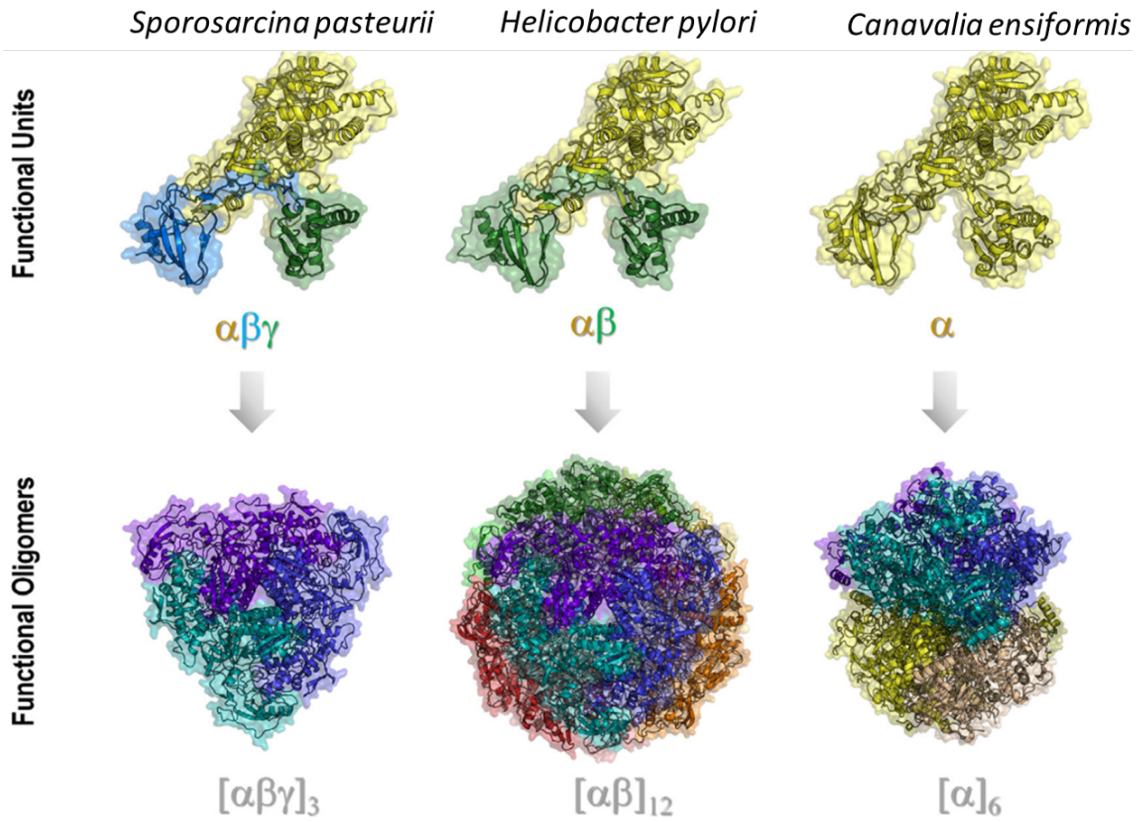

Figure 1-13: Comparing the supramolecular assembly of urease taken from different species. Image reprinted under Creative Commons Attribution-Non-Commercial-No Derivatives License.[116]

1.7.1 Mechanism of action

The crystal structure of urease is historically important, it was the first protein from *Canavalia ensiformis* (*C. ensiformis* (plant)) to be crystallised by James B Sumner in 1926, it showed that enzymes are proteins.[152] Since 1926, many ureases have been crystallised; demonstrating variability in their 3D structures and inhibitor binding (Fig. 1-13). Inhibitors such as AHA and β-mercaptoethanol, have been crystallised with urease, these structures inform on how the inhibitors bind and also provide information on the enzyme's mechanism of action (Section 1.5.2.1).[116] Alongside, mutagenesis studies, the mechanism of urease has been determined (Fig. 1-14).[153] Within the active site of the enzyme there are two Ni ions, coordinated by histidine amino acids, aspartate, and a carbamylated lysine.[154] In the absence of urea, three water molecules occupy the active site,(Fig. 1-14A), these are displaced when urea enters and binds to Ni(1) via the carbonyl oxygen on the urea (Fig. 1-14B). The carbonyl carbon becomes more electrophilic, urea binds to Ni(2) via the amino nitrogen atoms, this facilitates

the nucleophilic attack of water onto the carbonyl carbon (Fig. 1-14C), forming a tetrahedral intermediate (Fig. 1-14D). The ammonia, NH_3, and carbamate are released (Fig. 1-14E).[153]

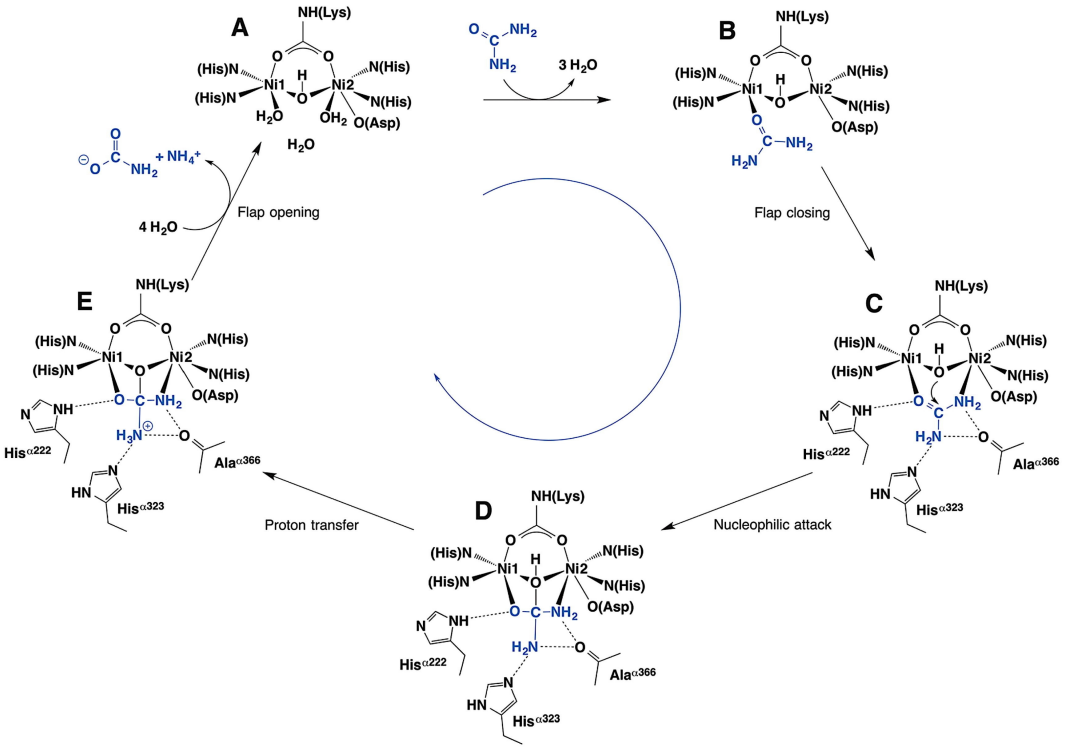

Figure 1-14: Mechanism of hydrolysing urea by urease, determined from structural data taken from the crystal structure of *Sporoscarcina pasteurii*. Reprinted with permission from Royal Society of Chemistry.[153]

1.7.2 Urease Inhibitors

As discussed in Section 1.5.2.1, urease inhibitors offer an alternative to antibiotic treatment of CAUTI. Research into urease inhibitors is not new, AHA was licensed in 1983, and it is not just inhibitors to treat catheter encrustations or *H. pylori* infections that have been investigated; they are also important in the agricultural sector.[118,155] Ammonia volatilisation occurs upon the application of nitrogen-based fertilisers to crops; urease-positive bacteria (and in some cases urease-positive plants) from the soil hydrolyze the urea causing ammonia to form, this reduces the effect of the fertilizer as the ammonia evaporates from the surface of the soil.[155] The urease inhibitor, *N*-(n-butyl) thiophosphoric triamide (NBPT), has been found to reduce the loss of nitrogen.[156] NBPT was routinely added to nitrogen fertilizers, however it has a short shelf-life and the effect on urease is short, therefore further research has been seeking alternat-

ives.[157] Urease inhibitors to treat CAUTI and *H. pylori* infection have been extensively reviewed by: Rego *et al.,* Modolo *et al.,* Kafarski *et al.,* Mazzei *et al.,* Krajewska *et al.,* Kosikowska *et al.,* and Kappaun *et al.,* they are summarised here.[158,159,160,153,48,161,116]

1.7.2.1 Urea Derivatives

Compounds containing fragments of urea or thiourea are an obvious starting point for inhibitor design as they mimic the natural substrate, urea.[160] These are competitive inhibitors, thiourea is often used a positive control in inhibitor design (itself cannot be used as an inhibitor owing to its toxic side effects).[162,163] A compound series based on urea derivatives and thiourea as a scaffold, included a *N*-acyl thiourea screen based on palmitic acid.[164] In which, top compound: 1-(4-chlorophenyl)-3-palmitoylthiourea had a IC_{50} of 0.02 μM against urease from *C. ensiformis*, the inhibition here was non-competitive and docking studies predicted the compounds bound to amino acids involved in the catalytic mechanism (R636) (thiourea IC_{50} = 4.720 μM) (Fig. 1-15).[164]

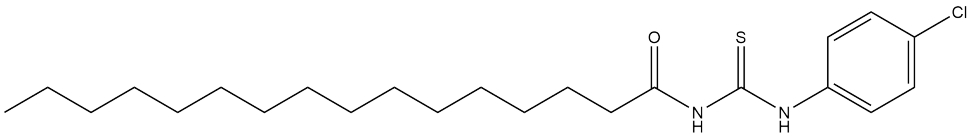

1-(4-chlorophenyl)-3-palmitoylthiourea

Figure 1-15: 1-(4-chlorophenyl)-3-palmitoylthiourea discovered by Saeeed *et al.,* taken from a series designed around palmititc acid.[164] Compound drawn using ChemDraw (PerkinElmer Informatics Inc, v. 19.0.1.28).

1.7.2.2 Organophosphorus Compounds

Phosphate was shown to inhibit urease by competitive inhibition in 1934.[165] Phosphoramidates have been shown to be particularly potent against urease, these were studies to identify an alternative to NBPT in fertilizers, however the compounds were not stable owing to P-N bond.[166] Phosphorodiamidic acid derivatives were studied against bacterial ureases, Fig. 1-16, shows a compound with a K_i of 0.108 μM against *S. pasteurii* urease and 0.202 μM against *P. mirabilis* urease (control of AHA with K_i of 3.3 μM against *S. pasteurii* urease and 5.7 μM against *P. mirabilis* urease).[167] Molecular modelling showed that the inhibitor coordinated with the Ni^{2+} ion in the active site as well as other amino acids involved in activity (A170 and A366) (modelled using urease from *S. pasteurii*).[167] Organophosphates have not been investigated extensively for clinical use owing to their high toxicity in mammals in various toxicity studies. Organophosphates (which are used in pesticides) demonstrated changes in sexual behaviour, the onset of puberty, gamete production, changes in the reproductive cycle,

and infertility in various mammalian studies.[168]

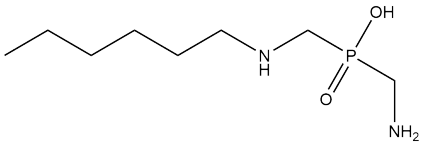

Figure 1-16: (Aminomethyl)((hexylamino)methyl)phosphinic acid, derivative of phosphorodiamidic acid with potency against *Sporoscarina pasteurii* and *Proteus mirabilis*.[167] Compound drawn using ChemDraw (PerkinElmer Informatics Inc, v. 19.0.1.28).

1.7.2.3 Heterocyclic Compounds

Both 5-member and 6-member heterocyclic compounds have been extensively explored as urease inhibitors. Benzimidazole, sulfur heterocycles, have been explored and demonstrated a mixed-type mechanism of inhibition; binding to the free-urease and enzyme-substrate complex. A K_i of 1.02 mM was measured against *C. ensiformis* urease (a 3-fold higher affinity compared to urea).[169] Another series of compounds of interest is the thiazolidine aliphatic esters, heptyl thiazolidine-4-carboxylate measured an IC_{50} of 0.30 μM against *S. pasteurii* urease (thiourea control IC_{50} = 15.66 μM)(Fig. 1-17).[170] The mechanism of inhibition was explored using computational docking analysis, which showed that the carbonyl oxygen coordinated with the Ni ions, whilst the nitrogen from the heterocyclic ring bonded with H322 (involved in catalytic mechanism). Aliphatic chains demonstrated a better potency compared to branched chains, it was hypothesised that the long chain could bind into the active site and subsequent studies showed the longer chained compounds had a higher potency compared to branched.[170,158]

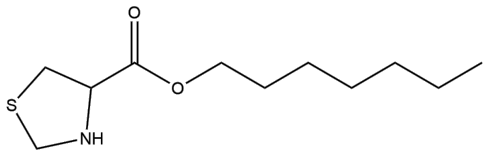

Figure 1-17: Heptyl thiazolidine-4-carboxylate identified as a potent inhibitor from a thiazolidine aliphatic ester series.[170] Compound drawn using ChemDraw (PerkinElmer Informatics Inc, v. 19.0.1.28).

1.7.2.4 Natural Products

Natural products historically have been the starting point for the identification of multiple pharmaceuticals especially antibiotics and antimicrobials[171]. Plant extracts have been explored, often for treatment of *H. pylori* infection; extracts from *Allium sativum* (garlic), *Allium cepa* (onion), *Allium porrum* (leek), *Brassica oleraceae* var.

capitata (cabbage), and *Brassica oleraceae* var. *gemmifera* (Brussels sprouts), have demonstrated urease inhibition.[172] The concentration of thiosulfinate within the extract was important for its ability to inhibit urease.[172] Methanolic, acetone, and alcoholic extracts or the oils of various plants have also shown urease inhibitory properties.[159]

Quinones demonstrate antibacterial and antifungal properties, and are involved in biological redox reactions, owing to their oxidising property; in the 1970s, 1,4-benzoquinone was identified as a urease inhibitor (Fig. 1-18).[173] Krajewska *et a.,* showed that 1,4-naphthoquinone was bound in a slow, concentration dependent manner suggesting a covalent bond formation with cysteine (found in the active site flap of urease (Fig. 1-11, 1-19)) (Section 1.7.2.5).[174] Additionally, it is suggested that quinones also inhibit by arylation and oxidation of thiol groups.[153,174] Fluoroquinolones are currently in use as antibiotics: Levofloxacin and Ciprofloxacin, these compounds inhibit DNA synthesis particularly in Gram-positive bacteria and have also been shown to act as urease inhibitors against *H. pylori* and *P. mirabilis* urease (Table 1.3).[160] The disadvantage of quinones as urease inhibitors is their reported cytotoxicity and carcinogenic properties.[161]

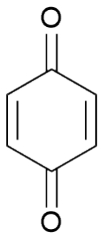

Figure 1-18: 1,4-benzoquinone identified as a potent inhibitor from a quinone series.[173] Compound drawn using ChemDraw (PerkinElmer Informatics Inc, v. 19.0.1.28).

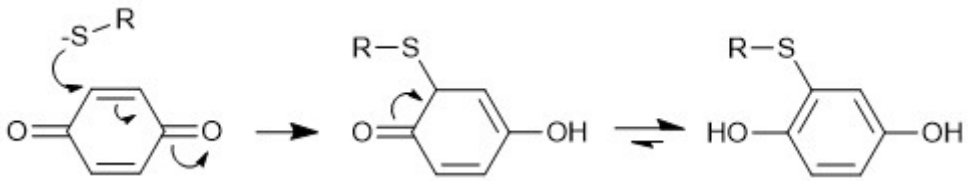

Figure 1-19: Michael acceptor mechanism drawn using ChemDraw (PerkinElmer Informatics Inc, v. 19.0.1.28).

Polyphenols, especially flavonoids are another group of compounds which exhibit urease inhibitory properties. Two studies investigated the inhibitory effects of naturally derived flavonoids and synthetically altered analogues; quercetin measured an IC_{50} of 11.2 μM against *H. pylori* urease (Fig. 1-20a).[175] Molecular modelling studies predicted

that quercetin bound to the active site flap of urease, and acted as a non-competitive inhibitor.[175] The best synthetic flavonoid is shown in Figure 1-20b, it measured an IC_{50} of 0.85 μM against *H. pylori* urease.[176] This compound demonstrated competitive inhibition and computationally docked into the active site cleft of urease.[176]

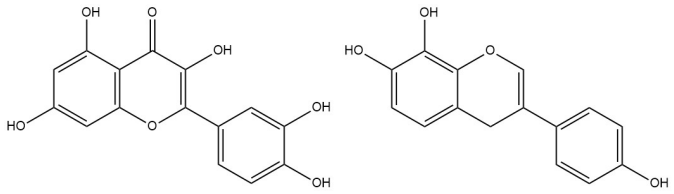

(a) Quercetin **(b)** Synthetic flavonoid

Figure 1-20: Flavonoid compounds drawn using ChemDraw (PerkinElmer Informatics Inc, v. 19.0.1.28).

1.7.2.5 Covalent Inhibitors

The majority of urease inhibitors studied (and in general most licensed clinical drugs) are not covalently bound, this means that they bind to their target site by hydrogen bonds, van der Waals forces, electrostatic interactions, and hydrophobic interactions.[132] Covalently bound compounds are of interest because they bind with a stronger bond, this means that these compounds can be more potent and therefore, can be administered in smaller doses. The disadvantages of covalent inhibitors are toxicity (binding covalently to non-target sites leading to adverse side effects), issues in the degradation of enzymes, and immunogenicity.[160] A common covalent interaction which is predicted is between quinones and cysteine, found in the active site flap (Section 1.7.2.4). One class of compounds which has been investigated is Michael acceptors, the most potent compound, acetylenedicarboxylic acid, shown in Figure 1-21a, is predicted to form a covalent bond with Cys322 and coordinate with the Ni ions in the active site (Fig. 1-21b).[177] This compound measured an IC_{50} of 88.6 μM against whole-cell *P. mirabilis*.

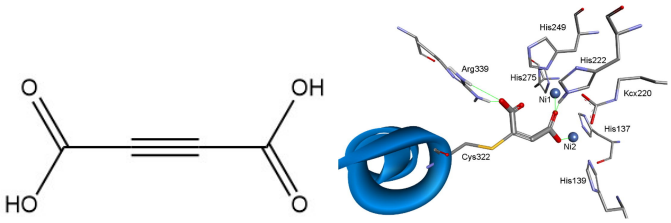

(a) Acetylenedicarboxylic acid.

(b) Computationally docked acetylenedicarboxylic acid, covalently bonded with with Cys322 and interactions with Ni ions in the active site.

Figure 1-21: Acetylenedicarboxylic acid, identified as a potent inhibitor of *Sporocarcina pasteurii* urease. (a) Compound drawn using ChemDraw (PerkinElmer Informatics Inc, v. 19.0.1.28). (b) Reprinted with permission from Bioorganic and Medicinal Chemistry Letters, Elsevier.[177]

1.7.2.6 2-mercaptoacetamide

Milo *et al.,* identified 2-mercaptoacetamide (2-MA) as an effective urease inhibitor.[178] The initial focus of this work came from a Carson *et al.,* study, which designed *N*-alpha mercaptoamide dipeptide inhibitors against the virulence factor: Zap A protease, an important enzyme in the establishment of *P. mirabilis* infection.[179] It was hypothesised that the war-head of these compounds could be effective against urease (unpublished) (Fig. 1-22). 2-MA demonstrated competitive inhibition, with an IC_{50} of 57.9 mM against *C. ensiformis* urease (AHA IC_{50} = 4.84 mM). 2-MA was not cytotoxic against *P. mirabilis*, and was able to significantly extend the lifetime of an *in vitro* catheter in a physiologically representative model of the catheterised tract infected with *P. mirabilis* compared to AHA treatment.[178]

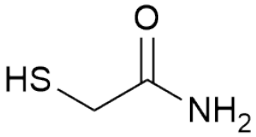

Figure 1-22: 2-mercaptoacetamide.[178] Compound drawn using ChemDraw (PerkinElmer Informatics Inc, v. 19.0.1.28).

1.7.2.7 Summary of Urease Inhibitors

In conclusion, urease inhibitors have been extensively studied for both agricultural and clinical use, both in treating recurrent catheter blockage and *H. pylori* stomach infections. Other inhibitor classes such as heavy metals, boric and boronic acids, bismuth compounds, and fluoride, which have not been discussed here, are reviewed by Krajewska *et al.,* Mazzei *et al.,* and Rego *et al.*[48,153,158] Most compounds identified are

predicted or known to be competitive inhibitors which are competing with the substrate, urea, to bind into the active site. Non-competitive inhibitors bind to a site other than the active site, often the active site flap, and inhibit the urease by an different mechanism.[132] Figure 1-11, showed the similarity in the active site between ureases from different species; however the supramolecular structure varies between species and could affect the access of compounds to the active site (Fig. 1-13). Fortunately, the structure and mechanism of urease has been extensively studied allowing an informed drug discovery process and the ability to use *in silico* drug discovery techniques (Section 1.6.1).[152,116] The majority of compounds are tested against *C. ensiformis* urease because it can be purchased (Merck, Germany) and is relatively stable.[158] However, if compounds are designed for bacterial urease targets, additional experiments are needed, such as a whole-cell bacterial assays, this allows experimentation into the ability of the compounds to access the urease. *P. mirabilis* urease is intracellular, whilst *H. pylori* is extracellular and intracellular, therefore experiments should be designed with assays involving the target bacteria specifically.[180,151]

1.8 Drug Delivery Systems (DDS)

The majority of drugs are delivered orally or by injection, and most small molecule drugs are delivered orally in tablet form.[181] The main types of DDS within the literature currently are: nanoparticle based cancer drugs, transdermal systems, microparticle-based depot formulations, oral DDS, pulmonary drug delivery, implants, and antibody-drug conjugates.[181] Drug delivery is all about getting the drug to the right place, at the right time, in the right quantity, without adversely affecting the patient. The urease inhibitor, AHA, is a small soluble molecule and therefore, is delivered orally where it enters the blood stream, is flushed from the blood stream into the urine in the kidneys where it can access *P. mirabilis*, cross the bacterial membrane and inhibit intracellular urease.[180] AHA is able to reach the bladder and is successful at preventing catheter blockage, however is not regularly used owing to its toxicity.[122]

A more obvious DDS for CAUTI is intravesical (delivery directly into the bladder), this is the principle behind bladder washouts (Section 1.4.1). The disadvantage of intravesical delivery is the frequent emptying of the bladder which often flushes the therapeutic away.[182] Therefore, research has focused on modifying the Foley catheter to ensure prolonged delivery, as described by antimicrobial catheters in Section 1.4.2. Biomodics ApS (Denmark) developed a novel delivery system, whereby the balloon of the catheter is modified to an interpenetrating polymer network (IPN), the balloon can be filled with the drug formulation and the drug diffuses across the IPN directly

into the bladder allowing sustained directed delivery (Fig. 1-23). The IPN consists of a hydrophilic poly(2-hydroxyethyl methacrylate-co-poly(ethylene glycol) methyl ether acrylate) (poly(HEMA-co-PEGMEA)) network which is integrated into the silicone elastomer of the catheter balloon.[183] The Biomodics catheter was effective at treating a Porcine model of *E. coli* CAUTI and in the treatment of bladder cancer.[184,185] Therefore, the Biomodics catheter offers a potential DDS for treating recurrent catheter blockage.

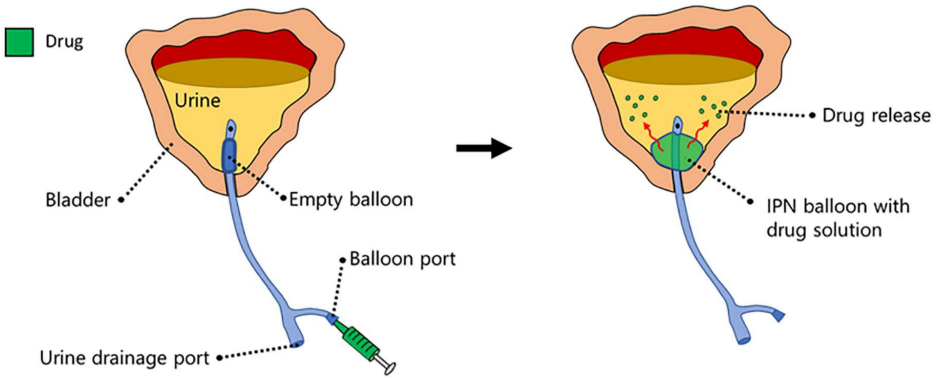

Figure 1-23: Schematic of the Biomodics catheter showing the delivery of the drug solution through the balloon membrane, directly into the bladder. Image reprinted under the Creative Commons Attribution License.[184]

1.9 Overall Aims and Objectives

The aim of this research has two branches: (1) optimisation and testing of a diagnostic device, the lozenge, to predict catheter blockage events; (2) rational drug design of urease inhibitors to treat recurrent catheter blockage. The manufacture of the lozenge will be optimised to allow the upscale of lozenge production and improvements in robustness shall be made (Chapter 3). A small scale pilot clinical trial will test the lozenge in urine donated by long-term catheterised patients (Chapter 4).

Rational drug design of urease inhibitors incorporates the current understanding of urease inhibitors (Section 1.7.2), with an *in silico* compound screen, followed by *in vitro* experimentation and cytotoxicity assessment. The final candidate compound will be tested using the Biomodics DDS on a *in vitro* model of the catheterised tract (Chapter 5). Finally, a natural product extract from the plant *Nasturtium officinale* (*N. officinale*, watercress) shall be examined for its urease inhibitory properties (Chapter 6).

1.10 Bibliography

[1] Zowawi HM, Harris PNA, Roberts MJ, Tambyah PA, Schembri MA, Pezzani MD, et al. The emerging threat of multidrug-resistant Gram-negative bacteria in urology. Nature Reviews Urology. 2015;12(10):570–584.

[2] Rowe TA, Juthani-Mehta M. Urinary tract infection in older adults. Aging Health. 2013;9(5):1–15.

[3] Totsika M, Gomes Moriel D, Idris A, A Rogers B, J Wurpel D, Phan MD, et al. Uropathogenic Escherichia coli Mediated Urinary Tract Infection. Current Drug Targets. 2012;13(11):1386–1399.

[4] Aydin A, Ahmed K, Zaman I, Khan MS, Dasgupta P. Recurrent urinary tract infections in women. International Urogynecology Journal. 2015;26(6):795–804.

[5] Barber AE, Norton JP, Spivak AM, Mulvey MA. Urinary tract infections: Current and emerging management strategies. Clinical Infectious Diseases. 2013;57(5):719–724.

[6] Sabih A, Leslie SW. Complicated urinary tract infections. StatPearls; 2020. Available from: https://www.ncbi.nlm.nih.gov/books/NBK436013/.

[7] Hanafy M, Saad M, Mohamed MAg. Ancient Egyptian Medicine Contribution to Urology. Urology. 1974;IV(1):114–120.

[8] Feneley RCL, Hopley IB, Wells PNT. Urinary catheters: History, current status, adverse events and research agenda. Journal of Medical Engineering and Technology. 2015;39(8):459–470.

[9] Carr HA. A short history of the Foley catheter: From handmade instrument to infection-prevention device. Journal of Endourology. 2000;14(1):5–8.

[10] Jacobsen SM, Stickler DJ, Mobley HLT, Shirtliff ME. Complicated catheter-associated urinary tract infections due to Escherichia coli and Proteus mirabilis. Clinical Microbiology Reviews. 2008;21(1):26–59.

[11] Jarow JP, Baxley JH. Medical devices: US medical device regulation. Urologic Oncology: Seminars and Original Investigations. 2015;33(3):128–132.

[12] European Commission DG Health and Consumer. Medical Devices: Guidence document - Classification of medical devices.; 2010. 6.

[13] Newman DK, Willson MM. Review of intermittent catheterization and current best practices. Urologic nursing. 2011;31(1).

[14] Getliffe KA. The characteristics and management of patients with recurrent hlockage of long-term urinary catheters. Journal of Advanced Nursing. 1994;20:140–149.

[15] Nicolle LE. Urinary Catheter - Associated Infections. Infectious Disease Clinics of North America. 2012;26(1):13–27. Available from: http://dx.doi.org/10.1016/j.idc.2011.09.009.

[16] Neoh KG, Li M, Kang ET, Chiong E, Tambyah PA. Surface modification strategies for combating catheter-related complications : recent advances and challenges. Journal of Materials Chemistry B. 2017;5:2045–2067. Available from: http://dx.doi.org/10.1039/C6TB03280J.

[17] Zarb P, Coignard B, Griskeviciene J, Muller A, Vankerckhoven V, Weist K, et al. The European Centre for Disease Prevention and Control (ECDC) pilot point prevalence survey of healthcare-associated infections and antimicrobial use. Euro Surveill. 2012;17(46):20316.

[18] Shackley DC, Whytock C, Parry G, Clarke L, Vincent C, Harrison A, et al. Variation in the prevalence of urinary catheters: A profile of National Health Service patients in England. BMJ Open. 2017;7(6):1–8. Available from: https://bmjopen.bmj.com/content/7/6/e013842.

[19] Prieto J, Wilson J, Bak A, Denton A, Flores A, Lusardi G, et al. A prevalence survey of patients with indwelling urinary catheters on district nursing caseloads in the United Kingdom: The Community Urinary Catheter Management (CCaMa) Study. Journal of Infection Prevention. 2020;21(4):129–135.

[20] Nicastri E, Leone S. Guide To Infection Control In The Healthcare Setting Hospital-Acquired Urinary Tract Infection; 2018. Available from: https://isid.org/guide/hospital/urinary-tract-infections/.

[21] Stickler D, Feneley R. The Indwelling Bladder Catheter: Attempts to Prevent Infection and the Development of Bacterial Biofilms. New York: Springer Science+Business Media New York; 2013.

[22] Gage H, Avery M, Flannery C, Williams P, Fader M. Community Prevalence of Long-Term Urinary Catheters Use. Neurourlogy and Urodyamics. 2017;36:293–296.

[23] Ramstedt M, Ribeiro IAC, Bujdakova H, Mergulhão FJM, Jordao L, Thomsen P, et al. Evaluating Efficacy of Antimicrobial and Antifouling Materials for Urinary Tract Medical Devices: Challenges and Recommendations. Macromolecular Bioscience. 2019;19(5):1–26.

[24] Nicolle LE. Catheter associated urinary tract infections. Antimicrobial Resistance & Infection Control. 2014;3(1):1–8. Available from: https://doi.org/10.1186/2047-2994-3-23.

[25] Smith DRM, Pouwels KB, Hopkins S, Naylor NR, Smieszek T, Robotham JV. Epidemiology and health-economic burden of urinary-catheter-associated infection in English NHS hospitals: a probabilistic modelling study. Journal of Hospital Infection. 2019;103(1):44–54. Available from: https://doi.org/10.1016/j.jhin.2019.04.010.

[26] Wong ES. Guideline for prevention of catheter-associated urinary tract infections. AJIC: American Journal of Infection Control. 1983;11(1):28–33.

[27] Kandil H, Cramp E, Vaghela T. Trends in Antibiotic Resistance in Urologic Practice. European Urology Focus. 2016;2(4):363–373. Available from: http://dx.doi.org/10.1016/j.euf.2016.09.006.

[28] Tambyah PA, Halvorson KT, Maki DG. A Prospective Study of Pathogenesis of Catheter-Associated Urinary Tract Infections. Mayo Clinic Proceedings. 1999;74(2):131–136. Available from: http://dx.doi.org/10.4065/74.2.131.

[29] Hooton TM, Bradley SF, Cardenas DD, Colgan R, Geerlings SE, Rice JC, et al. Diagnosis, prevention, and treatment of catheter-associated urinary tract infection in adults: 2009 international clinical practice guidelines from the Infectious Diseases Society of America. Clinical Infectious Diseases. 2010;10(5):321–324.

[30] Silhavy TJ, Kahne D, Walker S. The Bacterial Cell Envelope. Cold Spring Harb Perspect Biol. 2010;2:1–16. Available from: https://www.ncbi.nlm.nih.gov/pmc/articles/PMC2857177/pdf/cshperspect-PRK-a000414.pdf.

[31] Matsukawa M, Kunishima Y, Takahashi S, Takeyama K, Tsukamoto T. Bacterial colonization on intraluminal surface of urethral catheter. Adult Urology. 2005;65:440–444.

[32] Warren JW. The Catheter and Urinary Tract Infection. Medical Clinics of North America. 1991;75(2):481–493. Available from: http://dx.doi.org/10.1016/S0025-7125(16)30465-5.

[33] Clayton CL, Chawla JC, Stickler DJ. Some observations on urinary tract infections in patients undergoing long-term bladder catheterization. Journal of Hospital Infection. 1982;3:39–47.

[34] Chatterjee S, Pk M, Dey R, Ak K, Rk D. Biofilms on Indwelling Urologic Devices : Microbes and Antimicrobial Management Prospect. Annuals of Medical and Health Sciences Research. 2014;4(1):100–104.

[35] Donlan RM. Biofilms: Microbial Life on Surfaces. Emerging Infectious Diseases. 2002;8(9):881–890.

[36] Khatoon Z, McTiernan CD, Suuronen EJ, Mah TF, Alarcon EI. Bacterial biofilm formation on implantable devices and approaches to its treatment and prevention. Heliyon. 2018;4(12):e01067. Available from: https://doi.org/10.1016/j.heliyon.2018.e01067.

[37] Djeribi R, Bouchloukh W, Jouenne T, Menaa B. Characterization of bacterial biofilms formed on urinary catheters. American Journal of Infection Control. 2012;40(9):854–859. Available from: http://dx.doi.org/10.1016/j.ajic.2011.10.009.

[38] Lewis K. Persister Cells and the Riddle of Biofilm Survival. Biochemsitry (Moscow). 2005;70(2):327–336.

[39] Zhu Z, Wang Z, Li S, Yuan X. Antimicrobial strategies for urinary catheters. Journal of Biomedical Materials Research - Part A. 2019;107(2):445–467.

[40] Gaston JR, Andersen MJ, Johnson AO, Bair KL, Sullivan CM, Guterman LB, et al. Enterococcus faecalis polymicrobial interactions facilitate biofilm formation, antibiotic recalcitrance, and persistent colonization of the catheterized urinary tract. Pathogens. 2020;9(10):1–20.

[41] Armbruster CE, Smith SN, Johnson AO, Deornellas V, Eaton KA, Yep A, et al. The Pathogenic Potential of Proteus mirabilis Is Enhanced by Other Uropathogens during Polymicrobial Urinary Tract Infection. Infection and Immunity. 2017;85(2):e00808–16. Available from: https://doi.org/10.1128/IAI.00808-16.

[42] Williams FD, Schwarzhofj RH. Nature of Swarming. Annual Review Microbiology. 1978;32:101–22.

[43] Schnauffer JN, Pearson MM. Proteus mirabilis and Urinary Tract Infections. Mi-

crobiol Spectr. 2015;3(5):1032–1057. Available from: 10.1128/microbiolspec.UTI-0017-2013.

[44] Warren JW, Tenney JH, Hoopes JM, Muncie HL, Anthony WC. A prospective microbiologic study of bacteriuria in patients with chronic indwelling urethral catheters. Journal of Infectious Diseases. 1982;146(6):719–723.

[45] Armbruster CE, Mobley HLT, Pearson MM. Pathogenesis of Proteus mirabilis Infection. EcoSal Plus. 2018;8(1):1–73. Available from: https://doi.org/10.1128/ecosalplus.ESP-0009-2017.

[46] Stickler DJ. Bacterial biofilms in patients with indwelling urinary catheters. Nature Clinical Practice Urology. 2008;5(11).

[47] Chang A, Jeske L, Ulbrich S, Hofmann J, Koblitz J, Schomburg I, et al. BRENDA, the ELIXIR core data resource in 2021: New developments and updates. Nucleic Acids Research. 2021;49(D1):D498–D508. Available from: https://doi.org/10.1093/nar/gkaa1025.

[48] Krajewska B. Ureases I. Functional, catalytic and kinetic properties: A review. Journal of Molecular Catalysis B: Enzymatic. 2009;59(1-3):9–21.

[49] Konieczna I, Zarnowiec P, Kwinkowski M, Kolesinska B, Fraczyk J, Kaminski Z, et al. Bacterial Urease and its Role in Long-Lasting Human Diseases. Current Protein and Peptide Science. 2012;13(8):789–806. Available from: https://doi.org/10.2174{%}2F138920312804871094.

[50] Stickler DJ, Feneley RCL. The encrustation and blockage of long-term indwelling bladder catheters: A way forward in prevention and control. Spinal Cord. 2010;48(11):784–790. Available from: https://doi.org/10.1038/sc.2010.32.

[51] Bradbury RS, Reid DW, Champion AC. Urease production as a marker of virulence in Pseudomonas aeruginosa. British Journal of Biomedical Science. 2014;71(4):175–177. Available from: https://doi.org/10.1080/09674845.2014.11978060.

[52] García-Solache M, Rice LB. The enterococcus: A model of adaptability to its environment. Clinical Microbiology Reviews. 2019;32(2). Available from: https://doi.org/10.1128/CMR.00058-18.

[53] Stickler DJ, Morris NS, C W. Simple Physical Model to Study Formation and Physiology of Biofilms on Urethral Catheters. Methods in En-

zymology. 1999;310:494–501. Available from: https://doi.org/10.1016/S0076-6879(99)10037-5.

[54] Norsworthy AN, Pearson MM. From Catheter to Kidney Stone: The Uropathogenic Lifestyle of Proteus mirabilis. Trends in Microbiology. 2017;25(4):304–315. Available from: https://doi.org/10.1016/j.tim.2016.11.015.

[55] Armbruster CE, Mobley HLT. Merging mythology and morphology: the multifaceted lifestyle of Proteus mirabilis. Nature Reviews Microbiology. 2013;10(11):186–194.

[56] Iqbal MW, Youssef RF, Neisius A, Kuntz N, Hanna J, Ferrandino MN, et al. Contemporary management of struvite stones using combined endourologic and medical treatment: Predictors of unfavorable clinical outcome. Journal of Endourology. 2016;30(7):771–777.

[57] Choong S, Wood S, Fry C, Whitfield H. Catheter associated urinary tract infection and encrustation. International Journal of Antimicrobial Agents. 2001;17:305–310. Available from: https://doi.org/10.1016/s0924-8579(00)00348-4.

[58] Wilks SA, Fader MJ, Keevil CW. Novel insights into the proteus mirabilis crystalline biofilm using real-time imaging. PLoS ONE. 2015;10(10):1–13.

[59] Jones BD, Lockatell CV, Johnson DE, Warren JW, Mobley HLT. Construction of a urease-negative mutant of Proteus mirabilis: Analysis of virulence in a mouse model of ascending urinary tract infection. Infection and Immunity. 1990;58(4):1120–1123.

[60] Pearson MM, Rasko DA, Smith SN, Mobley HLT. Transcriptome of Swarming Proteus mirabilis. Infection and Immunity. 2010;78(6):2834–2845.

[61] Mobley HLT, Belas R, Lockatell V, Chippendale G, Trifillis AL, Johnson DE, et al. Construction of a Flagellum-Negative Mutant of Proteus mirabilis : Effect on Internalization by Human Renal Epithelial Cells and Virulence in a Mouse Model of Ascending Urinary Tract Infection. Infection and Immunity. 1996;64(12):5332–5340.

[62] Legnani-Fajardo C, Zunino P, Piccini C, Allen A, Maskell D. Defined mutants of Proteus mirabilis lacking flagella cause ascending urinary tract infection in mice. Microbial Pathogenesis. 1996;21:395–405.

[63] Armbruster CE, Forsyth-DeOrnellas V, Johnson AO, Smith SN, Zhao L, Wu W, et al. Genome-wide transposon mutagenesis of Proteus mirabilis: Essential genes, fitness factors for catheter-associated urinary tract infection, and the impact of polymicrobial infection on fitness requirements. PLoS Pathogens. 2017;13(6):1–43.

[64] Devillé WLJM, Yzermans JC, Duijn NPV, Bezemer D, Windt DAWMVD, Bouter LM. The urine dipstick test useful to rule out infections. A meta-analysis of the accuracy. BMC Urology. 2004;14:1–14.

[65] England PH. Diagnosis of urinary tract infections Quick reference tool for primary care for consultation and local adaptation About Public Health England; 2018. Available from: https://assets.publishing.service.gov.uk/government/uploads/system/uploads/attachment{_}data/file/927195/UTI{_}diagnostic{_}flowchart{_}NICE-October{_}2020-FINAL.pdf.

[66] NICE. UTI (catheter): antimicrobial prescribing; 2019. September. Available from: https://www.nice.org.uk/guidance/ng113.

[67] Milo S, Acosta FB, Hathaway HJ, Wallace LA, Thet NT, Jenkins ATA. Development of an Infection-Responsive Fluorescent Sensor for the Early Detection of Urinary Catheter Blockage. ACS Sensors. 2018;3(3):612–617. Available from: https://doi.org/10.1021/acssensors.7b00861.

[68] Evoniks. The Use of Advanced pH , Time or Microbial-Dependent Oral Drug Delivery Technologies for Precise Release in the Colon. American Pharmaceutical Review. 2018;1(October):100–103.

[69] Milo S, Tun N, Liu D, Nzakizwanayo J, Jones BV, Jenkins ATA. Biosensors and Bioelectronics An in-situ infection detection sensor coating for urinary catheters. Biosensors and Bioelectronic. 2016;81:166–172. Available from: http://dx.doi.org/10.1016/j.bios.2016.02.059.

[70] Stickler DJ, Jones SM, Adusei GO, Waters MG, Cloete J, Mathur S, et al. A clinical assessment of the performance of a sensor to detect crystalline biofilm formation on indwelling bladder catheters. BJU International. 2006;98(6):1244–1249. Available from: https://doi.org/10.1111/j.1464-410X.2006.06562.x.

[71] Malic S, Waters MGJ, Basil L, Stickler DJ, Williams DW. Development of an "early warning" sensor for encrustation of urinary catheters following Proteus in-

fection. Journal of Biomedical Materials Research - Part B Applied Biomaterials. 2012;100 B(1):133–137.

[72] Long A, Edwards J, Thompson R, Lewis DA, Timoney AG. A clinical evaluation of a sensor to detect blockage due to crystalline biofilm formation on indwelling urinary catheters. BJU International. 2014;114:278–285.

[73] Gould CV, Umscheid CA, Agarwal RK, Kuntz G, Pegues DA. Guidelines for prevention of catheter-associated urinary tract infections.; 2019.

[74] Evans A, Godfrey H. Bladder washouts in the management of long-term catheters. British journal of nursing (Mark Allen Publishing). 2000;9(14):111–114.

[75] Getliffe K. Managing recurrent urinary catheter blockage: Problems, promises, and practicalities. Journal of Wound, Ostomy and Continence Nursing. 2003;30(3):146–151.

[76] Shepherd AJ, Mackay WG, Hagen S. Washout policies in long-term indwelling urinary catheterisation in adults. Cochrane Database of Systematic Reviews. 2017;2017(3):1–55.

[77] Okorie CO. Is continuous bladder irrigation after prostate surgery still needed? World Journal of Clinical Urology. 2015;4(3):108.

[78] Getliffe KA. Bladder instillations and bladder washouts in the management of catheterized patients. Journal of Advanced Nursing. 1996;23(3):548–554.

[79] National Institute for Health and Care Excellence. Bladder instillations and urological surgery; 2022. Available from: https://bnf.nice.org.uk/treatment-summary/bladder-instillations-and-urological-surgery.html.

[80] Dance DAB, Pearson AD, Seal DV, Lowes JA. A hospital outbreak caused by a chlorhexidine and antibiotic-resistant Proteus mirabilis. Journal of Hospital Infection. 1987;10(1):10–16.

[81] Pannek J, Everaert K, Möhr S, Vance W, Van Der Aa F, Kesselring J. Tolerability and safety of urotainer® polihexanide 0.02% in catheterized patients: a prospective cohort study. BMC Urology. 2020;20(1):1–7.

[82] Brill FHH, Hambach J, Utpatel C, Mogrovejo DC, Gabriel H, Klock JH, et al. Biofilm reduction potential of 0.02% polyhexanide irrigation solution in sev-

eral types of urethral catheters. BMC Urology. 2021;21(1):1–6. Available from: https://doi.org/10.1186/s12894-021-00826-3.

[83] Davenport K, Keeley FX. Evidence for the use of silver-alloy-coated urethral catheters. Journal of Hospital Infection. 2005;60(4):298–303.

[84] Srinivasan A, Karchmer T, Richards A, Song X, Perl TM. A Prospective Trial of a Novel, Silicone-Based, Silver-Coated Foley Catheter for the Prevention of Nosocomial Urinary Tract Infections. Infection Control & Hospital Epidemiology. 2006;27(1):38–43.

[85] Belfield K, Betts H, Parkinson R, Bayston R. A tolerability and patient acceptability pilot study of a novel antimicrobial urinary catheter for long-term use. Neurourology and Urodynamics. 2019;38(1):338–345.

[86] Brosnahan J, Jull A, Tracy C. Types of urethral catheters for management of short-term voiding problems in hospitalised adults. Cochrane Database of Systematic Reviews. 2004;1:1–33.

[87] Stickler DJ, Morgan SD. Observations on the development of the crystalline bacterial biofilms that encrust and block Foley catheters. Journal of Hospital Infection. 2008;69(4):350–360.

[88] Morgan SD, Rigby D, Stickler DJ. A study of the structure of the crystalline bacterial biofilms that can encrust and block silver Foley catheters. Urological Research. 2009;37(2):89–93.

[89] Choong SKS, Hallson P, Whitfield HN, Fry CH. The physicochemical basis of urinary catheter encrustation. British Journal of Urology International International. 1999;83(7):770–775. Available from: https://doi.org/10.1046/j.1464-410x.1999.00014.x.

[90] Mathur S, Suller MTE, Stickler DJ, Feneley RCL. Prospective study of individuals with long-term urinary catheters colonized with Proteus species. British Journal of Urology International. 2006;97(1):121–128.

[91] Stickler DJ, Morgan SD. Modulation of crystalline Proteus mirabilis biofilm development on urinary catheters. Journal of Medical Microbiology. 2006;55(5):489–494. Available from: https://doi.org/10.1099/jmm.0.46404-0.

[92] Khan A, Housami F, Melotti R, Timoney A, Stickler D. Strategy to Control Catheter Encrustation With Citrated Drinks: A Randomized Crossover Study.

Journal of Urology. 2010;183(4):1390–1394. Available from: http://dx.doi.org/10.1016/j.juro.2009.12.024.

[93] Pappas E, Schaich KM. Phytochemicals of cranberries and cranberry products: Characterization, potential health effects, and processing stability. Critical Reviews in Food Science and Nutrition. 2009;49(9):741–781.

[94] Maki KC, Kaspar KL, Khoo C, Derrig LH, Schild AL, Gupta K. Consumption of a cranberry juice beverage lowered the number of clinical urinary tract infection episodes in women with a recent history of urinary tract infection. American Journal of Clinical Nutrition. 2016;103:1434–42.

[95] Thomas D, Rutman M, Cooper K, Abrams A, Finkelstein J, Chughtai B. Does cranberry have a role in catheter-Associated urinary tract infections? Canadian Urological Association Journal. 2017;11(11):E421–E424.

[96] Murray CJ, Ikuta KS, Sharara F, Swetschinski L, Robles Aguilar G, Gray A, et al. Global burden of bacterial antimicrobial resistance in 2019: a systematic analysis. The Lancet. 2022;399(10325):629–655.

[97] Munita JM, Arias CA. Mechanisms of antibiotic resistance. Microbiology Spectrum VMBF. 2016;4(2):1–24.

[98] Niël-Weise BS, Van Den Broek PJ. Urinary catheter policies for long-term bladder drainage. Cochrane Database of Systematic Reviews. 2012;1(8):1–36. Available from: https://doi.org/10.1002/14651858.CD004201.pub2.

[99] Rutschmann OT, Zwahlen A. Use of norfloxacin for prevention of symptomatic urinary tract infection in chronically catheterized patients. European Journal of Clinical Microbiology & Infectious Diseases. 1995;14(5):441–444.

[100] Mcosker CC, Fitzpatrick PM. Nitrofurantoin : mechanism of action and implications for resistance development in common uropathogens. Journal of Antimicrobial Chemotherapy. 1994;33(Suppl. A):23–30.

[101] Sandegren L, Lindqvist A, Kahlmeter G, Andersson DI. Nitrofurantoin resistance mechanism and fitness cost in Escherichia coli. Journal of Antimicrobial Chemotherapy. 2008;62:495–503.

[102] Brogden RN, Carmine AA, Heel RC, Speight TM, Avery GS. Trimethoprim : A Review of its Antibacterial Activity , Pharmacokinetics and Therapeutic Use in Urinary Tract Infections. Drugs. 1982;23:405–430.

[103] Huovinen P. Increases in Rates of Resistance to Trimethoprim. Clinical Infectious Diseases. 1997;24(Suppl 1):63–66.

[104] Weber DJ, Tolkoff-Rubin NE, Rubin RH. Amoxicillin and Potassium Clavulanate : An Antibiotic Combination and Adverse Effects. Pharmacotherapy. 1984;4:122–136.

[105] Suhani S, Purkaystha A, Begum MK, Islam J, Azad AK. Plasmids for Amoxicillin and Ciprofloxacin Resistance in Escherichia coli Isolate Causing Urinary Tract Infection Clinical Microbiology : Open Access. Clinical Microbiology. 2017;6(4).

[106] Dewar S, Reed LC, Koerner RJ. Emerging clinical role of pivmecillinam in the treatment of urinary tract infection in the context of multidrug-resistant bacteria. Journal of Antimicrobial Chemotherapy. 2014;69:303–308.

[107] National Center for Biotechnology Information. Cephalexin — C16H17N3O4S - PubChem; 2020. Available from: ttps://pubchem.ncbi.nlm.nih.gov/compound/Cephalexin.

[108] Manikandan S, Ganesapandian S, Singh M, Kumaraguru AK. Antimicrobial Susceptibility Pattern of Urinary Tract Infection Causing Human Pathogenic Bacteria. Asian Journal of Medical Sciences. 2011;3(2):56–60.

[109] Leflon-guibout V, Ternat G, Heym B, Nicolas-Chanoine MH. Exposure to co-amoxiclav as a risk factor for co-amoxiclav-resistant Escherichia coli urinary tract infection. Journal of Antimicrobial Chemotherapy. 2002;49:367–371.

[110] Wazait HD, Patel HRH, Veer V, Kelsey M, Meulen JHPVANDER, Miller RA, et al. Catheter-associated urinary tract infections : prevalence of uropathogens and pattern of antimicrobial resistance in a UK hospital (1996 – 2001). BJU International. 2003;91:806–809.

[111] Lebel M. Ciprofloxacin: Chemistry, Mechanism of Action, Resistance, Antimicrobial Spectrum, Pharmacokinetics, Clinical Trials, and Adverse Reactions. Pharmacotherapy. 1988;8(1):3–33.

[112] Gold B, Rodriguez WJ. Cefuroxime : Mechanisms of Action, Antimicrobial Activity, Clinical Applications, Adverse Reactions and Therapeutic Indications. Pharmacotherapy. 1983;3:82–100.

[113] Neu HC, Fu KP. Cefuroxime, a Beta-Lactamase-Resistant Cephalosporin with a

Broad Spectrum of Gram-Positive and -Negative Activity. Antimircobial, Agents and Chemiotherapy. 1978;13(4):657–664.

[114] Richards DM, Heel RC, Brogden RN, Speight TM, Avery G. Ceftriaxone A Review of its Antibacterial Activity, Pharmacological Properties and Therapeutic Use. Drugs. 1984;27:469–527.

[115] Krause KM, Serio AW, Kane TR, Connolly LE. Aminoglycosides : An Overview. Cold Spring Harbor Perspectives in Medicine. 2016;6:a027029.

[116] Kappaun K, Regina A, Regina C, Ligabue-braun R. Ureases: Historical aspects, catalytic, and non-catalytic properties – A review. Journal of Advanced Research. 2018;13:3–17. Available from: https://doi.org/10.1016/j.jare.2018.05.010.

[117] Burns JR, Gauthier JF. Prevention of Urinary Catheter Incrustations by Aacetohydroxamic Acid. The Journal of Urology. 1984;132(3):455–456. Available from: http://dx.doi.org/10.1016/S0022-5347(17)49689-3.

[118] Food and Drug Administration FDA. Approved Drug Products with Therapeutic Equivalence Evaluations. 40th ed. Food and Drug Administration FDA.; 2020. Available from: https://www.accessdata.fda.gov/scripts/cder/daf/index.cfm?event=overview.process{&}ApplNo=065110.

[119] Benini S, Rypniewski WR, Wilson KS, Miletti S, Ciurli S, Mangani S. The complex of Bacillus pasteurii urease with acetohydroxamate anion from X-ray data at 1.55 Å resolution. Journal of Biological Inorganic Chemistry. 2000;5(1):110–118. Available from: https://doi.org/10.1007/s007750050014.

[120] Griffith DP, Gleeson MJ, Lee H, Longuet R, Deman E, Earle N. Randomized, Double-blind Trial of Lithostat(TM) (Acetohydroxamic Acid) in the Palliative Treatment of Infection-Induced Urinary Calculi. European Urology. 1991;20(3):243–247.

[121] Zullo A, Hassan C, Morini S. Helicobacter pylori infection in patients with liver cirrhosis: Facts and fictions. Digestive and Liver Disease. 2003;35(3):197–205.

[122] Williams JJ, Rodman JS, Peterson CM. A Randomized Double-blind study of Acetohydroxamid acid in Struvite Nepholihiasis. The New England Journal of Medicine. 1974;311(12):760–764.

[123] National Center for Biotechnology Information PubChem Database. Aceto-

hydroxamic acid, CID=1990,; 2020. Available from: https://pubchem.ncbi.nlm.nih.gov/compound/1990{#}section=Pharmacology-and-Biochemistry.

[124] Wittebole X, De Roock S, Opal SM. A historical overview of bacteriophage therapy as an alternative to antibiotics for the treatment of bacterial pathogens. Virulence. 2014;5(1):226–235.

[125] Górski A, Borysowski J, Międzybrodzki R. Phage therapy: Towards a successful clinical trial. Antibiotics. 2020;9(11):1–7.

[126] Rice CJ, Kelly SA, O'brien SC, Melaugh EM, Ganacias JCB, Chai ZH, et al. Novel phage-derived depolymerase with activity against proteus mirabilis biofilms. Microorganisms. 2021;9(10).

[127] Eto DS, Jones TA, Sundsbak JL, Mulvey MA. Integrin-mediated host cell invasion by type 1-piliated uropathogenic Escherichia coli. PLoS Pathogens. 2007;3(7):0949–0961.

[128] Hadjifrangiskou M, Gu AP, Pinkner JS, Kostakioti M, Zhang EW, Greene SE, et al. Transposon mutagenesis identifies uropathogenic Escherichia coli biofilm factors. Journal of Bacteriology. 2012;194(22):6195–6205.

[129] Flores-mireles AL, Walker JN, Caparon M, Hultgren SJ. Urinary tract infections: epidemiology, mechanisms of infection and treatment options. Nature Reviews Microbiology. 2015;13(5):269–284.

[130] Cusumano CK, Pinkner JS, Han Z, Greene SE, Ford BA, Crowley JR, et al. Treatment and Prevention of Urinary Tract Infection with Orally Active FimH Inhibitors. Sci Transl Med. 2011;3(109):1–22.

[131] Fiori-Duarte AT, Rodrigues RP, Kitagawa RR, Kawano DF. Insights into the design of inhibitors of the urease enzyme - a major target for the treatment of Helicobacter pylori infections. Current Medicinal Chemistry. 2019;26:1–15.

[132] Berg J, Tymoczko J, Stryer L. Biochemistry. 8th ed. W H Freeman, New York; 2015.

[133] Hughes JP, Rees SS, Kalindjian SB, Philpott KL. Principles of early drug discovery. British Journal of Pharmacology. 2011;162(6):1239–1249.

[134] Lombardino JG, Lowe JA. The role of the medicinal chemist in drug discovery - Then and now. Nature Reviews Drug Discovery. 2004;3(10):853–862.

[135] Wouters OJ, McKee M, Luyten J. Estimated Research and Development Investment Needed to Bring a New Medicine to Market, 2009-2018. JAMA. 2020;323(9):844–853.

[136] Sliwoski G, Kothiwale S, Meiler J, Lowe EW. Computational Methods in Drug Discovery. Pharmacological Reviews. 2014;66(1):334–395.

[137] Yuriev E, Ramsland PA. Latest developments in molecular docking: 2010-2011 in review. Journal of Molecular Recognition. 2013;26(5):215–239.

[138] Lipinski CA, Lombardo F, Dominy BW, Feeney PJ. Experimental and computational approaches to estimate solubility and permeability in drug discovery and development settings. Advanced Drug Delivery Reviews. 1997;23:3–25.

[139] Sulimov VB, Kutov DC, Taschilova AS, Ilin IS, Tyrtyshnikov EE, Sulimov AV. Docking Paradigm in Drug Design. Current Topics in Medicinal Chemistry. 2020;21(6):507–546.

[140] Azizian H, Nabati F. Large-scale virtual screening for the identification of new Helicobacter pylori urease inhibitor scaffolds. J Mol Model. 2012;18:2917–2927.

[141] Moore K, Rees S. Cell-Based Verses Isolated Target Screening: How Lucky Do You Feel? Journal of Biomolecular Screening. 2001;6(2):69–74.

[142] Fotakis G, Timbrell JA. In vitro cytotoxicity assays: Comparison of LDH, neutral red, MTT and protein assay in hepatoma cell lines following exposure to cadmium chloride. Toxicology Letters. 2006;160(2):171–177.

[143] Amin K, Dannenfelser RM. In Vitro Hemolysis: Guidance for the Pharmaceutical Scientist. Journal of pharmaceutical sciences. 2006;95(6):1173–1176.

[144] Nzakizwanayo J, Pelling H, Milo S, Jones BV. An In Vitro Bladder Model for Studying Catheter-Assoicated Urinary Tract Infection and Asssoicated Analysis of Biofilms. Humana Press; 2019. Available from: https://link.springer.com/protocol/10.1007/978-1-4939-9601-8{_}14.

[145] Pawlik TM, Sosa JA, editors. Clinical trials. 2nd ed. Switzerland: Springer; 1989. Available from: https://acsjournals.onlinelibrary.wiley.com/doi/abs/10.1002/1097-0142{%}2819900915{%}2966{%}3A6{%}3C1091{%}3A{%}3AAID-CNCR2820660602{%}3E3.0.CO{%}3B2-F.

[146] Corpet F. Multiple sequence alignment with hierarchical clustering. Nucleic Acids Research. 1988;16(22):10881–10890.

[147] Robert X, Gouet P. Deciphering key features in protein structures with the new ENDscript server. Nucleic Acids Research. 2014;42(W1):320–324.

[148] Heimer SR, Mobley HLT. Interaction of Proteus mirabilis Urease Apoenzyme and Accessory Proteins Identified with Yeast Two-Hybrid Technology. Journal of Bacteriology. 2001;183(4):1423–1433.

[149] Jones BD, Mobley HLT. Proteus mirabilis Urease : Genetic Organization , Regulation , and Expression of Structural Genes. Journal of Bac. 1988;170(8):3342–3349.

[150] Yang W, Feng Q, Peng Z, Wang G. An overview on the synthetic urease inhibitors with structure-activity relationship and molecular docking. European Journal of Medicinal Chemistry. 2022;234:114273. Available from: https://doi.org/10.1016/j.ejmech.2022.114273.

[151] Ha Nc, Oh St, Sung JY, Cha KA, Lee MH, Oh Bh. Supramolecular assembly and acid resistance of Helicobacter pylori urease. Nature Structural Biology. 2001;8(6):505–509. Available from: https://www.nature.com/articles/nsb0601{_}505.

[152] Sumner JB. The isolation and crystallization of the enzyme urease. J Biol Chem. 1926;69:435–441. Available from: http://www.jbc.org/content/69/2/435.full.pdf+html.

[153] Mazzei L, Musiani F, Ciurli S. The Biological Chemistry of Nickel, Chapter 5, Urease. 10. Royal Society of Chemistry; 2017. Available from: https://doi.org/10.1039/9781788010580.

[154] Maroney MJ, Ciurli S. Nonredox Nickel Enzymes. Physiology & behavior. 2014;114(8):4206–4228.

[155] Cameron KC, Di HJ, Moir JL. Nitrogen losses from the soil/plant system: A review. Annals of Applied Biology. 2013;162(2):145–173. Available from: https://doi.org/10.1111/aab.12014.

[156] Watson CJ, Miller H, Poland P, Kilpatrick DJ, Allen MDB, Garrett MK, et al. Soil properties and the ability of the urease inhibitor N-(n-butyl) thiophosphoric triamide (nBTPT) to reduce ammonia volatilization from surface-applied urea.

Soil Biology and Biochemistry. 1994;26(9):1165–1171. Available from: https://doi.org/10.1016/0038-0717(94)90139-2.

[157] Cantarella H, Otto R, Soares JR, Silva AGdB. Agronomic efficiency of NBPT as a urease inhibitor: A review. Journal of Advanced Research. 2018;13:19–27. Available from: https://doi.org/10.1016/j.jare.2018.05.008.

[158] Rego YF, Queiroz MP, Brito TO, Carvalho PG, Queiroz VTD, Fátima ÂD, et al. A review on the development of urease inhibitors as antimicrobial agents against pathogenic bacteria. Journal of Advanced Research. 2018;13:69–100. Available from: https://doi.org/10.1016/j.jare.2018.05.003.

[159] Modolo LV, de Souza AX, Horta LP, Araujo DP, de Fátima Â. An overview on the potential of natural products as ureases inhibitors: A review. Journal of Advanced Research. 2015;6(1):35–44. Available from: https://doi.org/10.1016/j.jare.2014.09.001.

[160] Kafarski P, Talma M. Recent advances in design of new urease inhibitors: A review. Journal of Advanced Research. 2018;13:101–112. Available from: https://www.sciencedirect.com/science/article/pii/S2090123218300171.

[161] Kosikowska P, Berlicki Ł. Urease inhibitors as potential drugs for gastric and urinary tract infections: a patent review. Expert Opinion on Therapeutic Patents. 2011;21(6):945–957. Available from: https://doi.org/10.1517/13543776.2011.574615.

[162] Kistiakowsky GB, Shaw WHR. On the Mechanism of the Inhibition of Urease. Journal of the American Chemical Society. 1953;75(4):866–871. Available from: https://doi.org/10.1021/ja01100a030.

[163] National Center for Biotechnology Information. PubChem Compound Summary for CID 2723790, Thiourea.; 2020. Available from: https://pubchem.ncbi.nlm.nih.gov/compound/Thiourea.

[164] Saeed A, ur Rehman S, Channar PA, Larik FA, Abbas Q, Hassan M, et al. Long chain 1-acyl-3-arylthioureas as jack bean urease inhibitors, synthesis, kinetic mechanism and molecular docking studies. Journal of the Taiwan Institute of Chemical Engineers. 2017;77:54–63. Available from: http://dx.doi.org/10.1016/j.jtice.2017.04.044.

[165] Howell SF, Sumner JB. The Specific Effects of Buffers Upon Urease Activity.

Journal of Biological Chemistry. 1934;104(3):619–626. Available from: http://dx.doi.org/10.1016/S0021-9258(18)75737-2.

[166] Domínguez MJ, Sanmartín C, Font M, Palop JA, San Francisco S, Urrutia O, et al. Design, synthesis, and biological evaluation of phosphoramide derivatives as urease inhibitors. Journal of Agricultural and Food Chemistry. 2008;56(10):3721–3731. Available from: https://doi.org/10.1021/jf072901y.

[167] Macegoniuk K, Dziełak A, Mucha A, Berlicki Ł. Bis(aminomethyl)phosphinic acid, a highly promising scaffold for the development of bacterial urease inhibitors. ACS Medicinal Chemistry Letters. 2015;6(2):146–150. Available from: https://doi.org/10.1021/ml500380f.

[168] Maitra SK, Kumar Maitra S. Reproductive Toxicity of Organophosphate Pesticides. Annals of Clinical Toxicology. 2018;1(1):1004. Available from: https://www.remedypublications.com/open-access/reproductive-toxicity-of-organophosphate-pesticides-1072.pdf.

[169] Pereira Araujo D, Santos Morais VS, De Fátima Â, Modolo LV. Efficient sodium bisulfite-catalyzed synthesis of benzothiazoles and their potential as ureases inhibitors. RSC Advances. 2015;5(36):28814–28821. Available from: https://doi.org/10.1039/C5RA01081K.

[170] Lodhi MA, Shams S, Khan KM. Thiazolidine Esters: New Potent Urease Inhibitors. Journal Chemical Society Pakistan. 2014;36(5):858–864. Available from: https://jcsp.org.pk/PublishedVersion/1b76c1dd-0243-4eb9-917a-577412e4b28dManuscriptno12,FinalGallyProofof9914{_}SulaimanShams{_}.pdf.

[171] Harvey AL, Edrada-Ebel R, Quinn RJ. The re-emergence of natural products for drug discovery in the genomics era. Nature Reviews Drug Discovery. 2015;14(2):111–129. Available from: https://www.nature.com/articles/nrd4510.

[172] Olech Z, Zaborska W, Kot M. Jack bean urease inhibition by crude juices of Allium and Brassica plants. Determination of thiosulfinates. Food Chemistry. 2014;145:154–160. Available from: http://dx.doi.org/10.1016/j.foodchem.2013.08.044.

[173] Bremner JM, Douglas LA. Inhibition of urease activity in soils. Soil Biology and Biochemistry. 1971;3(4):297–307.

[174] Krajewska B, Zaborska W. Double mode of inhibition-inducing interactions of 1,4-naphthoquinone with urease: Arylation versus oxidation of enzyme thiols. Bioorganic and Medicinal Chemistry. 2007;15(12):4144–4151. Available from: https://doi.org/10.1016/j.bmc.2007.03.071.

[175] Xiao ZP, Wang XD, Peng ZY, Huang S, Yang P, Li QS, et al. Molecular Docking, Kinetics Study, and Structure-Activity Relationship Analysis of Quercetin and Its Analogous as Helicobacter pylori Urease Inhibitors. Journal of Agricultural and Food Chemistry. 2012;60(42):10572–10577. Available from: https://pubs.acs.org/doi/pdf/10.1021/jf303393n.

[176] Xiao ZP, Peng ZY, Dong JJ, He J, Ouyang H, Feng YT, et al. Synthesis, structure-activity relationship analysis and kinetics study of reductive derivatives of flavonoids as Helicobacter pylori urease inhibitors. European Journal of Medicinal Chemistry. 2013;63:685–695. Available from: http://dx.doi.org/10.1016/j.ejmech.2013.03.016.

[177] Macegoniuk K, Kowalczyk R, Rudzińska A, Psurski M, Wietrzyk J, Berlicki Ł. Potent covalent inhibitors of bacterial urease identified by activity-reactivity profiling. Bioorganic and Medicinal Chemistry Letters. 2017;27(6):1346–1350. Available from: https://doi.org/10.1016/j.bmcl.2017.02.022.

[178] Milo S, Heylen RA, Glancy J, Williams GT, Patenall BL, Hathaway HJ, et al. A small-molecular inhibitor against Proteus mirabilis urease to treat catheter-associated urinary tract infections. Scientific Reports. 2021 dec;11(1):3726. Available from: http://www.nature.com/articles/s41598-021-83257-2.

[179] Carson L, Cathcart GR, Scott CJ, Hollenberg MD, Walker B, Ceri H, et al. Comprehensive inhibitor profiling of the Proteus mirabilis metalloprotease virulence factor ZapA (mirabilysin). Biochimie. 2011;93(10):1824–1827. Available from: http://dx.doi.org/10.1016/j.biochi.2011.06.030.

[180] Mclean RJC, Cheng KJ, Gould WD, Nickel JC, Costerton WJ. Histochemical and biochemical urease localization in the periplasm and outer membrane of two Proteus mirabilis strains. Canadian Journal of Microbiology. 1986;32(10):772–778. Available from: https://doi.org/10.1139/m86-142.

[181] Anselmo AC, Mitragotri S. An overview of clinical and commercial impact of drug delivery systems. Journal of Controlled Release. 2014;190:15–28. Available from: http://dx.doi.org/10.1016/j.jconrel.2014.03.053.

[182] Zacchè MM, Srikrishna S, Cardozo L. Novel targeted bladder drug-delivery systems: A review. Research and Reports in Urology. 2015;7:169–178. Available from: https://www.ncbi.nlm.nih.gov/pmc/articles/PMC4664547/.

[183] Alm M, Langer S. A method of producing a delivery device (patent). European Patent Office; 2012. Available from: http://repositorio.unan.edu.ni/2986/1/5624.pdf.

[184] Stærk K, Grønnemose RB, Palarasah Y, Kolmos HJ, Lund L, Alm M, et al. A Novel Device-Integrated Drug Delivery System for Local Inhibition of Urinary Tract Infection. Frontiers in Microbiology. 2021 jun;12(June):1–14. Available from: https://www.frontiersin.org/articles/10.3389/fmicb.2021.685698/full.

[185] Stærk K, Hjelmager JS, Alm M, Thomsen P, Andersen TE. A new catheter-integrated drug-delivery system for controlled intravesical mitomycin C release. Urologic Oncology: Seminars and Original Investigations. 2022;40(9):409.e19–409.e26. Available from: https://doi.org/10.1016/j.urolonc.2022.05.022.

Chapter 2

General Materials and Methods

2.1 Materials

Uropathogenic bacterial species: *P. mirabilis* B4 and *E. coli* NSM59 were obtained from the Jenkins Group collection, University of Bath.

The following materials were purchased form Merck, Germany: acetic acid; acetone; AHA; ammonium chloride; anhydrous sodium sulphate; calcium chloride; dimethyl sulfoxide (DMSO); disodium hydrogen phosphate heptahydrate; DNA extraction kit; ethylenediaminetetraacetic acid (EDTA); gelatine; isopropanol; lactose; magnesium chloride hexahydrate; nuclease-free water; phenethyl isothiocyanate (PE-ITC); phenol; potassium chloride; potassium di-hydrogen orthophosphate; sodium acetate; sodium chloride; sodium dihydrogen phosphate; sodium fluorescein; sodium hypochlorite; sodium hydroxide; sodium nitroprusside; sodium oxalate; triethyl citrate; tris base; trisodium citrate; urea; urease from *C. ensiformis*.

The following were purchased from Thermo Fisher Scientific, USA: 16S rRNA universal primers Table 4.1; ammonia hydroxide (FisherScientific); bacteriological agar; Columbia blood agar (CBA) (5% sheep blood); Cysteine-Lactose-Electrolyte Deficient (CLED) agar; Dulbecco's Eagle Medium complete (DMEM) (Gibco); glycerol; Luria-Bertani (LB) agar; LB broth; MaConkey (MC) agar; Müller Hinton (MH) agar; minimum essential media (MEM) (Gibco); MTT (Invitrogen); Phosphate buffer saline (PBS) (FisherScientific); PHUSION high-fidelity enzyme mix; triton X-100 (FisherScientific); trypsin (Gibco); tryptone; tryptone soya broth (TSB); yeast extract;

Firmapress, purchased from LFA Machines LTD, UK. Talcum powder, purchased from Johnson and Johnson, USA. Eudragit S100, kindly gifted from Evoniks, Germany. CHROMID agar plates, purchased from bioMérieu, UK. Polmerase chain reaction (PCR) tubes, purchased from Greiner. Wizard SV Gel and PCR Clean-up System, purchased from Promega. *N,N'*-Bis(3-pyridinylmethyl)thiourea (BisTU), purchased from Fluorochem, UK.

2.2 Methods

2.2.1 Bacterial growth

Throughout any bacterial experimentation aseptic techniques were used, all work was conducted within a Grade II laminar flow hood. All buffers, broths, and agar are sterilized in an autoclave at 121 °C, under pressurized steam for 30 min prior to use. The stages of bacterial growth are described in Figure 2-1, the growth of bacteria can be monitored by measuring the OD_{600} for growth in liquid culture, this measures the scat-

tering of light which correlates with the cell density. Lag phase is where the bacterial cells are synthesizing DNA replication enzymes and preparing for cell replication (Fig. 2-1A). Next the logarithmic phase takes place where the bacterial cells are replicating logarithmically (Fig. 2-1B). The stationary phase occurs when the media and nutrients have become depleted, the rate of growth of new cells matches the rate of cell death (Fig. 2-1C). Once all of the nutrients have been used up and the quantity of inhibitory waste products have increased, the cells begin to die (Fig. 2-1D).

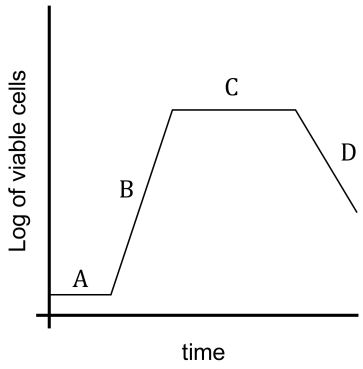

Figure 2-1: Typical bacterial growth curve (A) Lag phase, (B) Logarithmic phase, (C) Stationary Phase, and (D) Death phase. Graph drawn on GraphPad Prism v. 9.5.0.

Bacteria are stored at -80 °C in a freezer stock solution which consists of LB broth with 15% glycerol. Bacterial freezer stocks are streaked onto solid agar plates; for *E. coli* a LB agar plate (20 g/L in deionised water) is used, whilst for *P. mirabilis* a non-swarming LB plate (NSLB) is used, Table 2.1 describes the components in NSLB plates. NSLB plates are required to prevent *P. mirabilis* swarming, as described in Section 1.2.3. Plates are grown statically at 37 °C overnight.

Table 2.1: Components for non-swarming Luria-Bertani (NSLB) agar

NSLB components	**Mass (g/L)**
Tryptone	10
Yeast extract	5
Bacteriological agar	15

To generate a liquid culture, 10 mL of LB broth (25 g/L) was inoculated with a single colony from an agar plate. Broth was grown at 37 °C for 18 h with agitation (200 rpm). The overnight cultures are centrifuged (3100 *g*, 10 min, at 4 °C, 5810 R Eppendorf), the

supernatant is discarded and the pellet of cells re-suspended in PBS (1 tablet dissolved in 200 mL of deionised water).

2.2.1.1 Bacterial Quantification

Bacteria were quantified using the Miles and Misra technique.[1] Serial dilutions, 10-fold, to 10^{-8} of bacteria were prepared using PBS and vortexed; onto a solid agar plate 3 drops of each dilution (10 μL) were placed and allowed to dry. Plates were incubated at 37 °C overnight, the section containing between 3-30 colonies were counted and the CFU/mL was determined using equation 2.1.

$$CFU/mL = \frac{average\ number\ of\ colonies}{d \times V} \tag{2.1}$$
$$d = dilution\ factor, V = volume$$

2.2.2 Minimum Inhibitory Concentration (MIC) assay

An overnight culture of bacteria was grown up as described in Section 2.2.1, it was diluted to a concentration of 1×10^6 CFU/mL. Twice the maximum concentration to be tested of the compound is prepared in LB. To the first column of a 96-well plate (Corning, UK), 200 μL of the compound is added. It is serially diluted (2-fold) across the plate to column 10. The subculture of bacteria is added to first 10 columns (100 μL). LB broth is only added to column 11 (200 μL) negative control and to column 12 just the subculture of bacteria is added (200 μL), the positive control. Each column contains three biological repeats and two technical repeats per biological. The plate is incubated for 18 h at 37 °C. Using a spectrometer (SPECTROstar Omega BMG LabTech, Germany) the growth of the bacteria is monitored at an OD600 at regular timepoints. The plate is shaken at 200 rpm for 10 s prior to readings being taken. MIC is defined as the lowest concentration of compound which permits bacterial growth. Initially, the MIC is determined visually by assessing the turbidity and then also by examination of the growth curves measured at OD_{600}.

2.2.3 *In vitro* bladder models

Physiological bladder models were initially described by Stickler *et al.*[2] A detailed description of set-up and preparation of the bladder model is explained by Nzakizwanayo *et al.*[3] Artificial urine (AU) is prepared according to Nzakizwanayo *et al.*,[3] and is described in Table 2.2 & 2.3.

Table 2.2: Part 1: components 5x artificial urine, dissolved in 1 L of deionised water and autoclaved.

Components	Mass (g)
Anhydrous sodium sulphate	11.50
Magnesium chloride hexahydrate	3.25
Sodium chloride	23.00
Tri-sodium citrate	3.25
Sodium oxalate	0.10
Potassium di-hydrogen orthophosphate	14.00
Potassium chloride	8.00
Ammonium chloride	5.00
Gelatine	25.00
Tryptone soya broth	5.00

The pH was adjusted to pH = 5.7 by the addition of sodium hydroxide.

Table 2.3: Part 2: components 5x artificial urine, dissolved in 400 mL of deionised water.

Components	Mass (g)
Urea	125.00
Calcium chloride	2.45

To dissolve the urea in part 2, the solution is stirred and warmed to approximately 40 °C. Sterilization of part 2 is achieved by filtration through a 0.22 μm syringe filter (Millipore, UK). Part 1 AU and Part 2 AU are combined with 3.6 L of deionised water. The pH of the final solution is checked and adjusted to 6.1 prior to use.

To setup the *in vitro* bladder models all the tubing and bladders were autoclaved. An outline of the bladder and tubing set up is shown in Figure 2-2. A water bath set to 37 °C is connected to the bladder to maintain a temperature of 37 °C within. Size 14, silicone catheters (Dahlhausen, Germany)(unless otherwise stated) are inserted aseptically into the bladder, the balloon is inflated with 10 mL of sterile water (unless otherwise stated) and connected to a drainage bag. A peristaltic pump (Ismatec ISM1077A/Watson-Marlow, 323S/D) is used to deliver AU from the 'kidney', (5 L glass Duran with bottom side arm outlet) to the bladder, it is calibrated to deliver a flow rate of 0.5-1.0 mL/min.

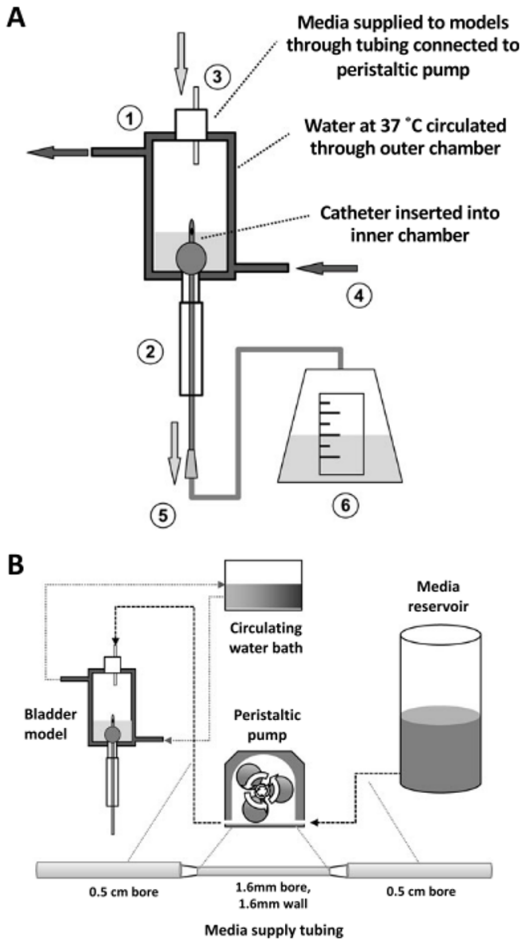

Figure 2-2: Diagram of the *in vitro* bladder model. A. (1) glass bladder, (2) Foley catheter, (3) sterile artificial urine, (4) water jacket, (5) catheter connected to drainage bag, (6) drinage bag. B. overall tubing size and connections. Reprinted with permission from Springer Nature [3].

Bladders were inoculated with the desired level of infection; in late-stage models this was 10^8 CFU/mL. After inoculations the bladders were incubated for 1 h before the peristaltic pump is started. Throughout the experiment, samples are removed to monitor the models. Variables measured are: time to block, pH of urine in drainage bag or in bladder, and quantity of bacteria with drainage bag or in bladder. Time-lapse photography was set up using a Nikon D3100 camera, which took a photograph every 2 min. The photographs were compiled into time-lapse videos and used to monitor the models overnight.

2.2.4 *In silico* Docking and Screen Design

In silico docking was used to predict the binding of ligands against the crystal structure of urease. Two different structures of urease were used, owing to difference in applications. The crystal structure of urease from *Sporosarcina pasteurii* (*S. pasteurii*) (Protein Data Bank (PDB): 4UBP) (formally known as *Bacillus pasteurii*) and *Helicobacter pylori* (*H. pylori*) (PDB: 1E9Y).[4,5] Both of these structures have a high resolution of 1.55 Å and 2.8 Å respectively, a high resolution is important for *in silico* docking because it allows ligands to be docked to a higher accuracy; therefore, the results are more likely to be accurate predictions. The ligands were designed to target *P. mirabilis*, unfortunately, a crystal structure of *P. mirabilis* urease does not exist; however, the sequences between bacterial ureases are well conserved and the active sites are identical (Figure 1-11). Ligand docking was completed using Cresset® Flare™ 4.0.2 (Revision: 40719, Cresset, Litlington, Cambridgeshire, UK).[6,7,8] The software was used to prepare the crystal structure and complete the docking using the 'accurate but slow' setting. Ligand structures were prepared using ChemDraw 19.1.1.21 (PerkinElmer Informatics, Waltham, Massachusetts, US). For ligands which were docked covalently, the target amino acid was identified prior to docking. A grid box was designed 10 Å around Ni 6057 (C Ni 798) found in the active site of the enzyme. For compounds which were larger or had predicted alternative docking site the grid box was altered. The quality of ligand docking was assessed using the Lead Finder (LF) dG score, this has been optimized for protein-ligand binding energy, $\triangle$G, which assumes the pose of the compound is correct. The more negative the score, the better the binding. Ligands were also assessed visually, examining contacts made with urease, those within 3.5 Å were counted.

For urease docking from *S. pasteurii* the quality of the docking experiment was checked by removing the crystallised structure of AHA and re-docking AHA back onto urease. These are called control docking experiments, the root mean square deviation (RMSD) of the computationally docked AHA is compared to the crystallised AHA. A RMSD of $<$2 Å is considered a 'well-docked' ligand and predicts that the docking experiment would accurately dock ligands.[9] Control docking experiment for AHA gave a calculated RMSD of 0.997 Å indicating that the crystal was prepared correctly, and the software is working as expected (Figure 2-3a). The RMSD experiment could not be repeated using *H. pylori* urease because despite the published paper describing that the enzyme was crystallised with AHA, the PDB structure did not show AHA in the active site; therefore, the direct comparison could not be made. However, visually the docked AHA appeared to dock as expected in to the active site (Figure 2-3b).

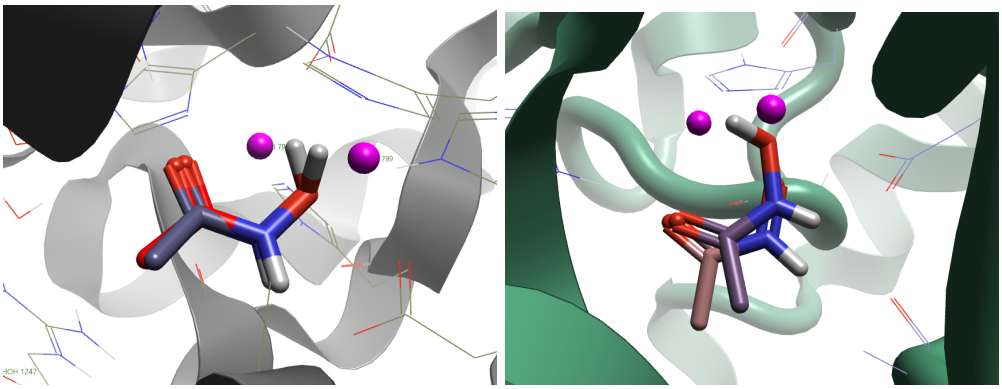

(a) Computationally docked acetohydroxamic acid (AHA) (top) compared to crystallized AHA (bottom) in *Sporosarcina pasteurii* urease.[4]

(b) Computationally docked AHA (top) compared to crystallised nitrosocaronylmethane (bottom) in *Helicobacter pylori* urease.[5]

Figure 2-3: Comparing AHA and crystallised compounds in the active site of urease. Image generated using Flare™ from Cresset®.

2.2.4.1 Comparing crystal structures of Urease

The following crystal structures were overlaid using Cresset® Flare™: *H. pylori* (PDB: 1E9Y), *S. pasteurii* (PDB: 4UBP), and *Klebisella aerogenes* (*K. aerogenes*) (PDB 1FEW).[5,4,10]

2.2.5 *In vitro* Urease Activity Assay

The assay used to measure urease activity is called the Berthelot reaction.[11,12] The assay measures the accumulation of ammonia over time, the reaction mechanism is shown in Figure 2-4. The amount of ammonia produced is proportional to the amount of blue indophenol, the accumulation of indophenol is measured using an spectrometer (SPECTROstar Omega BMG LabTech, Germany) at an wavelength of 636 nm. Sodium nitroprusside acts as a catalyst for the reaction. Solutions are prepared according to Table 2.4.

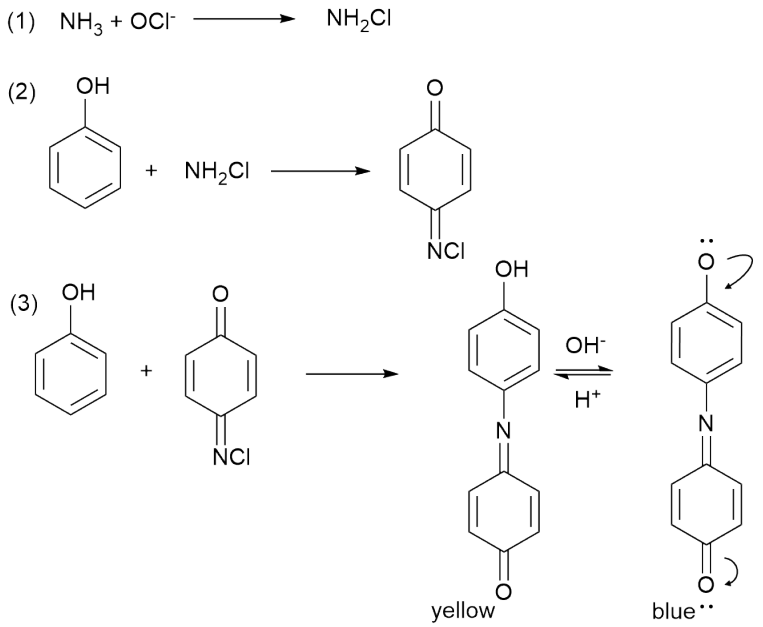

Figure 2-4: (1) Hypochlorite reacts with ammonia forming monochloramine. (2) Phenol from Solution A (Table 2.4) reacts with monochloramine forming benzoquinone chlorimine. (3) Benzoquione chlorimine reacts with phenol to produce indophenol, which in a basic pH (caused by Solution B (Table 2.4)) and turns blue.[12]

Table 2.4: Solutions for preparation: Berthelot assay

Solution	**Composition**
0.004 mg/mL urease in 0.1 M $NaPO_4$, pH 7.4	Sodium dihydrogen phosphate (0.0246 M) and disodium hydrogen phosphate heptahydrate (0.0754 M)
Urea buffer: 0.1 M $NaPO_4$, 0.05 M urea, pH 7.4	Sodium dihydrogen phosphate (0.0246 M), disodium hydrogen phosphate heptahydrate (0.0754 M) and 0.05 M urea
Solution A (106 mM phenol, 191 μM sodium nitroprusside)	Phenol (0.5 g), solution C (5 mL), make up to 50 mL with deionised water
Solution B (125 mM sodium hydroxide and sodium hypochlorite)	Sodium hydroxide (50 mg), sodium hypochlorite (410 μL), make up to 50 mL in deionised water
Solution C	Sodium nitroprusside (25 mg) in 50 mL deionised water.

2.2.5.1 Preparation of Compounds and *N. officinale* extract

Compounds were purchased in powder form and stored at -20 °C. A 1 M solution was made in 100% DMSO which was then diluted down to the desired concentration of 10 mM. *N. officinale* extract was kindly prepared and donated by the Watercress Research Ltd. *N. officinale* extract is an aqueous extract prepared by blending the WC, followed by a filtration step which removes the extract from the pulp. The extract is initially filtered through a cheesecloth and then finally through a 0.2 μm filter which also removes any bacteria present.

2.2.5.2 Urease Activity assay with *C. ensiformis* urease

Purified urease taken from *C. ensiformis* (Jack Bean plant) is used to assess urease activity over time or in the presence of inhibitors. Into each well of a 96-well plate (Corning, UK) 10 μL of 0.5% sulfuric acid is added. *C. ensiformis* urease in 0.1 M sodium phosphate, pH 7.4, is incubated with desired compound (at different concentrations) or control (just PBS) and urea for 30 min at 37 °C. Post-incubation, 20 μL is removed and added to the 96-well plate (including two technical repeats). Each incubation is repeated in triplicate (biological repeats). To each well, 20 μL of 60 mM sodium hydroxide is added. Then 50 μL of Solution A and 50 μL of Solution B. The plate is incubated, whilst covered in foil for 30 min at 37 °C. The absorbance is read at 636 nm. For measurements over time, during incubation samples are removed and added to the 96-well plate at regular time points. Urease activity was calculated according to equation 2.2.

$$Urease\ activity\ \% = \frac{(test\ well - negative\ control)}{(positive\ control - negative\ control)} \times 100 \tag{2.2}$$

2.2.5.3 Urease Activity assay with whole-cell *P. mirabilis*

An overnight culture of *P. mirabilis* is prepared according to Section 2.2.1. The culture was centrifuged, 3100 *g*, 10 min, 4 °C (5810 R Eppendorf) and the supernatant was discarded. The pellet was re-suspended in PBS. The assay was prepared as described in Section 2.2.5.2, with the culture replacing the *C. ensiformis* urease.

2.3 Bibliography

[1] Miles AA, Misra SS, Irwin JO. The estimation of the bactericidal power of the blood. Journal of Hygiene. 1938;38(6):732–749. Available from: https://www.ncbi.nlm.nih.gov/pmc/articles/PMC2199673/.

[2] Stickler DJ, Morris NS, C W. Simple Physical Model to Study Formation and Physiology of Biofilms on Urethral Catheters. Methods in Enzymology. 1999;310:494–501. Available from: https://doi.org/10.1016/S0076-6879(99)10037-5.

[3] Nzakizwanayo J, Pelling H, Milo S, Jones BV. An In Vitro Bladder Model for Studying Catheter-Assoicated Urinary Tract Infection and Asssoicated Analysis of Biofilms. Humana Press; 2019. Available from: https://link.springer.com/protocol/10.1007/978-1-4939-9601-8{_}14.

[4] Benini S, Rypniewski WR, Wilson KS, Miletti S, Ciurli S, Mangani S. The complex of Bacillus pasteurii urease with acetohydroxamate anion from X-ray data at 1.55 Å resolution. Journal of Biological Inorganic Chemistry. 2000;5(1):110–118. Available from: https://doi.org/10.1007/s007750050014.

[5] Ha Nc, Oh St, Sung JY, Cha KA, Lee MH, Oh Bh. Supramolecular assembly and acid resistance of Helicobacter pylori urease. Nature Structural Biology. 2001;8(6):505–509. Available from: https://www.nature.com/articles/nsb0601{_}505.

[6] Cheeseright T, Mackey M, Rose S, Vinter A. Molecular Field Extreme as Descriptors of Biological Activity: Definition and Validation. Journal of Chemical Information and Modeling. 2006;46(2):665–676. Available from: https://doi.org/10.1021/ci050357s.

[7] Bauer MR, Mackey MD. Electrostatic Complementarity as a Fast and Effective Tool to Optimize Binding and Selectivity of Protein-Ligand Complexes. Journal of Medicinal Chemistry. 2019;62(6):3036–3050. Available from: https://doi.org/10.1021/acs.jmedchem.8b01925.

[8] Kuhn M, Firth-Clark S, Tosco P, Mey ASJS, MacKey M, Michel J. Assessment of Binding Affinity via Alchemical Free-Energy Calculations. Journal of Chemical Information and Modeling. 2020;60(6):3120–3130. Available from: https://doi.org/10.1021/acs.jcim.0c00165.

[9] Gohlke H, Hendlich M, Klebe G. Predicting binding modes , binding affinities

and ‘ hot spots ’ for protein-ligand complexes using a knowledge-based scoring function. Perspectives in Drug Discovery and Design. 2000;20:115–144. Available from: https://doi.org/10.1023/A:1008781006867.

[10] Pearson MA, Michel LO, Hausinger RP, Karplus PA. Structures of Cys319 variants and acetohydroxamate-inhibited Klebsiella aerogenes urease. Biochemistry. 1997;36(26):8164–8172. Available from: https://pubs.acs.org/doi/10.1021/bi970514j.

[11] Weatherburn MW. Phenol-Hypochlorite Reaction for Determination of Ammonia. Analytical Chemistry. 1967;39(8):971–974. Available from: https://doi.org/10.1021/ac60252a045.

[12] Searle PL. The Berthelot or Indophenol Reaction and Its Use in the Analytical Chemistry of Nitrogen. Analyst. 1984;109:549–568. Available from: https://doi.org/10.1039/AN9840900549.

Chapter 3

Optimisation of a Lozenge-based Sensor for Detecting Impending Blockage of Urinary Catheters

3.1 Chapter Overview

This Chapter researches the optimisation of the lozenge sensor, initially developed by Milo *et al.,* for patient use and manufacture.[1]

3.2 Introduction

The lozenge technology is introduced in Section 1.3.1. As discussed in Section 1.2.2, catheter blockage can cause serious clinical consequences such as: kidney infections, kidney stones, and urosepsis.[2] Currently, there is no diagnostic device in clinical use which detects impending catheter blockage. Diagnostic dipsticks may be used between catheter changes; however, this requires high patient/carer compliance and is not routine in the UK. Stickler *et al.,* developed a bromothymol blue indicator (Section 1.3.2), although it did not make it into clinical use owing to poor diagnostic specificity.[3] The bromothymol blue sensor detected the change in pH of the urine due to urease activity (Section 1.2.1). The basis of the lozenge is the same however, instead of detecting change in pH using an indicator; a pH sensitive polymer is used to detect the pH change. Eudragit S100 breaks down at pH >7, this polymer was used to coat the hydrogel sensors developed by Milo *et al.*[1] Figure 3-1 shows a schematic of the lozenge function.

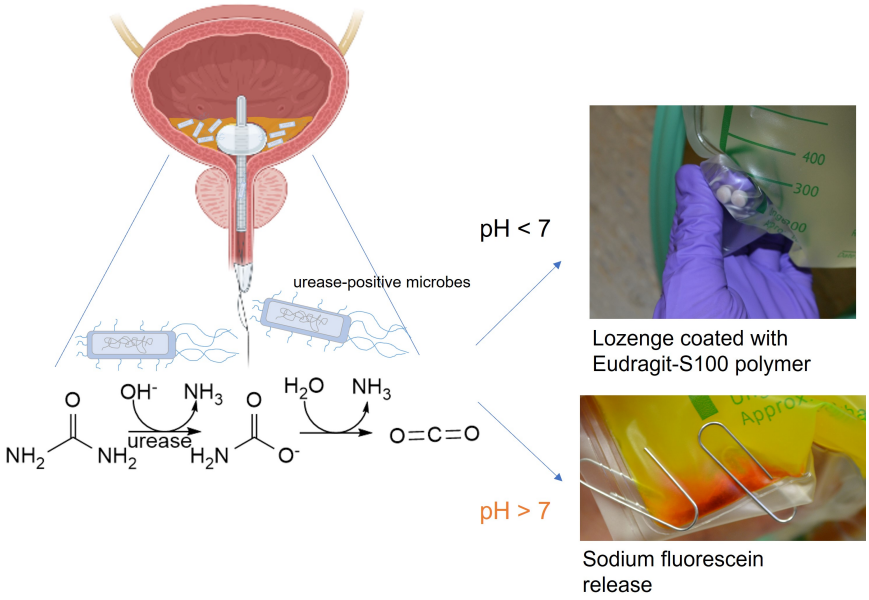

Figure 3-1: Schematic of the diagnostic lozenge. Urease-positive bacteria, such as: *Proteus mirabilis* cause an increase in pH within the bladder. The urine within the drainage bag increases causing the lozenge to release sodium fluorescein into the drainage bag.

3.3 Methods

General methods are described in Chapter 2. The following methods are specific to this Chapter.

3.3.1 Manufacture of Lozenge

The lozenge was initially designed as a poly(vinyl-alcohol) (PVA) hydrogel impregnated with 5(6)carboxyfluroescein (CF) coated in a Eudragit S100 polymer, however this was fragile and difficult to coat.[1] Therefore, the centre of the lozenge was changed from a hydrogel to a tablet, Table 3.1, describes the composition and optimisation of the tablet mixtures. Additionally, CF was changed to sodium fluorescein (SF). Firmapress is a packing solution used to form the tablets, it consists of: microcrystalline cellulose, magnesium stearate, silica di-oxide, and di-calcium phosphate. Lactose and talcum powder were added to the mixture to improve the manufacture of the tablets. Tablets were manufactured on a hand-held TDP 0 Desktop Tablet Press (LFA Machines Ltd. UK)(Fig. 3-2).

Table 3.1: Tablet manufacture, composition of tablet batches

Batch	**Sodium fluorescein (% (w/w))**	**Firmapress (% (w/w))**	**Talcum powder (% (w/w))**	**Lactose (% (w/w))**
1	20	80	-	-
2	20	75	5	-
3	20	65	5	10
4	20	45	5	30

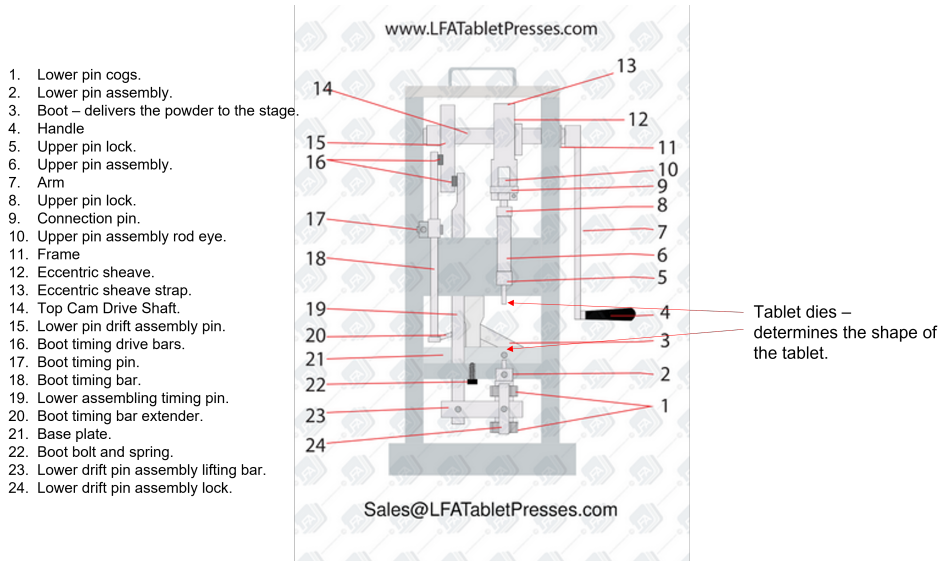

Figure 3-2: Diagram of the tablet press containing the labels for each of the parts. Adapted from diagram taken from the LFA website.

3.3.1.1 Preparation of Eudragit S100

Eudragit S100 is a pH sensitive polymer (Fig. **??**), preparation is described in Table 3.2.[4] The Eudragit S100 was added to half the solution mix until it had dissolved, ∼60 min. Talcum powder and triethyl citrate were added to the other half of the solution. The total solution was stirred with a high shear mixer, e.g. a vortex; for 10 min. The two solutions were combined with constant stirring. The talc was removed by vacuum filtration and solution stored at room temperature.

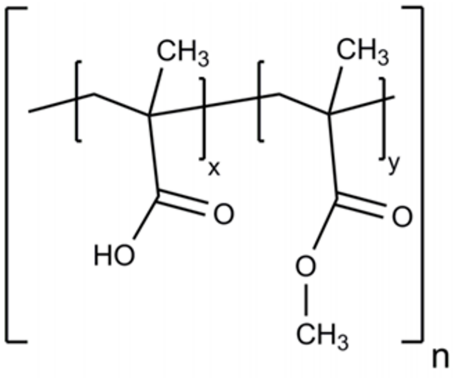

Figure 3-3: Chemical structure of Eudragit S100.

Table 3.2: Composition of Eudragit S100 solution

Component	Mass /g	Volume /mL
Eudragit S100	15.6	-
Triethyl citrate	1.6	-
Talc	7.8	-
Acetone	-	108.6
Isopropanol	-	163.6
Deionised water	-	10.8

3.3.1.2 Dip-Coating of Lozenge

The tablets were pressed using the ingredients described in Section 3.3.1. During the pressing process thin cotton thread was placed on top of the tablet mix when the dies (the two pieces of metal which compress the tablet mix and determine the shape of the tablet) compress the thread was secured within the tablet. This allowed the tablet to be hung. Tablets were dipped 60 times into Eudragit S100 (Table 3.2). Between each dip the tablets were allowed to dry for 5 min.

3.3.1.3 Drum-Coating of Lozenge

The lozenges were drum-coated by Nina Hauschildt from Evonik, Germany. She carried out the coating procedure using Eudragit S100 polymer and the following quantity of coating assessment. Drum-coating is a manufacturing process routinely used in coating tablets, the tablets are rotated in a drum whilst the polymer coating is sprayed onto them, the drum is cooled so that the polymer coating dries quickly, a uniform coating is provided, and the tablets do not stick together. The quantity of coating for each tablet was 10 mg/cm^2. A total of 250 g of tablets were drum-coated producing a lozenge with a diameter of 7 mm.

3.3.2 Testing the Lozenge

3.3.2.1 Functionality testing of SF release

To test the functionality of the lozenge releasing SF, different pH buffers were prepared, as detailed in Table 3.3. The pH of the buffers was checked and adjusted if necessary to desired pH $\pm$0.1. Calibration curves were prepared using measured masses of SF were dissolved in 10 mL of buffer (Table 3.3). Into a black 96-well plate (Corning, UK), 200 μL of SF solution was added to three wells to achieve three technical repeats and the fluorescence was measured (excitation and emission wavelengths: 485 nm and 520

nm respectively) (SPECTROstar Omega BMG LabTec, Germany). The procedure was repeated a further two times to achieve three repeats.

Table 3.3: Buffer components for functionality testing.

Buffer	Formulated buffer components
pH 5.0	0.1 M sodium acetate: sodium acetate (0.0673 M) and acetic acid (0.0343 M).
pH 6.0	0.1 M sodium phosphate buffer: sodium dihydrogen phosphate (0.0863 M) and disodium hydrogen phosphate heptahydrate (0.0137 M).
pH 7.5	0.1 M sodium phosphate: sodium dihydrogen phosphate (0.0754 M) and disodium hydrogen phosphate heptahydrate (0.0246 M).
pH 8.0	0.1 M tris base: tris base (0.099 M).

To measure the release of SF, a lozenge was placed in 10 mL of buffers at different pHs (Table 3.3), pH 5 and 6 buffers represent healthy urine, whilst those at pH 7.5 and 8 represent urine infected with *P. mirabilis*. Lozenges were shaken, to represent the movement of a drainage bag attached to the leg. Fluorescence was measured at 30 min intervals for the first 3 h and then at hourly intervals. Aliquots of 200 μL were removed for measurements and returned after so the total volume remained the same. Unless the sample required a dilution step, in which case only 10 μL was removed. The quantity of SF released was determined using the calibration curves.

3.3.2.2 Functionality testing using *P. mirabilis*

Overnight cultures of *P. mirabilis* were prepared as described in Section 2.2.1 and AU was prepared as described in Section 2.2.3. An overnight culture grows $\sim 7.2 \times 10^9$ CFU/mL, this was diluted with AU to $1{\times}10^7$ CFU/mL. The lozenge was added to the cultures and regular measurements of pH were taken every hour. An additional sample was taken for bacterial quantification (Section 2.2.1.1). The release of SF from the lozenge was observed visually and photographs were taken. Three biological repeats were completed, from each overnight two separate dilutions were prepared one to measure pH and the other for bacterial quantification, this prevented contamination from the pH probe.

3.3.2.3 Testing the lozenge in *in vitro* bladder models

In vitro bladder models were set up as described in Section 2.2.3. A lozenge was placed in each drainage bag. Each bladder was inoculated with either $1{\times}10^8$ CFU/mL

of *P. mirabilis* B4 (urease-positive), *E. coli* NSM59 (urease negative), or no bacteria (control). Throughout the experiment, samples were removed from the drainage bag and the pH and quantity of bacteria were measured. Time lapse photography (details in Section 2.2.3) was used to visually determine when the lozenge released.

3.3.2.4 Stability of the lozenge

The stability of the lozenge was assessed in the *in vitro* bladder model experiments described in Section 3.3.2.3. Any lozenge which released within the *E. coli* or control, or released earlier than other biological repeats in the *P. mirabilis* drainage bag was considered a false positive (fail). Those that released within the *P. mirabilis* drainage bag were described as a positive pass and those which did not release in the *E. coli* and control bladders were described as a negative pass. The sensitivity, specificity and accuracy were determined using equations: 3.1, 3.2, and 3.3 respectively. Sensitivity measures how well a diagnostic test/device can identify a positive result; specificity estimates how good the test/device is at identifying negative results; and accuracy determines how good the device/test is at identifying a positive result and excluding a negative.

$$Sensitivity = \frac{TP}{(TP + FN)} \times 100 \tag{3.1}$$
$$TP = true\,positive,\ FN = false\,negative$$

$$Specificity = \frac{TN}{(FP + TN)} \times 100 \tag{3.2}$$
$$FP = false\,positive,\ TN = true\,negative$$

$$Accuracy = \frac{(TP + TN)}{(TP + TN + FP + FN)} \times 100 \tag{3.3}$$
$$TP = true\,positive,\ TP = true\,negative,$$
$$FP = false\,positive,\ FN = false\,negative$$

The stability of the lozenge was also assessed in healthy human urine. Ethics approval was given by the Research Ethics Approved Committee for Health (REACH), reference number: EP 19/20 089, for the donation of human urine from healthy volunteers. Informed consent was given by 12 healthy adults (healthy was defined as not currently taking antibiotics or using a urinary catheter). Participants donated a morning sample so that all donations were taken at a similar timepoint. Urine was collected and transported in a sterile falcon tube and refrigerated (3-5 °C) upon arrival. Urine was tested on the day of donation and discarded within 48 h. From the urine sample, 10 mL was removed into a separate falcon and a lozenge was added, the sample was now left at room temperature. At regular time points, the pH was measured (using a pH probe solely used for human samples), 200 μL of urine was removed and the fluorescence was measured (the 200 μL was returned back after the measurement). A positive control was prepared, a lozenge was placed into a pH 8.0 buffer (described in Table 3.3), the fluorescence was measured at 24 h time point for the positive control. SF release from the lozenge was observed visually and photographs were taken.

3.3.2.5 Sterilisation of the lozenges

Drainage bags and catheters are sterilised by ethylene oxide (EO). The stability of the lozenges during an EO sterilisation cycle was tested. Lozenges (32) were packaged separately to mimic placement within drainage bags, and a bulk of 100 lozenges were packed together. EO sterilisation was conducted by Sterigenics, A Sotera Health company (US), on a fully qualified cycle. After the cycle the lozenge integrity was checked visually and the functionality tested, as described in Section 3.3.2.1.

3.4 Results and Discussion

3.4.1 Optimisation of the Lozenge and Functionality Testing

The main limitations of the coated PVA-hydrogel lozenge design was that it was difficult to coat, fragile, and had high variability between sensors.[1] To optimise the lozenge each of these limitations was addressed: a solid tablet was developed using a tablet press, this ensured that there was less variability between the sensors and ensured the sensors were not as fragile. A biconvex tablet was produced, this tablet was small with a domed surface on the top and bottom (Fig. 3-4). To ensure a solid biconvex tablet was produced the tablet mix was optimised, excipents: lactose and talcum powder were added to the tablet binder, Firmapress, improve integrity and flow through the tablet press during manufacture. Caking is where the tablet mixture sticks to the dies

(impressions used to form the tablet shape), the addition of lactose and talcum powder also prevented caking occurring. This improved the manufacture of the tablets because the process was continual instead of having to stop and clean the press.

Figure 3-4: Photograph of a coated lozenge. Scale in cm.

The CF dye used in the initial design was replaced with SF, this is a less expensive dye which is suitable for use in a mass production of the lozenge and in clinical use (Fig. 3-5).

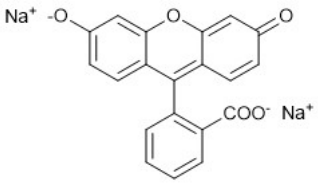

Figure 3-5: Structure of sodium fluorescein. Compound drawn using ChemDraw (PerkinElmer Informatics Inc, v. 19.0.1.28).

Initially, the hydrogels were coated using dip-coating; whereby a thread was passed through the hydrogel and the hydrogel was manually dipped into Eudragit S100 polymer. This process was attempted with the solid tablets and thread was compressed between the powder during the formation of the tablet. This led to uneven coating on the tablet and where the thread came through the tablet it was not coated as well and this acted as a leaching point for the dye. This led to large variability in the kinetic release of SF in different pH buffers (Fig. 3-6). Lozenges took three hours until they demonstrated release in pH To improve the coating coverage a drum-coating procedure was used. This is a standard manufacturing technique used to coat tablets in polymers, Eudragit S100 is sprayed onto to the tablets whilst they are being mixed and air-dried; this process prevents the tablets sticking together and allows an even coating to be distributed onto the tablet surface.

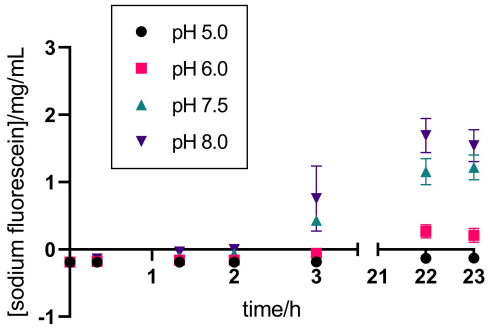

Figure 3-6: Release of sodium fluorescein from dip-coated tablets in buffers of varying pH. Release quantified using calibration curves (Appendix 3-16). Graph drawn using GraphPad Prism 8, n=4, error bars represent standard deviation.

The kinetics of release of the drum coated tablet was measured in buffers of varying pH over 24 h (Fig. 3-7). There was less variation between the tablets compared to the dip-coating (Fig. 3-6). The tablets performed as expected; releasing the SF dye at pH >7. Release for the drum coated lozenges occurred within two hours of incubation, compared to the dip-coated lozenges (Fig. 3-6 & 3-7). Interestingly the release in the drum-coated lozenges was faster and reach a higher release, this is likely due to a thinner and more even coating of the polymer. The lozenges also demonstrated stability within the 24 h only showing release at pH 7.0 and 8.5 and not at pH 5.0 and 6.0 (Fig. 3-8).

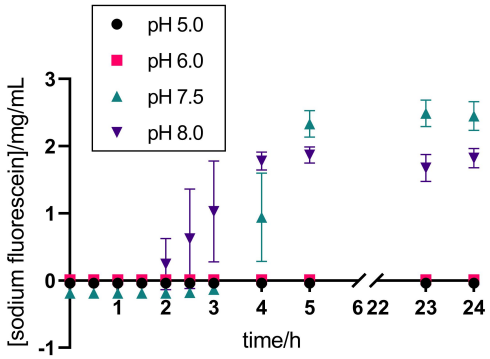

Figure 3-7: Release of sodium fluorescein from drum-coated lozenges in buffers of varying pH. Release quantified using calibration curves (Appendix 3-16). Graph drawn using GraphPad Prism 8, n=4, error bars represent standard deviation.

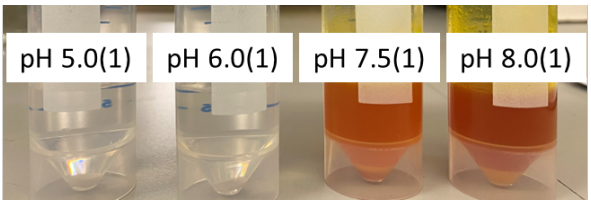

Figure 3-8: Lozenges placed in falcon tubes containing different pH buffers, demonstrating visual release of sodium fluorescein after 24 h.

3.4.1.1 Functionality testing using *P. mirabilis*

Here the lozenge was tested against bacterial bioburden. This assessed that when the bacterial concentration increased, the urease concentration increased and therefore, a subsequent increase in pH was observed. The bioburden of bacteria signifies the infection, it was important to ensure that the lozenge did not release too early; in order to prevent unnecessary catheter changes. The lozenge was placed in a AU which had been inoculated with *P. mirabilis*. The pH was measured, bacteria quantified, and the the lozenge visually assessed for release. The increase in pH correlates with the bacterial load (Fig. 3-9a). For the first 3 h, the bacterial load remains low (lag phase); this is slightly elongated in AU, compared to LB where the lag phase is 2.5 h.[5] During the hours of 3-7, the bacterial growth is exponential and at 7 h the growth plateaues and has reached stationary phase (Fig. 2-1). As the bacteria grows the pH increases, there is a slight lag in the increase in pH suggesting there is a delay in the metabolism of urea to ammonia. After 8 h the lozenge has started releasing SF, correlating with the pH >7 and a higher bacterial titre (Fig. 3-9b). The lozenge remained stable in the early hours and did not release when the pH <7 or when the bacterial bioburden was $< 10^8$ CFU/mL.

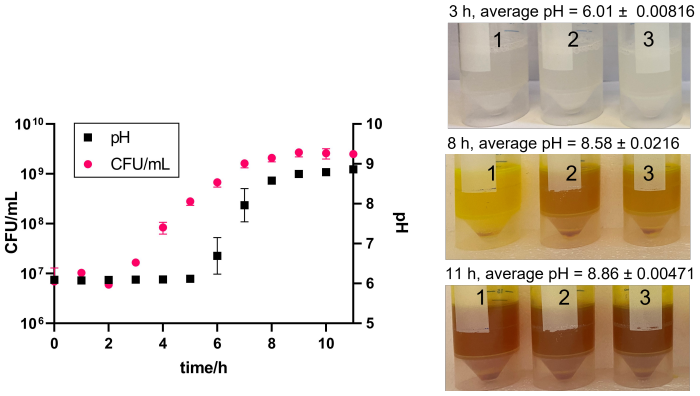

(a) Quantification of *Proteus mirabilis* and pH in artificial urine over time.

(b) Visual analysis of the lozenges a timepoints: 3, 8, and 11 h; showing the release of lozenge at pH >7.

Figure 3-9: Lozenge vs bacterial bioburden. Plots were prepared using GraphPad 9. Mean from three independent experiments, error bars represent standard deviation.

3.4.1.2 Functionality testing in *In vitro* Bladder Models

The lozenge was tested in a physiologically representative model of the catheterised tract.[6] This tested the function and stability of the lozenge. The bladders were inoculated with urease-positive *P. mirabilis* and urease-negative *E. coli*. *E. coli* is the most common micro-organism that causes UTIs.[7,8] The control bladder model was not infected with bacteria. As *E. coli* is urease negative it was predicted that it would not cause catheter blockage or cause lozenge switch on. The bladders were inoculated with 1×10^8 CFU/mL to mimic a late stage infection; pH and bacterial bioburden within the drainage bags was monitored throughout (Fig. 3-10).

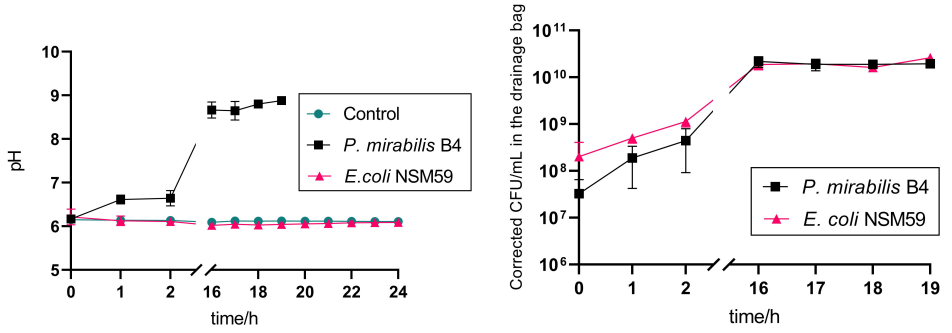

(a) pH of the drainage bag measured over time for control (no bacteria), *P. mirabilis* and *E. coli*.

(b) Viable cell count of the drainage bag over time for *P. mirabilis* and *E. coli*, corrected for the increase in volume in the drainage bag over time.

Figure 3-10: *In vitro* bladder model experiments. Plots were prepared using GraphPad 9. Mean from three independent experiments, error bars represent standard deviation.

The pH did not rise in the control or *E. coli* drainage bag, though it did rise, as expected, in the *P. mirabilis* drainage bag. The quantification of the viable bacteria was consistent between the *E. coli* and *P. mirabilis* drainage bags. There was no significant difference between the viable bacteria counts in either drainage bag: *P. mirabilis* (2.19×10^{10} CFU/mL, n=3) and *E. coli* (1.87×10^{10} CFU/mL, n=3) after 16 h (unpaired t-test with Welch's correction, p=0.7242). There was a significant difference in the pH of the drainage bag between *P. mirablis* and *E. coli* infected bladders: *P. mirabilis* pH=8.67 (n=3) and *E. coli* pH=6.02 (n=3) at 16 h (unpaired t-test with Welch's correction, p=0.0363). It took on average 18 h for the *P. mirabilis* bladder to block, the control and *E. coli* bladders ran freely until the experiment ended at 24 h. Heylen *et al.,* Supplementary Video, shows the time-lapse photography of the drainage bags and the release of the lozenge.[9] There is a distinctive colour difference between the drainage bag from *P. mirabilis* compared to *E. coli* and the control (Fig. 3-11). This visual indication is a clear warning to the patient that catheter blockage is imminent. The average early warning which the lozenge gave (calculated using the time-lapse photography) was 6.7 h (±0.58). This is an optimum warning time as it gives patients enough time to have their catheter changed or flushed, thus preventing serious clinical outcomes associated with catheter blockage (Section 1.2.2).

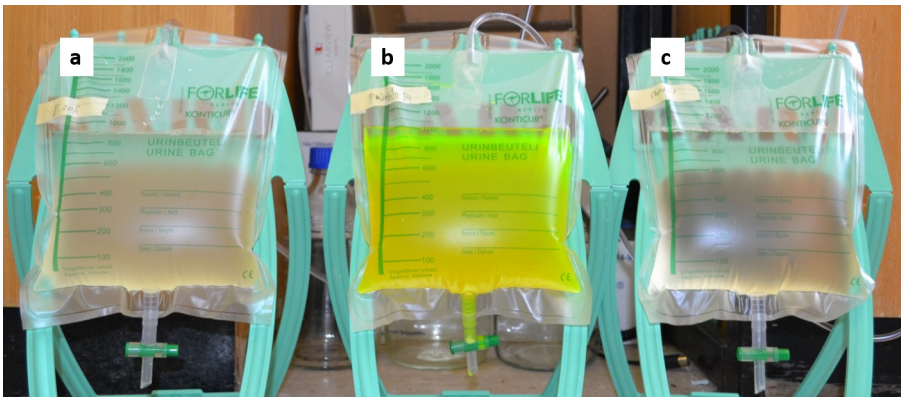

Figure 3-11: Visual analysis of the drainage bags from the *in vitro* bladder models. (a) Drainage bag from *Escherichia coli* infected bladder. (b) Drainage bag from *Proteus mirabilis* infected bladder. (c) control bladder with no bacteria.

3.4.2 Investigating Stability of the Lozenge

Part of the aim of this research was to assess the lozenge for bulk manufacturing. It is important that the lozenges produced by the solid tablet press and subsequently drum-coated, are robust and have consistent performance. A total of 30 tablets were assessed for stability, those that released (as expected) in the *P. mirabilis* drainage bags were termed 'positive pass', those that did not release in the *E. coli* and control drainage bags are termed 'negative pass' and those that released in the *E. coli* and control bladders, or released earlier than other biological repeats in the *P. mirabilis* drainage bags are false positives (fails) (Table 3.4). The lozenge stability data here calculates to give a sensitivity of 100%, specificity of 71%, and accuracy of 80%. Overall, 80% (24/30) of the lozenges were stable over 24 h. The reason a lozenge failed is likely due to the manual manufacture of the tablets, which may have led to a tablet not capping properly. This would have subsequently resulted in an unequal polymer coating during the drum-coating process. The manufacturing could be improved by motorising tablet manufacture, which would lead to more uniform tablets being produced. Additionally, the thickness of the Eudragit S100 coating could be increased from 10 mg/cm^2; however, this would also decrease the warning time interval as the Eudragit S100 would take longer to dissolve.

Table 3.4: Assessing the stability of lozenges during *in vitro* bladder model experiments. Positive pass is lozenge that released in the *Proteus mirabilis* drainage bag; negative pass is a lozenge that released in *Escherichia coli* and control drainage bags; and a fail is a lozenge which released within the 24 h in the *E. coli* or control drainage bags or released earlier than the other biological repeats in the *P. mirabilis* drainage bag. Experiments 1-2 had one lozenge placed in each bag, whilst experiments 3-6 had two lozenges in each bag.

Experiment	Positive pass	Negative pass	Fail
1	1	2	-
2	1	1	1
3	2	1	3
4	2	3	1
5	2	4	-
6	1	4	1
Total	9	15	6

The lozenge is designed to predicted impending blockage in long-term catheterised patients. Therefore, it is important to test that it does not release in healthy human urine. Healthy human urine has a pH <7 therefore, the lozenge should not release SF dye for healthy urine.[10,11] A morning sample of urine was donated by 12 healthy volunteers. The donor's urine remained below pH of 7 for over 26 h (Fig. 3-12a). The average pH of the donor's urine was 5.63 ±0.30 at 0 h, this was in agreement to literature.[10,11] The fluorescent intensity remained constant over time and was significantly lower than the control (unpaired t-test, Welch's correction, p=0.0001). It was concluded, that no SF released in healthy urine therefore, there are no components in healthy urine which could cause the lozenge to release (Fig. 3-13). The lozenge is unlikely to cause false positive results in clinical application.

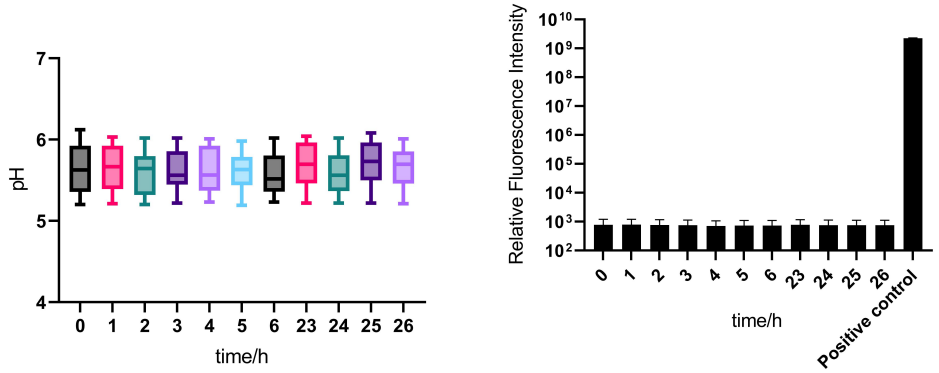

(a) Variation in pH over 26 h demonstrated using box and whisker diagrams, showing the mean and variation between the human samples.

(b) Variation in fluorescence after 24 h of the lozenge being incubated within the human urine. Positive control was the lozenge incubated in pH 8 tris buffer.

Figure 3-12: Testing the lozenge in healty human urine. Plots were prepared using GraphPad 9. Mean from three independent experiments, error bars represent standard deviation.

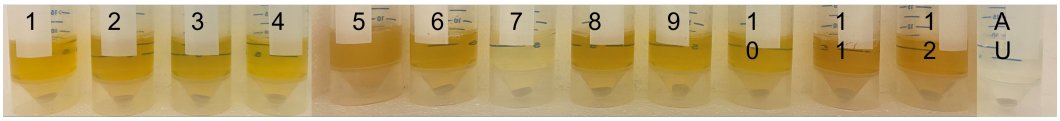

Figure 3-13: Visual analysis of the donor urine with the lozenge after 24 h. 1-12 are urine samples and 13 is artificial urine.

3.4.3 Sterilisation of Lozenges

It is common for medical devices to be sterilised with EO (Fig. 3-14). EO is toxic to micro-organisms, it can sterilise microbes because of its alkylating property and high diffusivity, it alkalises cellular components such as DNA and functional proteins therefore killing the microbes.[12] EO is routinely used in the sterilization of urinary catheters and drainage bags. For the clinical application, the lozenge would be placed with in the drainage bag, then sterilised. Therefore, whether the lozenges were stable during EO sterilisation was assessed. It is important that the lozenges do not leach SF dye during the sterilisation process. In this experiment, 132 lozenges were tested: 32 lozenges were individually packaged, and 100 were packaged together for group sterilisation. Post-sterilisation showed that the Eudragit S100 polymer was still intact. The functionality and stability of the lozenge was assessed as described in Section 3.4.1. Figure 3-15, shows that the lozenges were functioning as expected and were able to release SF dye at pH >7. Lozenges which were sterilised demonstrated a higher release of SF compared to those which were not sterilised (Fig. 3-7 & 3-15). Potentially, the EO is affecting the integrity of the polymer however the trend of kinetic release is

similar just a higher release was measured. It is unlikely that would affect the ability of the lozenge to function as an early-warning sensor, therefore, the lozenges can be sterilised by EO.

Figure 3-14: Structure of ethylene oxide. Compound drawn using ChemDraw (PerkinElmer Informatics Inc, v. 19.0.1.28).

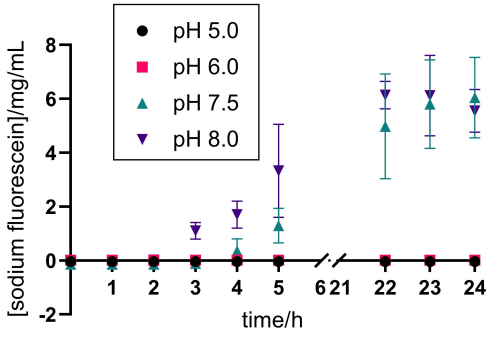

Figure 3-15: Release of sodium fluorescein from drum-coated, sterilised lozenges in buffers of varying pH. Release quantified using calibration curves (Appendix 3-16). Graph drawn using GraphPad Prism 8, n=4, error bars represent standard deviation.

3.5 Conclusion

The lozenge has been optimised from its original design, allowing easier manufacturing, scale-up, and clinical use. It still remains functional as a sensor in detecting impending catheter blockage. It provides a warning time of 6.7 h, thus allowing users time to change or flush the catheters before serious clinical consequences occur. The lozenge remains stable in healthy human urine and can be sterilised using EO. The next step for the lozenge is to test it in urine from patients with long-term catheters, thus allowing the diagnostic performance of the lozenge to be tested.

3.6 Appendix

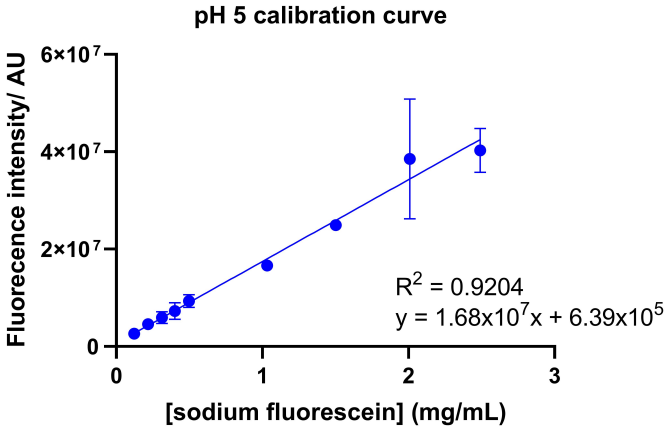
pH 5 calibration curve
Fluorecence intensity/ AU
6×10^7
4×10^7
2×10^7
0
0
1
2
3
[sodium fluorescein] (mg/mL)
R^2 = 0.9204
y = 1.68x10^7x + 6.39x10^5

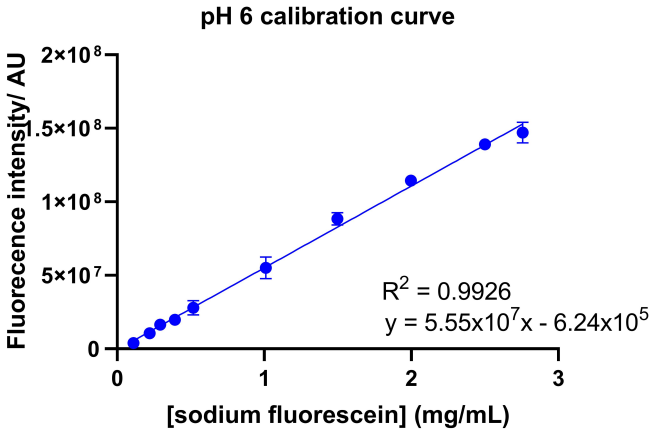
pH 6 calibration curve
Fluorecence intensity/ AU
2×10^8
1.5×10^8
1×10^8
5×10^7
0
0
1
2
3
[sodium fluorescein] (mg/mL)
R^2 = 0.9926
y = 5.55x10^7x - 6.24x10^5

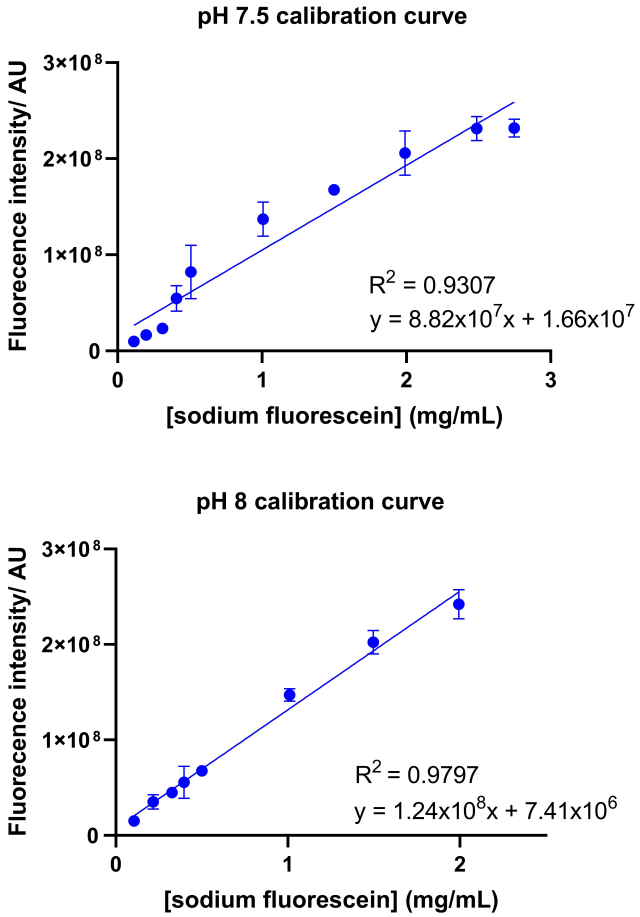

Figure 3-16: Calibration curves of sodium fluorescein in buffers of varying pH. Graph drawn using GraphPad Prism 8, n=3, error bars represent standard deviation.

3.7 Bibliography

[1] Milo S, Acosta FB, Hathaway HJ, Wallace LA, Thet NT, Jenkins ATA. Development of an Infection-Responsive Fluorescent Sensor for the Early Detection of Urinary Catheter Blockage. ACS Sensors. 2018;3(3):612–617. Available from: https://doi.org/10.1021/acssensors.7b00861.

[2] Armbruster CE, Mobley HLT, Pearson MM. Pathogenesis of Proteus mirabilis Infection. EcoSal Plus. 2018;8(1):1–73. Available from: https://doi.org/10.1128/ecosalplus.ESP-0009-2017.

[3] Stickler DJ, Jones SM, Adusei GO, Waters MG, Cloete J, Mathur S, et al. A clinical assessment of the performance of a sensor to detect crystalline biofilm formation on indwelling bladder catheters. BJU International. 2006;98(6):1244–1249. Available from: https://doi.org/10.1111/j.1464-410X.2006.06562.x.

[4] Milo S, Thet NT, Liu D, Nzakizwanayo J, Jones BV, Jenkins ATA. An in-situ infection detection sensor coating for urinary catheters. Biosensors and Bioelectronics. 2016;81:166–172. Available from: http://dx.doi.org/10.1016/j.bios.2016.02.059.

[5] Milo S, Heylen RA, Glancy J, Williams GT, Patenall BL, Hathaway HJ, et al. A small-molecular inhibitor against Proteus mirabilis urease to treat catheter-associated urinary tract infections. Scientific Reports. 2021 dec;11(1):3726. Available from: http://www.nature.com/articles/s41598-021-83257-2.

[6] Nzakizwanayo J, Pelling H, Milo S, Jones BV. An In Vitro Bladder Model for Studying Catheter-Assoicated Urinary Tract Infection and Asssoicated Analysis of Biofilms. Humana Press; 2019. Available from: https://link.springer.com/protocol/10.1007/978-1-4939-9601-8{_}14.

[7] Dhakal BK, Kulesus RR, Mulvey MA. Mechanisms and consequences of bladder cell invasion by uropathogenic Escherichia coli. European Journal of Clinical Investigation. 2008;38(SUPPL.2):2–11. Available from: https://doi.org/10.1111/j.1365-2362.2008.01986.x.

[8] Tambyah PA, Halvorson KT, Maki DG. A Prospective Study of Pathogenesis of Catheter-Associated Urinary Tract Infections. Mayo Clinic Proceedings. 1999;74(2):131–136. Available from: http://dx.doi.org/10.4065/74.2.131.

[9] Heylen RA, Branson M, Gwynne L, Patenall BL, Hauschildt N, Urie J, et al. Optimisation of a lozenge-based sensor for detecting impending blockage of urin-

ary catheters. Biosensors and Bioelectronics. 2022;197(November 2021):113775. Available from: https://doi.org/10.1016/j.bios.2021.113775.

[10] Kaye D. Antibacterial activity of human urine. The Journal of Clinical Investigation. 1968;47(10):2374–2390. Available from: https://doi.org/10.1172/JCI105921.{%}0AResearch.

[11] Landry DW, Bazari H. Approach to the Patient with Renal Disease. vol. 1. 24th ed. Elsevier Inc.; 2012. Available from: http://dx.doi.org/10.1016/B978-1-4377-1604-7.00116-0.

[12] Mendes GCC, Brandão TRS, Silva CLM. Ethylene oxide sterilization of medical devices: A review. American Journal of Infection Control. 2007;35(9):574–581.

Chapter 4

Pilot Clinical Trial to Test the Function of a Diagnostic Sensor in Predicting Impending Urinary Catheter Blockage in Long-term Catheterised Patients

4.1 Chapter Overview

The aim of this Chapter was to set-up and conduct a pilot feasibility trial to test the functionality of a sensor (lozenge, Chapter 3) in predicting impending catheter blockage in human urine.

4.2 Introduction

A diagnostic sensor was developed for clinical use in Chapter 3.[1] This pilot trial is not a medical device trial because the participant will not directly be using the diagnostic device themselves. Therefore, the sensor does not have to be manufactured under a GMP licence. Instead this is a cohort study, with the aim to recruit 48 participants. In Section 3.4.2, the sensor was tested for stability in healthy human urine. This study will use donated urine from long-term catheterised patients. The primary outcome is to functionality test the sensor and owing to a three-week follow-up phone call, the ability of the sensor to predict impending blockage shall be analysed. Secondary outcomes include assessment of participants QoL, and analysis of the microbial composition of the urine.

4.3 Methods

4.3.1 Study Design for Pilot Clinical Trial

Set up and design of the pilot clinical trial was conducted with the assistance of the Clinical Team: Dr. Edward Jefferies, and Mrs Annette Moreton (Royal United Hosptial, Bath). Study design, registration of the trial, completion of the Integrated Research Application System (IRAS) form, and submission to Research Ethics Committee (REC) was completed by Dr June Mercer-Chalmers and Prof. A. Toby. A. Jenkins (University of Bath (UoBath)). The study was sponsored by the UoBath. An overview of the study design and sample processing is described in Figure 4-1.

Study aims: (1) investigate the feasibility of testing the lozenge (diagnostic sensor) in a larger scale randomized clinical trial. (2a) determine the predictability of the sensor; (b) the functionality of the sensor; and (c) deduce the microbiological diversity of the drainage bag. The study was registered with the International Standard Registered Clinical/soCial sTudy Number (ISRCTN) as 51644058, the trial was submitted as Integrated Research Application System (IRAS) number: 261095 and approved by the Research Ethics Committee (REC) number: 20/LO/0094.

4.3.1.1 Participants

Participants to the study had to be adults with a long-term indwelling urinary catheter. Participants were recruited through attendance to the Outpatient Urology Clinic at the RUH, Bath. Inclusion in trial was voluntary and participants signed a consent form prior to donation. Participants had the opportunity to read the trial leaflet and ask questions to the research nurse (Mrs Annette Moreton). Upon consent to the study, a case record form (CRF) was completed; this contained various questions are the participants health and the type of catheter they were using. Participants completed a QoL questionnaire, designed by Cotterill *et al.*, an International Consultation on Incontinence Questionnaire (ICIQ).[2] Participants donated their full (>150 mL) drainage bag and catheter. Samples were anonymised by staff at RUH and stored between 2-8 °C prior to transport to the UoBath. Three weeks after donation, research nurses at the RUH contacted participants via a telephone call; to determine if a blockage event had occurred and whether there had a been a change in their catheter treatment. The target sample number was 48. This was determined through consultation with the RUH, taking into account: staffing restrictions, time, and capacity at the RUH. A sample number of 48 was felt sufficient for a pilot feasibility study. The trial was designed to commence in the March 2020; however, was severely delayed owing to the COVID-19 pandemic.

4.3.2 Sample Processing

All participant samples were anonymised at the RUH, researchers at the UoBath had no identifiable link between the participant and their sample. CRF was completed by the research nurses upon recruitment, it was not analysed until after the samples had been assessed to prevent bias. Prior to processing samples were stored between 2-8 °C, processing of the samples was completed within 24 h of donation. Analysis took place within a microbiological Class 2 sterile cabinet to prevent contamination. Photographs were taken of the catheter and bag at the beginning of analysis, assessment of the colour of the urine, and whether the catheter tip was encrusted or not, was recorded. Urine from the drainage bag (10 mL) was aliquoted into 6x 50 mL Falcon tubes (Corning, UK). Positive and negative controls were prepared, positive control was AU (prepared according to Section 2.2.3) and the pH adjusted to >8 using 1 M NaOH. Negative control was just AU alone. Sensors were added to 5 out of the 6 tubes and the control tubes, one tube was a no sensor control. Tubes were photographed in a light box, camera distance of 30 cm, with consistent camera settings (Nikon D3100, 35 mm lens zoom). pH and temperature were measured for three of the tubes, then

averaged. Tubes were incubated at room temperature for 18 h. Post-incubation tubes were photographed, pH and temperature re-measured, and the release of the sensor visually determined.

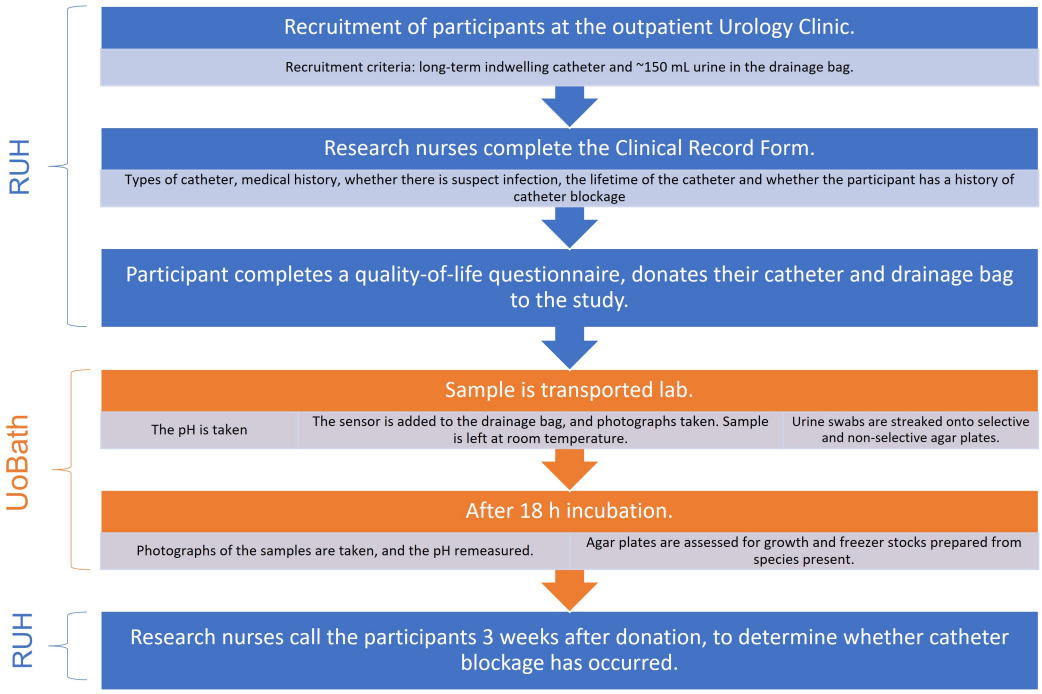

Figure 4-1: Schematic of the study design and process of samples from the RUH to the UoBath.

4.3.2.1 Microbial Analysis

From each participant's donation a 10 μL loop of urine was streaked onto the following agars to achieve single colonies, selective plates: CLED, CHROMID agar plates, MC; non-selective: MH, LB, NSLB (Table 2.1), and CBA (5% sheeps blood). This was used to assess the morphology of the bacteria and isolate different species. An additional CBA plate was prepared using a semi-quantitative streaking method. All plates were incubated statically overnight at 37 °C. Post incubation plates were photographed and individual colonies were visually assessed for: rough/smooth edges, color, and size. Using the CBA semi-quantitative plate an approximation of quantification was made using Appendix 4-4. In samples which were polymicrobial plates were re-streaked to obtain plates containing single species. Individual colonies were picked from the plates, grown overnight in LB or MH broth and freezer stocks were prepared, as described in Section 2.2.1. From the plates a tentative assessment of bacterial species was made based on appearance from selective agar plates (CLED, CHROMID, and MC) and urease activity test.

Each species was tested for urease activity using the phenol red method. A small quantity of bacteria was mixed with phenol red solution (10% (w/v) urea and 0.02% (w/v) phenol red). A positive result is a color changed from yellow to red.

4.3.2.2 16S rRNA Sequencing

The bacteria which were isolated from the participant's urine were identified by 16S rRNA sequencing. 16S is a ~1500 base pair (bp) molecular marker from the 30S subunit of the ribosome. It has desirable characteristics which allow for phylogenetic relationships between species of bacteria to be explored and thus allows the identification of bacterial genus and in many cases the species.[3] From the frozen stocks of bacteria, plates were grown statically (Section 2.2.1). The preparation of colony PCR was completed within a sterile Class 2 micro cabinet. Owing to the 16S rRNA marker being located in all species of bacteria, a sterile cabinet was used to prevent contamination from other bacteria. Primers for 16S rRNA sequence are shown in Table 4.1.[3] Primers were diluted in nuclease-free water to a concentration of 100 μM. A single colony was picked from the bacterial plate and added to nuclease-free water (100 μL) and microwaved on high for 3 min. Into an autoclaved PCR tube: 2 μL of colony preparation and 18 μL master mix was added. Master mix consists of: 10 μL PHUSION high-fidelity enzyme mix; 1 μL 27F primer; 1 μL 1392R primer; and 6 μL of nuclease-free water, per reaction. PCR was run using PHUSION method: melting temperature of 56 °C, and extension time of 1 min for 35 cycles at 72 °C. Resulting PCR product was run on a 1% (w/v) agarose gel at 110 V for 30 min, against a 1 kb ladder to confirm the size of the PCR product.

Table 4.1: Universe 16S rRNA primers purchased from ThermoScientific UK.[3]

27F	5'-AGAGTTTGATCCTGGCTCAG-3'
1392R	5'- GGTTACCTTGTTACGACTT-3'

If the colony PCR failed to yield the desired PCR product then the DNA was extracted from the bacteria. To extract DNA the Gram status (Section 1.1.2.1) of the bacteria is required; if it was not known for these samples from the tentative assessment made using the selective agar plates (Section 4.3.2.1), then the method was completed for both Gram-positive and negative. DNA was extracted using a Sigma (Merck) DNA extraction kit and the PCR was repeated as described above. PCR product was cleaned up using a Wizard SV Gel and PCR Clean-up System. DNA concentration was determined using spectrometer (A_{260}) and diluted to desired concentration (10 ng/μL)

with nuclease-free water. For each bacterial samples, two sequencing samples were prepared: one to be sequenced in the 27F primer direction and the other to be sequenced in the 1392R primer direction. Each sample had 2 μL of the desired primer added to it. Therefore, the PCR product was sequenced in two directions, the maximum length which could be sequenced was 1000 bp, so sequencing in both directions allowed greater coverage of the 16S rRNA molecular marker ($\sim$1500 bp). Solutions were sequenced by Eurofins, Germany; quality of the sequence analysed and trimmed to remove less reliable base reads. Sequences were scanned against the EzBioCloud Database of 16S rRNA sequences and the identification analysed both the 27F and 1392R sequences were run separately and result compared to the tentative assessment (Section 4.3.2.1).

4.3.2.3 Statistical Analysis

The clinical trial was a small-scale pilot trial, no randomization could take place because the number of participants was too low and the study was not powered. The following tests were used to determine significance: Fisher Exact test and χ^2 test.

4.4 Results

4.4.1 Recruitment

The study aimed to collect 48 participant's samples however only 35 samples were collected from 28 individuals. The total number of recruits was not met owing to staffing restrictions at the RUH. The recruitment trial time was over 5 months, participants were invited to the trial at 15 outpatient clinics at the Department of Urology, RUH. An average of 2.3 participants recruited/clinic. Most outpatients were invited to the trial, the main reason for recruitment failure was because they did not have >150 mL of urine in their drainage bag (a requirement of inclusion). No samples were excluded from the study and all samples were tested. Table 4.2 describes the baseline demographics of the study.

Table 4.2: The baseline demographics and clinical characteristics of the study participants.

Variable	Participants
Number of Males	23/28 (82.1%)
Number of Females	5/28 (17.9%)
Average age, yr. (range)	72.6 (41-94)
Ethnicity:	
White: British	26/28 (92.9%)
White: Other	2/28 (7.1%)
Common Co-morbidities:	
Heart Disease	11/28 (39.2%)
Hypertension	10/28 (35.7%)
Prostrate Cancer/History of	6/28 (21.5%)
Type 2 Diabetes	5/28 (17.9%)
Multiple Sclerosis	4/28 (14.2%)
Osteroporosis	4/28 (14.2%)
Stroke Disease	4/28 (14.2%)
Inguinal/Hiatus hernia/been repaired	4/28 (14.2%)
Urinary catheter:	
Urethral	23/28 (82.1%)
Supra-pubic	(5/28%)

The majority of the participants were male (82.1%). Shackley *et al.,* reported a 3:2 ratio in males vs females in patients who were catheterised (total number 1 194 902).[4] As observed in Table 4.2, this ratio is not observed in this study which is likely due to sample size, Shackley *et al.,* also included short-term catheterised patients and therefore this ratio might not be representative of a long-term catheterised population. Additionally, owing to a small sample size it is difficult to apply the baseline demographics to a larger population. The mean age was 72.6 yrs and all participants were white; which is the main demographic in the Bath and North-East Somerset Trust, UK where 90% of the population is White: British.[5] The lack of diversity and representation of other ethnic groups is a major limitation of this study, this was difficult to mitigate owing to the size of the study and the geographical location.

Table 4.3, describes the different catheter manufacturers used. There was quite a wide range of manufacturers used for such a small sample size, demonstrating the large variability in catheters on offer to long-term patients.

Table 4.3: Summary of the different catheter manufacturers used.

Catheter manufacturer	Participants
Rusch	4
Bard	4
Coloplast Coude	4
Coloplast Porges	3
Yushin	3
Brilliant AquaFlate	2
Mediplus	2
Medicath	1
Libra	1
Not recorded	4

4.4.2 QoL Responses

The QoL questionnaire was completed by all participants, this demonstrated the impact of long-term catheter use on participants lifestyle (Table 4.4). Catheter function and concerns had a score of 11.2, compared to the results reported by Cotterill *et al.,* this was below their reported score of 14.5 (n = 199) although was within ±1 standard deviation.[2] Similarly, the lifestyle impact score (7.0) was also lower than previously reported data (8.6, n = 202) but within ±1 standard deviation. In conclusion, this QoL questionnaire was comparable to the larger dataset (Appendix 4.7).[2] Question 6 was included in Table 4.4, as it was particularly relevant to this study. There was a low score for this question, therefore participants in this study population were not concerned about catheter blockage (Table 4.4). Although for 10 of the 27 responses participants were 'sometimes' or for 1 participant 'all the time' thinking about catheter blockage.

Table 4.4: Scores and the ranges from the quality-of-life questionnaire designed by Cotterill *et al.*, and calculated as designed. Responses to Question 6 are included here owing to the relevance to this particular study.

Domain	**Score**
Catheter function and concerns (n = 28)	Range = 1-23, mean = 11.5
Lifestyle impact (n = 28)	Range = 3-15, mean = 7.0
Q6a: 'Is the possibility of the catheter blocking on your mind?' (n = 27)	Range = 0-4, mean = 1.04
Q6b: 'How much does this bother you?' (n = 27)	Range = 0-10, mean = 2.44

4.4.3 Sensor Performance

To measure whether the sensor could predict impending catheter blockage, the sensor was tested in the urine donated by the participants and incubated for 18 h. The result from the sensor was tested to see whether it correlated with a blockage event, which was assessed by a three week telephone call. Only two participants reported a blockage event within the three weeks (Fig. 4-2A). For the two blockers the sensor did accurately detect the event. However, 42% of the sensors turned on without a blockage event (false positives). This gave a sensitivity of 100% and a specificity of 58.06%. The low specificity is likely because of the three week follow up period, the catheters are designed to be *in situ* for up to three months. Therefore, it is likely that the three week cut off period missed many of the blockage events even for the recurrent 'blockers' because the catheters were not *in situ* for long enough.

To test the functionality of the sensor, the pH of the donated urine was compared to whether the sensor turned on or not (Fig. 4-2B). As urease activity is known to increase the pH of the urine, and an increase in pH increases the likelihood of a blockage event; catheter users with void urine pH >7 are more likely to be recurrent blockers.[6,7,8,9] In total 173 sensors were tested, a sensitivity of 78.75% and specificity of 96.77% was determined for the functionality of the sensors. Therefore, the sensors demonstrated a strong evidence that they turn-on in pH >7 ($p = 2.06 \times 10^{-24}$, χ^2 test).

One of the questions in the CRF was about whether the participant used flush out solutions or bladder maintenance solutions(Q31-32), as described in Section 1.4.1. As previously discussed these washout/maintenance solutions are prescribed to clear the debris and prevent further blockage; however, the current evidence suggests they are not effective.[10] From the dataset, three individuals (6 samples) were prescribed washout

solutions. These are only used by frequent blockers and therefore indicate participants that are likely to experience blockage events. These participants were added to the predictability test (Fig. 4-2C). The sensitivity was re-calculated as 100% and the specificity was improved to 70.37%. This allowed the use of the Fisher Exact test to demonstrate significance between sensor turn on and participants prescribed maintenance solution/reporting a blockage event ($p = 0.029$). There was no correlation between the length of time the catheter was indwelling and whether the sensor turned on. All participants who reported blockages or were prescribed maintenance solution had a pH >7 (except RUH07 = 6.73, rising to 7.44 after 18 h incubation). Average pH of the urine for this group was 8.20, range: 6.73-8.80.

The participant's concerns about blockages were reported in the QoL questionnaire (Section 4.4.2). The correlation between sensor turn on and concern about blockage was assessed. Table 4.4, showed the mean of catheter blockage concern was 1.04. For the Q6 responses: <2 (never (0), occasionally (1)), and ≥2 (somewhat (2), most-of-the-time (3), all-of-the-time (4)). If the threshold of ≥2 is taken and correlated with sensor turn on; a sensitivity of 70.59% and specificity of 63.64% was determined. This suggests that participants which were more concerned with catheter blockage were more likely to get sensor activation. This result is in isolation to the physiological measurements, such as, blockage events or high urine pH. If participants were more concerned about catheter blockage, it is likely they have experienced a blockage event before or are a frequent blocker. The literature states that once a patient experiences a blockage event they are much more likely to suffer recurrent blockage events; owing to the presence of the urease-positive infection within the bladder, which is able to remain *in situ* between catheter changes.[7,8]

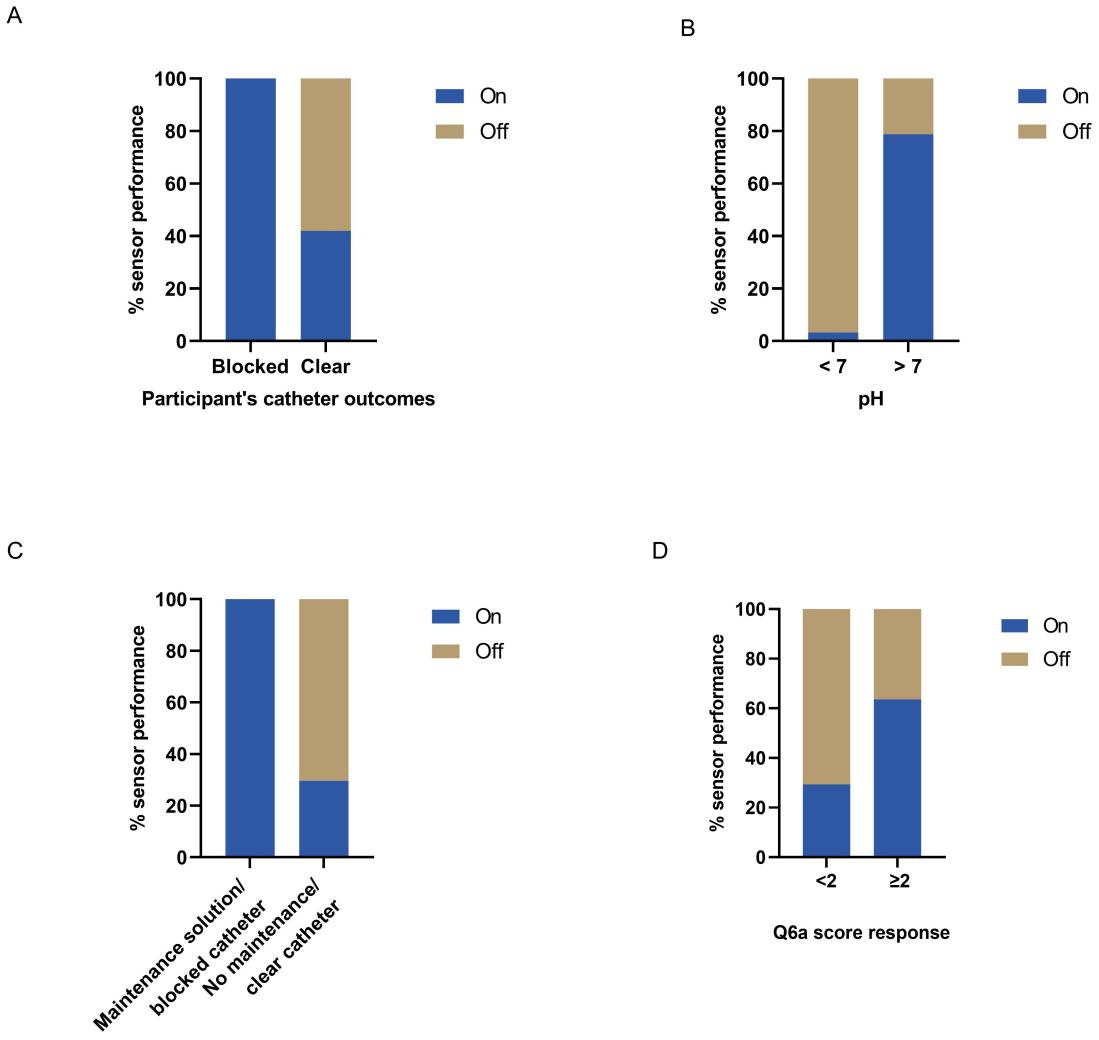

Figure 4-2: Sensor Performance. A. Predictability of the sensor, the number of sensors which turned on compared to the reported blockage events. B. Functionality of the sensor measured by the number of sensors which turned on compared to measured pH. C. Comparing the predictability of the sensors to reported blockage events and use of bladder maintenance solutions. D. The ability of the sensor to predict blockage compared to the concern for catheter blockage measured in a quality of life questionnaire. Graphs were prepared using GraphPad Prism v. 9.4.1.

4.4.4 Microbial Analysis

From the donated urine, 90 strains of bacteria were isolated. Initially, the bacterial species were identified via selective plate analysis, this allowed for a tentative assessment of the bacterial species. Redundancy from the selective plate analysis identified 71 strains that required further identification by 16S rRNA sequencing. Five strains failed

to be sequenced after three attempts: RUH07-01, RUH14-02, RUH16-01, RUH20-02, and RUH30-01. Identification of these bacteria was made using the selective plate analysis, the exception was RUH30-01, it was not possible to identify this bacteria because it was isolated on a non-selective CBA plate. Of the 35 samples donated: 22/35 (62.9%) were polymicrobial and 13/35 (37.1%) had one species infection. All urine donated contained bacteria. From the responses in the CRF; 33/35 of the participants reported they did not have a suspect infection (Q2, CRF), suggesting that most of the infections were asymptomatic. Thus, agreeing with literature that all patients with long-term catheters have chronic bacteriuria.[8] There is a risk that the bacteria identified were present owing to contamination by the nurses removing the catheter; however, all nurses routinely use aseptic technique on catheter removal and insertion therefore the risk of contamination is low. Table 4.5 describes the frequency of different species present within the donated urine, whilst Appendix Table 4.6 describes the bacteria found within each sample.

Table 4.5: Frequency of different bacteria species identified in the donated urine and their urease activity status.

Bacterial species	**Frequency**	**Urease activity**
Proteus spp.	13	Positive[6]
Pseudomonas spp.	10	Variable[11]
Enterococcus spp.	10	Negative[12]
Klebisella spp.	9	Positive[13]
Escherichia spp.	8	Negative[14]
Staphylococcus spp.	4	Variable[14]
Citrobacter koseri	3	Variable[15]
Enterobacter spp.	2	Variable[16]
Other	5	N/A

Participants which had urease-positive bacteria identified within their urine (Table 4.5) were more likely to report a catheter blockage or use a bladder maintenance solution, this was in agreement with the literature (Fig. 4-3A).[17,6,18,19,20,21] For over half the participants urease activity was identified but there was no associated catheter blockage. It can be hypothesized that there are complex interactions between the participant's immune system and the urease-positive bacteria which could be suppressing the pathology, and maintain the bacterial load below the infection threshold. Additionally, many of these participants have a polymicrobial infection; therefore, there is a possibility of intra-species competition between the bacterial populations. The converse is that the

urease activity is enhanced by difference species as described by Armbruster *et al.,* who observed synergy between *P. mirabilis* and *Providencia stuartii* which led to enhanced urease activity.[22,21]

During this study it was not possible to quantify the bacteria within the urine. An alternative semi-quantitative method was used to estimate bacterial burden, described in Section 4.3.2.1. However, this did not provide details on the different quantities of the bacterial species. To determine the different levels of bacterial populations 16S rRNA sequencing on urine collected from the bladder (not drainage bag) would be required, as this would have been a true reflection of the CAUTI. Urine cannot be frozen, owing to the likelihood of it affecting the downstream microbial analysis, additionally permission to store urine was not requested. So the analysis would have had to be done immediately after collection and this was not possible. Another limitation of the study was that only aerobic bacteria were analysed, anaerobic bacteria could have been present and interacting with the aerobic species. Despite these limitations, the testing done here was more rigorous than standard clinical testing and provided species-level detail on the CAUTI.

The sensor performed well in detecting the urease-positive infections; sensitivity measured at 63.64% and specificity at 84.62% (Fig. 4-3B). Interestingly, two of the participants which had a blocked catheter or used maintenance solutions had *P. mirabilis* and *Enterococcus faecalis* infections; Gaston *et al.,* reported polymicrobial interactions between these species led to antibiotic recalcitrance, biofilm formation, and persistence within the catheterised urinary tract.[23]

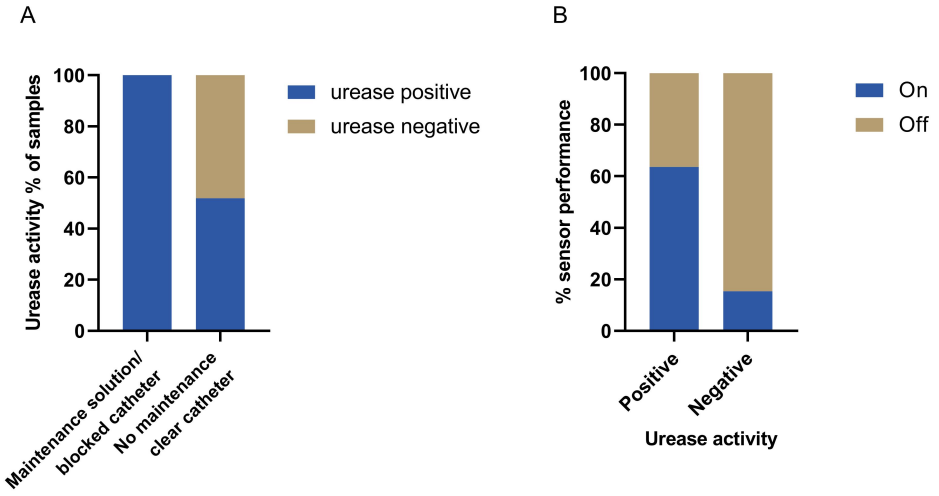

Figure 4-3: Comparing microbial analysis to other datasets. A. Relationship between participants reported blockage events and use of maintenance solution compared to whether a urease-positive infection is present within their urine. B. Correlation between the sensor turn on predictability and whether urease activity was measured. Graphs were prepared using GraphPad Prism v. 9.4.1.

4.5 Discussion

4.5.1 Limitations

The two main limitations of this study are the small sample size and lack of variation in baseline characteristics (Table 4.2). The sample size resulted in limited statistical analysis and the study was not powered; therefore, whether the sensor could predict impending catheter blockage could not be determined. Another major limitation in the study was the three week delay between the catheter change and the follow-up telephone call. This discrete timepoint did not allow future participant follow up and whether the catheter blocked after three weeks was not known. Consequently, only two participants reported blockage events within the three week time period. Conducting a larger clinical trial will mitigate these limitations. A larger sample size will allow statistical analysis and recruitment from multiple centres can ensure a variable population is investigated. The development of a participant electronic CRF (eCRF) which will allow capture of blockage events in real-time via a phone or tablet device. This would allow for continuous monitoring of the participant and their sensor.

4.5.2 Sensor Performance

The sensor correctly identified the two blockage events which occurred. Additionally, it was able to detect the prescription of maintenance solutions for participants which were common 'blockers' and identify urease-positive infections (Fig. 4-2A & C, 4-3B). Despite these promising results the sensor did have a high false-positive rate, detecting that participants would experience blockage events when blockages did not occur. In the future, prediction of catheter blockage will likely require a two-fold verification: (1) sensor turns on in the drainage bag; (2) determination of how the participant is feeling, whether there has been an increase in the use of maintenance solutions or reduced urine output. This two-step verification will require testing in a larger clinical trial.

4.5.3 Microbial Analysis

Although urinary catheters have been in use since 1929 (Foley) and are the most commonly prescribed medical device; there is limited research describing the microbiological profile within long-term users.[24,25] Indeed, the majority of studies (like this one) have a small sample size and similar limitations; such as, the culture of aerobic bacteria exclusively.[8,26,27,28] Two of these studies identified bacterial species using MacConkey and blood agar plates.[8,27] Whilst the others used standard microbiology testing, which in the UK consists of CLED agar streaking and culture. In this study, both selective agar culture and 16S rRNA sequencing was completed. Sequencing of the 16S rRNA gene allowed species-level identification of bacterial species. Thus allowing differentiation between *E. coli* and *S. flexneri*, which is not possible via the selective agar culturing method. Interestingly, the selective agar plates mis-identified 50 strains compared to their sequencing results, this demonstrates the importance of sequence-level identification.

4.6 Conclusion

This chapter describes the results of a pilot clinical trial, using participants who use a long-term urinary catheter. It demonstrates the functionality and predictability of a sensor in diagnosing urinary catheter blockage. The sensor correctly identified the blockage events which occurred during the study. Owing to low sample numbers the study was not powered and powered statistical analysis could not be completed.

4.7 Appendix

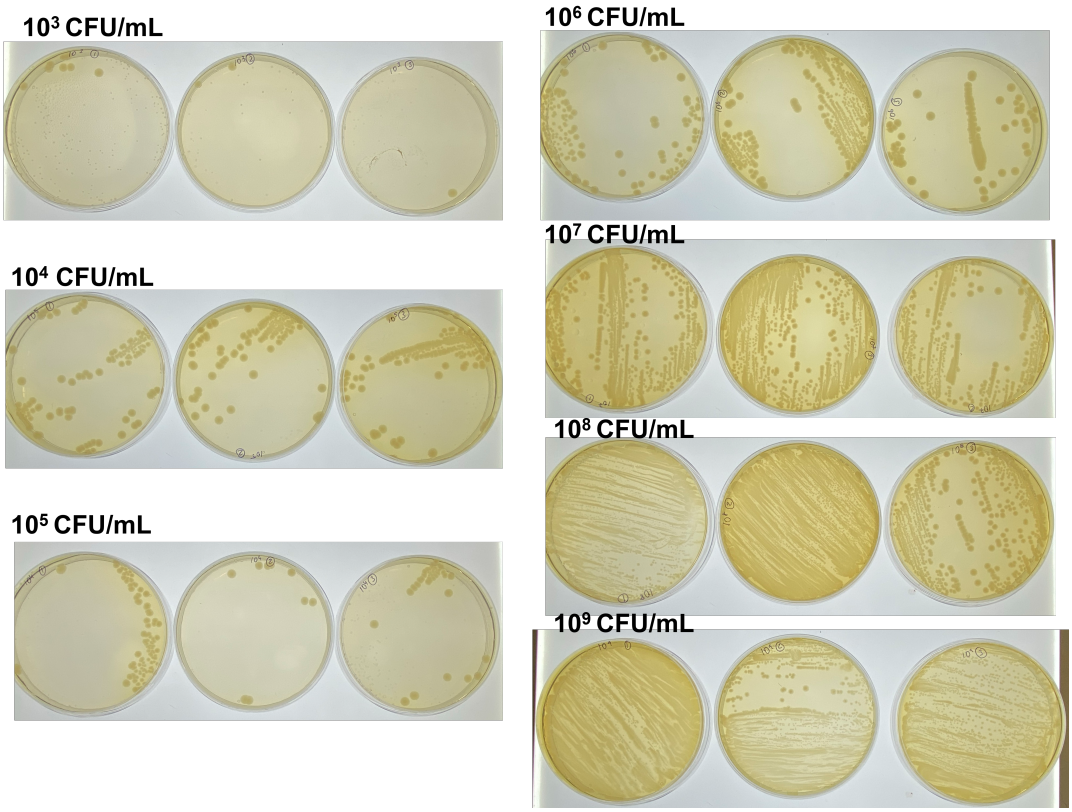

Figure 4-4: Standard concentrations of bacteria streaked on to LB agar, used to semi-quantify bacteria present in the drainage bag from participants.

Table 4.6: Bacteria identified in each of the samples donated by the participants.

Study ID	**Species identified**
RUH01	*Shigella flexneri* *Pseudomonas aeruginosa* *Enterococcus faecalis*
RUH02	*Shigella flexneri*
RUH03	*Pseudomonas aerugionosa*
RUH04	*Staphylococcus epidermidis*
RUH05	*Enterococcus faecium*
RUH06	*Proteus mirabilis*
RUH07	*Enterococcus faecalis* *Proteus mirabilis*
RUH08	*Brevibacterium frigoritolerans* *Proteus alimentorum*
RUH09	*Escherichis spp.* *Pseudomonas aeruginosa* *Proteus mirabilis*
RUH10	*Mammaliiococcus lentus* *Proteus mirabilis* *Staphylococcus epidermidis*
RUH11	*Escherichia spp.* *Proteus mirabilis*
RUH12	*Klebsiella michiganensis* *Proteus mirabilis*
RUH13	*Proteus mirabilis*
RUH14	*Klebisella michiganensis* *Morganella morganii*
RUH15	*Enterobacter hormaechei*
RUH16	*Enterococcus faecalis* *Proteus mirabilis*
RUH17	*Klebisella quasivariicola* *Pseudomonas aeruginosa* *Shigella flexneri*

RUH18	*Escherichia fergusonii* *Shigella flexneri*
RUH19	*Proteus mirabilis*
RUH20	*Citrobacter koseri* *Enterobacter faecalis*
RUH21	*Pseudomonas junteni* *Staphylococcus schweitzeri*
RUH22	*Klebsiella pneumoniae* *Pseudomonas aeruginosa*
RUH23	*Enterococcus faecalis* *Pseudomonas aeruginosa*
RUH24	*Enterococcus faecalis* *Escherichia fergusonii* *Pseudomonas aeruginosa*
RUH25	*Citrobacter koseri*
RUH26	*Proteus mirabilis*
RUH27	*Klebsiella aerogenes*
RUH28	*Enterococcus faecalis* *Enterobacter hormaechei*
RUH29	*Enterococcus faecalis* *Corynebacterium spp.*
RUH30	*Enterococcus faecalis* *Pseudomonas aeruginosa*
RUH31	*Klebsiella michiganensis* *Proteus mirabilis*
RUH32	*Klebisella michiganensis* *Proteus mirabilis*
RUH33	*Staphylococcus epidermidis* *Klebsiella michiganensis*
RUH34	*Providencia spp.* *Klebsiella pneumoniae*
RUH35	*Pseudomonas aeruginosa* *Citrobacter koseri*

Table 4.7: Quality of Life questionnaire scores

Participant ID	**Type of catheter**	**Q4a**	**Q5b**	textbfQ6b	**Q8b**	**Q9b**	**Q10b**	**Q11b**	**Q12a**	**Catheter Function**	**Lifestyle**	**Q16b**	**Q17b**	**Q18b**	**Q19b**
RUH01	urethal	0	0	0	0	2	2	3	3	6	5	-	-	-	-
RUH02	urethal	7	2	3	3	7	8	4	9	17	0	8	0	0	0
RUH03	urethral	2	2	1	1	0	0	0	0	7	12	8	0	0	0
RUH04	supra-pubic	3	3	4	4	0	10	7	2	14	9	-	5	0	-
RUH05	urethral	6	8	7	6	6	5	7	8	21	15	4	7	5	-
RUH06	supra-pubic	0	0	0	0	0	0	0	0	3	6	0	0	0	0
RUH07	supra-pubic	8	7	7	5	9	8	9	8	27	14	0	-	8	-
RUH08	urethal	1	8	1	5	1	1	6	9	20	7	-	9	5	-
RUH09	urethal	2	0	2	4	5	1	0	0	9	5	0	- 2	0	-
RUH10	urethal	0	3	3	0	0	0	0	0	2	9	0	0	0	-
RUH11	urethal	1	1	0	0	0	0	0	2	11	5	7	0	0	0
RUH12	urethal	2	1	3	0	3	3	3	2	13	7	8	2	2	0
RUH13	supra-pubic	5	7	5	2	0	4	6	4	13	13	4	8	5	1
RUH14	supra-pubic	1	8	5	3	0	5	5	5	17	5	10	0	5	-
RUH15	urethal	0	2	2	2	0	0	0	0	7	15	0	0	4	-
RUH16	urethal	10	3	10	5	1	5	9	8	23	9	0	10	5	0
RUH17	urethal	1	1	0	0	0	1	2	3	5	6	1	0	1	0
RUH18	urethal	1	0	0	0	0	0	0	0	5	6	2	2	0	0
RUH19	supra-pubic	8	7	7	5	2	2	1	5	16	9	7	4	5	-
RUH20	urethal	0	0	0	0	0	0	0	0	4	3	0	1	0	0
RUH23	urethal	10	10	0	5	0	4	1	8	19	6	1	3	0	6
RUH24	supra-pubic	0	5	-	-	-	-	-	-	1	6	0	0	0	5
RUH25	urethal	0	2	-	5	3	0	0	0	6	4	0	2	0	0
RUH27	urethal	5	2	0	3	0	0	0	1	7	4	1	2	0	-
RUH28	urethal	5	7	2	1	2	1	5	9	17	-	-	5	10	-
RUH29	urethal	8	5	4	2	5	0	2	4	15	5	0	5	0	-
RUH33	supra-pubic	1	1	0	0	0	10	5	0	7	6	2	2	2	8
RUH34	urethal	1	5	0	0	2	0	0	4	11	6	1	1	0	1

4.8 Bibliography

[1] Heylen RA, Branson M, Gwynne L, Patenall BL, Hauschildt N, Urie J, et al. Optimisation of a lozenge-based sensor for detecting impending blockage of urinary catheters. Biosensors and Bioelectronics. 2022;197(November 2021):113775. Available from: https://doi.org/10.1016/j.bios.2021.113775.

[2] Cotterill N, Fowler S, Avery M, Cottenden AM, Wilde M, Long A, et al. Development and Psychometric Evaluation of the ICIQ-LTCqol: A Self-Report Quality of Life Questionnaire for Long-Term Indwelling Catheter Users. Neurourology and Urodynamics. 2016;35:423–428. Available from: https://doi.org/10.1002/nau.22729.

[3] Srinivasan R, Karaoz U, Volegova M, MacKichan J, Kato-Maeda M, Miller S, et al. Use of 16S rRNA gene for identification of a broad range of clinically relevant bacterial pathogens. PLoS ONE. 2015;10(2):1–22. Available from: https://doi.org/10.1371/journal.pone.0117617.

[4] Shackley DC, Whytock C, Parry G, Clarke L, Vincent C, Harrison A, et al. Variation in the prevalence of urinary catheters: A profile of National Health Service patients in England. BMJ Open. 2017;7(6):1–8. Available from: https://bmjopen.bmj.com/content/7/6/e013842.

[5] Cox T. Bath and North East Somerset Clincial Commissioning Group.; 2018. Available from: https://bsw.icb.nhs.uk/wp-content/uploads/sites/6/2022/06/Annual-Report-BaNES-CCG-2018-19-FINAL-1.pdf.

[6] Stickler DJ, Feneley RCL. The encrustation and blockage of long-term indwelling bladder catheters: A way forward in prevention and control. Spinal Cord. 2010;48(11):784–790. Available from: https://doi.org/10.1038/sc.2010.32.

[7] Kunin CNM. Blockage of urinary catheters: Role of microorganisms and constituents of the urine on formation of encrustations. Journal of Clinical Epidemiology. 1989;42(9):835–842. Available from: https://doi.org/10.1016/0895-4356(89)90096-6.

[8] Nicolle LE. Catheter associated urinary tract infections. Antimicrobial Resistance & Infection Control. 2014;3(1):1–8. Available from: https://doi.org/10.1186/2047-2994-3-23.

[9] Choong SKS, Hallson P, Whitfield HN, Fry CH. The physicochemical basis of urinary catheter encrustation. British Journal of Urology International International.

1999;83(7):770–775. Available from: https://doi.org/10.1046/j.1464-410x.1999.00014.x.

[10] Hagen S, Sinclair L, Cross S. Washout policies in long-term indwelling urinary catheterisation in adults. Cochrane Database of Systematic Reviews. 2017;2017(3). Available from: https://doi.org/10.1002/14651858.CD004012.pub5.

[11] Bradbury RS, Reid DW, Champion AC. Urease production as a marker of virulence in Pseudomonas aeruginosa. British Journal of Biomedical Science. 2014;71(4):175–177. Available from: https://doi.org/10.1080/09674845.2014.11978060.

[12] García-Solache M, Rice LB. The enterococcus: A model of adaptability to its environment. Clinical Microbiology Reviews. 2019;32(2). Available from: https://doi.org/10.1128/CMR.00058-18.

[13] Mobley HLT, Island MD, Hausinger RP. Molecular Biology of Microbial Ureases. Microbiological Reviews. 1995;59(3):451–480. Available from: https://doi.org/10.1128/mr.59.3.451-480.1995.

[14] Konieczna I, Zarnowiec P, Kwinkowski M, Kolesinska B, Fraczyk J, Kaminski Z, et al. Bacterial Urease and its Role in Long-Lasting Human Diseases. Current Protein and Peptide Science. 2012;13(8):789–806. Available from: https://doi.org/10.2174{%}2F138920312804871094.

[15] Brenner DJ, O'Hara CM, Grimont PAD, Janda JM, Falsen E, Aldova E, et al. Biochemical Identification of Citrobacter Species Defined by DNA Hybridization and Description of Citrobacter gillenii sp. nov. (Formerly Citrobacter Genomospecies 10) and Citrobacter murliniae sp. nov. (Formerly Citrobacter Genomospecies 11). Journal of Clinical Microbiology. 1999;37(8):2619–2624. Available from: https://doi.org/10.1128/JCM.37.8.2619-2624.1999.

[16] Davin-Regli A, Lavigne JP, Pagès JM. Enterobacter spp.: Update on Taxonomy, Clinical aspects, and Emerging Antimicrobial Resistance. Clinical Microbiology Reviews. 2019;32(4):1–32. Available from: https://doi.org/10.1128/CMR.00002-19.

[17] Norsworthy AN, Pearson MM. From Catheter to Kidney Stone: The Uropathogenic Lifestyle of Proteus mirabilis. Trends in Microbiology. 2017;25(4):304–315. Available from: https://doi.org/10.1016/j.tim.2016.11.015.

[18] Choong S, Wood S, Fry C, Whitfield H. Catheter associated urinary tract infection

and encrustation. International Journal of Antimicrobial Agents. 2001;17:305–310. Available from: https://doi.org/10.1016/s0924-8579(00)00348-4.

[19] Schnauffer JN, Pearson MM. Proteus mirabilis and Urinary Tract Infections. Microbiol Spectr. 2015;3(5):1032–1057. Available from: 10.1128/microbiolspec.UTI-0017-2013.

[20] Getliffe K, Newton T. Catheter-associated urinary tract infection in primary and community health care. Age and Ageing. 2006;35(5):477–481. Available from: https://doi.org/10.1093/ageing/afl052.

[21] Armbruster CE, Smith SN, Johnson AO, Deornellas V, Eaton KA, Yep A, et al. The Pathogenic Potential of Proteus mirabilis Is Enhanced by Other Uropathogens during Polymicrobial Urinary Tract Infection. Infection and Immunity. 2017;85(2):e00808–16. Available from: https://doi.org/10.1128/IAI.00808-16.

[22] Armbruster CE, Mobley HLT, Pearson MM. Pathogenesis of Proteus mirabilis Infection. EcoSal Plus. 2018;8(1):1–73. Available from: https://doi.org/10.1128/ecosalplus.ESP-0009-2017.

[23] Gaston JR, Andersen MJ, Johnson AO, Bair KL, Sullivan CM, Guterman LB, et al. Enterococcus faecalis polymicrobial interactions facilitate biofilm formation, antibiotic recalcitrance, and persistent colonization of the catheterized urinary tract. Pathogens. 2020;9(10):1–20.

[24] Carr HA. A short history of the Foley catheter: From handmade instrument to infection-prevention device. Journal of Endourology. 2000;14(1):5–8.

[25] Stickler D, Feneley R. The Indwelling Bladder Catheter: Attempts to Prevent Infection and the Development of Bacterial Biofilms. New York: Springer Science+Business Media New York; 2013.

[26] Singh R, Rohilla RK, Sangwan K, Siwach R, Magu NK, Sangwan SS. Bladder management methods and urological complications in spinal cord injury patients. Indian Journal of Orthopaedics. 2011;45(2):141–147.

[27] Kunin CM, Chin QF, Chambers S. Formation of encrustations on indwelling urinary catheters in the elderly: A comparison of different types of catheter materials in 'blockers' and 'nonblockers'. Journal of Urology. 1987;138(4):899–902. Available from: http://dx.doi.org/10.1016/S0022-5347(17)43412-4.

[28] Kohler-Ockmore J, Feneley RCL. Long-term catheterization of the bladder: Prevalence and morbidity. British Journal of Urology. 1996;77(3):347–351.

Chapter 5

Rational Design of New Urease Inhibitors to treat Long-term Urinary Catheter Blockage

5.1 Chapter Overview

The aim of this research was to identify a urease inhibitor which could be utilized as a preventative treatment for patients with recurrent urinary catheter blockage. Additionally, this chapter explores a 'rational drug design method' whereby *in silico* docking is used to predicted potential compounds prior to *in vitro* experimentation.

5.2 Introduction

As introduced during Section 1.2.1, urease is a pivotal enzyme in causing catheter blockage. Therefore, it is surprising that currently there is only one licensed urease inhibitor: AHA (Section 1.5.2.1). Milo *et al.*, discovered 2-MA, a small compound with urease inhibitory activity and natural compounds have been identified as urease inhibitors (Section 1.7.2.4).[1] The majority of new small-molecule drugs are discovered using HTS, synthetic Chemists produce large libraries of compounds which are tested against enzymatic targets in activity assays or against bacteria in MIC assays - when identifying new antibiotics. This is a costly and expensive process, therefore this step was replaced with *in silico* docking of ligands designed around known urease inhibitors. During the design of the ligand screen, we did not want the screen to be restricted therefore, whether the compound could be synthesised was not taken into account at the beginning. N. Cusick (who designed the screen) used rational decisions based on how the ligand was docking into the active site of urease and what binding contacts were made with the amino acids present in the active site. Newly identified potential urease inhibitors were then tested in *in vitro* enzymatic assays and whole-cell urease assays. Employment of the *in vitro* catheterised bladder model allowed testing of the key compound in its ability to prevent catheter blockage. Delivery of the compound was important, utilizing the Biomodics IPN catheter allowed a site-directed drug delivery mechanism. This is advantageous because targeted delivery means the drug can be delivered at a higher concentration to the right place. For patients already using a long-term catheter the use of a Biomodics catheter would not impact their care and with the employment of a urease inhibitor the catheter would last longer and have less complications. Standard cytotoxicity assays were also completed to determine whether the compound was toxic.

5.3 Methods

General methods are described in Chapter 2. The following methods are specific to this Chapter.

5.3.1 Designing the Compound Series

The compound series of ligands was designed by Nicola Cusick as part of her chemistry Masters research project, which was supervised by Rachel Heylen.

There is already existing research into urease inhibitors (Section 1.7.2). The aim in the design of the compound series was to use the knowledge of urease inhibitors and design various compounds based on these structures. We called this rational design. The following inhibitors were used to design five series: (A) thiourea,[2,3,4,5] (B & C) 2-MA,[1] (D) quercetin,[6,7] and (E) quercetin and 2-MA. Each of the compounds designed were assessed for whether they contain: HBA and HBD groups, hydrophobic chains, aromatic groups, and sulfur-containing groups. Appendix 5-16, 5-17, 5-18, 5-19, 5-20; shows all the compounds within each of the series. All compounds were prepared using ChemDraw 19.1.1.21 (PerkinElmer Informatics, Waltham, Massachusetts, US), and 3D models generated using Chem3D 15.0 (PerkinElmer Informatics, Waltham, Massachusetts, US). Compounds were docked as described in Section 2.2.4. Ligands which were enantiomers, were docked in both 'R' and 'S' configurations. The outline for the rational drug design is shown in Figure 5-1.

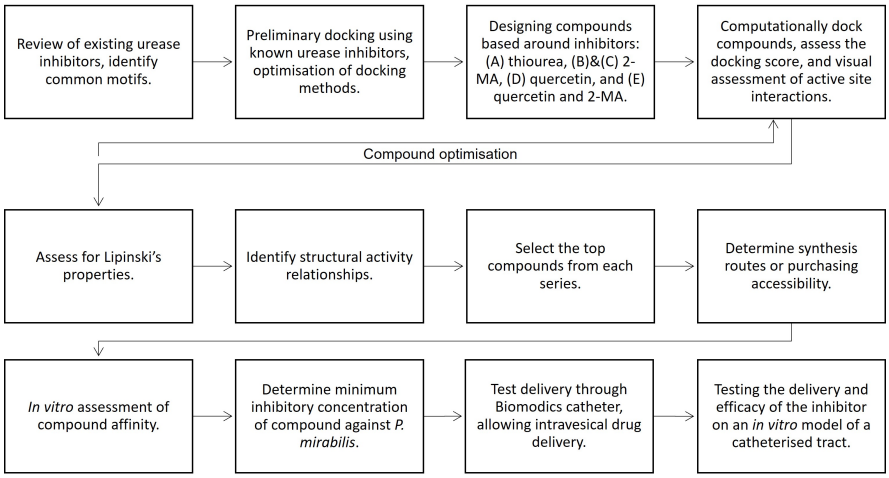

Figure 5-1: Flow diagram showing the strategy for identifying new urease inhibitors.

5.3.2 Biomodics Catheter Kinetic Release Studies

The Biomodics catheter is described in Section 1.8. The Biomodics catheter has a balloon made from an IPN, thus allowing the diffusion of a drug solution directly into the bladder. It is believed that the hydrogel (poly(HEMA-co-PEGMEA)) forms

pores within the silicone surface, therefore allowing the diffusion of drugs. As this is still a relatively new device, the optimal properties for the drug delivery through the membrane are not yet known. Prior to using the Biomodics catheter in an *in vitro* bladder model, it was important to test whether the drug solution could cross the IPN and enter the bladder. AHA and Bis-TU were measured using UV-vis spectroscopy using a quartz cuvette (1 cm pathlength) (Agilent Cary 60 UV-vis spectrometer). A calibration curve was prepared using range of concentrations of AHA and Bis-TU, full wavelength spectra were performed and the peak of each spectra; absorbances 235 nm and 239 nm were used to determine the quantity of AHA and Bis-TU release, respectively (Appendix 5-21). The spectrometers were blanked using AU.

To measure the release, sterile 50 mL beakers were used to mimic the bladder. Each beaker was filled with AU (30 mL), the catheter was inflated with the compound (10 mL); AHA (320 mM, 10% (v/v) DMSO) or Bis-TU (85 mM, 10% (v/v) DMSO) dissolved in AU. The catheters were secured within the beaker and submerged, they were kept in place with paper clips and covered with paraffin to prevent evaporation. The Biomodics catheter was compared to a standard silicone catheter (Tiga-Med, Germany). Catheters were incubated at 37 °C for 12 h, at every hour 1 mL of solution was removed and the absorbance measured. The sample was returned to the beaker, to keep the volume consistent. The quantity of compound was calculated using the calibration curve. Limit of detection (LOD) was calculated according to equation 5.1.

$$LOD = \frac{3\sigma}{slope} \tag{5.1}$$

$$\sigma = standard\ deviation\ of\ the\ lowest\ concentration.$$

5.3.2.1 Testing the Biomodics catheter and compounds in an *in vitro* bladder models

In vitro bladder models were set up as described in Section 2.2.3. A different pump was used: Watson-Marlow 323S/D (030.3134.3DU), calibrated to deliver 0.8 mL/min. Models were catheterised with Biomodics catheters (donated by Biomodics ApS, Denmark). The catheter balloons were inflated with 10 mL of the drug solutions: control bladder: saline (10% (v/v) DMSO) (150 mM sodium chloride) and DMSO; Bis-TU bladder: 20 mM Bis-TU (dissolved in saline, 10% (v/v) DMSO); and AHA bladder: 20 mM AHA (dissolved in saline, 10% (v/v) DSMO. To prevent bursting of the balloon the solutions were gradually injected into the balloon, prior to insertion, the balloon

material was stretched and manually manipulated into a round shape. Models were filled with AU until the catheter began to drain, the pump was stopped, and the compound solution allowed to diffuse through the balloon and equilibrate with the AU for 18 h. Bladders were inoculated with *P. mirabilis* diluted to 3.7×10^7 CFU/mL (5 mL) which was added to each bladder; this mimicked a late stage infection. At regular times during the experiment samples were removed aseptically from each bladder for bacterial quantification (Section 2.2.1.1) and to measure the pH. The end of the experiment was when the catheter blocked, time to block. Models were monitored by time-lapse photography overnight using a Nikon D31000 camera with photographs taken every 2 min.

5.3.3 Cytotoxicity Testing

5.3.3.1 *Ex vivo* Hemolysis Assay

This experiment was ethically approved by REACH reference: EP 18/19 108. Target solutions of compounds tested were prepared at concentrations of 10 mM with 1% (v/v) DMSO. Compounds tested here were AHA and Bis-TU. Compounds were serially diluted across a 96-well plate (100 μL). Whole blood was obtained from three consenting donors. It was drawn directly into lithium heparin-coated vacutainer tubes. The whole blood was centrifuged, 500 g for 10 min at 4 °C (5810 R Eppendorf), the supernatant (plasma) was removed and replaced with double the volume of saline solution (150 mM sodium chloride). Erythrocyte pellet was re-suspended and the solution re-centrifuged. This washing method was repeated three times. The erythrocyte pellet was finally diluted 1% (v/v) with saline and incubated in a 96-well plate (100 μL) with the concentrations of compounds, including a negative control (just saline) and a positive control (1% triton), for 1 h at 37 °C under steady rotation. Post-incubation the plate was centrifuged at 500 g for 5 min and the supernatant was transferred to a new 96-well plate. The absorbance was measured at 404 nm (Tecan Sunrise) and the degree of hemolysis calculated using equation 5.2.

$$\%\, hemolysis = \frac{absorbance\, of\, sample\, cells}{absorbance\, of\, lysed\, cells} \times 100 \tag{5.2}$$

5.3.3.2 HepG2 Mammalian Cell Viability Assay

HepG2 cells were kindly gifted by Prof. David Tosh. HepG2 cells are often used to test for toxicity in pharmaceutical research.[8] Freezer stocks of HepG2 cells were defrosted and re-suspended in DMEM. A T75 (Nunc) flask was seeded with 10 mL of complete DMEM and grown for 3-4 days until adherent cells were achieved, 37 °C, 5% CO_2. The old media was washed away and 5 mL of PBS was added to wash the cells, this was removed and cells were incubated with 3 mL of 0.25% trypsin in PBS (which was pre-warmed to 37 °C) for 7 min at 37 °C. Post incubation cells were checked using a microscope (Nikon TMS inverted phase contrast) to ensure they were no longer adherent. Cells were dissociated with 4 mL of media and re-suspended by pipetting 10 mL approximately 20 times. Cells were centrifuged for 3 min at 1000 rpm and the media aspirated away. The cell pellet is re-suspended in 1 mL of media. Cells are counted using a hemocytometer and new flasks are seeded with 200 μL of cells to 10 mL of media. To maintain stocks, cells are subcultured every 2-3 days.

Compounds were prepared at 10 mM with 1% (v/v) DMSO in DMEM, compounds tested here were AHA and Bis-TU. Compounds were serially diluted across a 96-well plate (100 μL). MTT (Invitogen) assay was used to measure the cells metabolic activity. Cell culture plates, 96-well (Nunc) were seeded with 1×10^4 cells/well and grown for 24 h. The media/compound was aspirated away and MTT (1 mg/mL) in DMEM (which was filter sterilized) was added to each well (100 μL). The plate is incubated for 60 min at 37 °C and then the MTT is removed. Isopropanol (150 μL) is added to each well and the plate is incubated in foil for 15 min on an orbital shaker. Absorbance is measured at 590 nm (reference filter 620 nm) (Sunrise Tecan). The % survival is calculated using equation 5.3.

$$\%\, survival = \frac{absorbance\, of\, treated\, cells}{absorbance\, of\, untreated\, cells} \times 100 \tag{5.3}$$

5.4 Results and Discussion

5.4.1 *In silico* Docking Results

The compound series was designed based on known urease inhibitors, these were docked on to the crystal structure of urease from *S. pasteurii*. The LF dG score has been optimised for describing protein-ligand binding, the more negative the score the better

the binding. Known urease inhibitors, AHA (Fig. 5-2) and the substrate, urea, were docked into the active site to test the docking procedure (Fig. 5-3). Figure 5-4, shows the compound series generated for the screen, full structures of the compounds can be found in the Appendix 5.6.

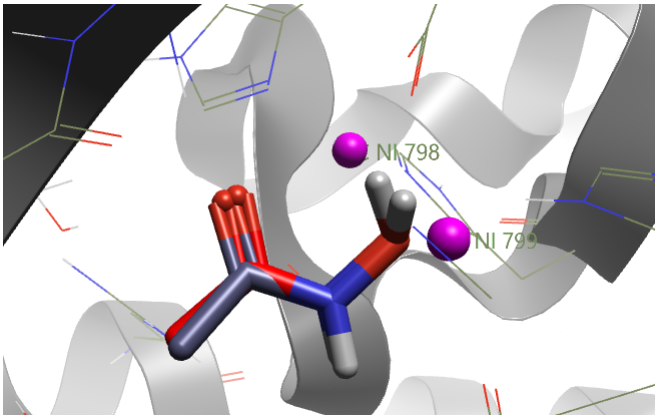

Figure 5-2: Acetohydroxamic acid (AHA) docked into the active site. The top compound is the crystallized AHA and the bottom is the docked ligand AHA, RMSD = 0.977 Å. Pink spheres indicate the Ni ions in the active site. Image generated using Flare™ from Cresset®.

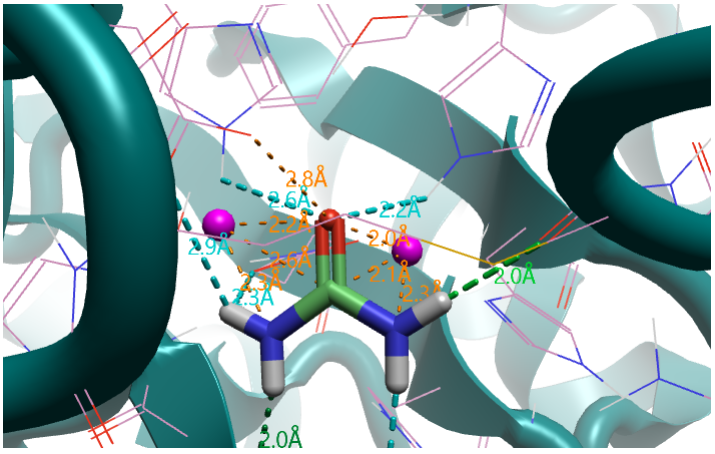

Figure 5-3: Urea the substrate of urease, docked into the active site. Pink spheres indicate the Ni ions in the active site. Image generated using Flare™ from Cresset®.

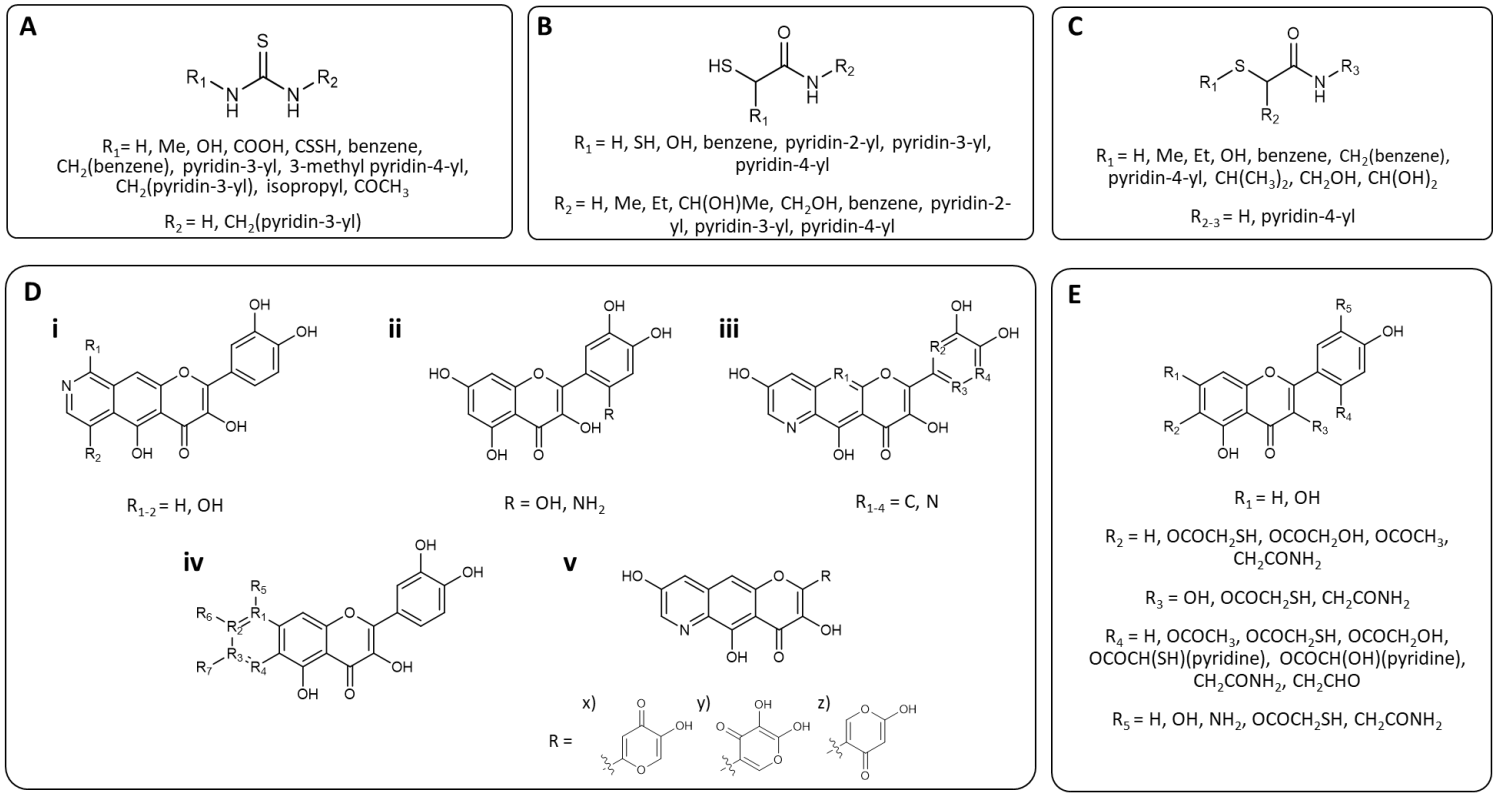

Figure 5-4: The chemical structures of the compounds docked to urease. Series (A) is based around thiourea, (B) and (C) 2-mercaptoacetamide (2-MA), (D) quercetin and (E) 2-MA and quercetin. Compounds are drawn using ChemDraw 19.1.1.21 (PerkinElmer Informatics, Waltham, Massachusetts, US).

In silico docking is a useful tool for assessing potential compounds however, care should be taken in the interpretation of the results. Higher molecular weight compounds tend to bias towards a higher docking score.[9] Therefore, it is good practice to also assess the images of the compounds docked into the active site and identify contacts between the protein and the ligand. Docking of the known inhibitor, thiourea, showed the formation of two hydrogen bonds between the amine hydrogen on the thiourea and Asp-383 and Gly-280 on urease (Fig. 5-5A). During the design of Series A, which was based around thiourea, the N-H was kept thus maintaining the hydrogen bond donor capacity. Series A, compounds A1-A17 were docked and it was observed that the carboxylic derivative was forming a hydrogen bond with the His-222, this allowed the alignment of the compound to ensure coordination with the Ni^{2+} ions. This was in agreement with literature where a carboxyl was identified as interacting with the Ni centre, resulting in increased urease inhibition.[10] Hydrogen bond formation was also observed by the pyridine ring interacting with His-222 and cation-pi interactions with the nitrogen from Arg-339 (Fig. 5-5B).

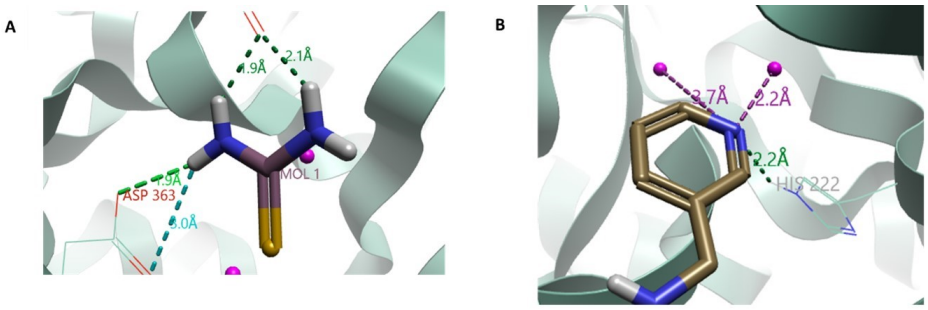

Figure 5-5: (A) Thiourea docked into the active site of urease. Distance measured from the amine hydrogen to Asp-383 and Gly-280, show the predicted hydrogen bonds which have formed. (B) Compound A11 docked and forming hydrogen bonds between the pyridine ring and His-222 and interactions between the Ni^{2+} ions in the active site. Ni^{2+} ions shown as pink spheres. Urease (PDB: 4UBP) shown as green ribbon, selected amino acids as thin sticks and compound docked as thick sticks. Molecules docked and images generated with Cresset®Flare™ v. 4.0.2.

Series B was designed with the incorporation of 2-MA, which has been shown to increase the lifetime of a catheter in an *in vitro* bladder model.[1] The pyridine ring from series A was incorporated into this series. B17 had the most negative score, this contained azaheterocycles (Fig. 5-6A). For series C, the compound design was optimised by increasing the length of the compound. It was hypothesised that this increase in length would improve the hydrophobic interactions between the compound and the active site. Originally a sulfide had been included as this was present in 2-MA and thiourea, however it was observed that there were no predicted interactions involving the sulfide.

Therefore, it was replaced with a carbonyl because it was predicted that the oxygen would be less toxic compared to the sulfur and would cause fewer unspecific interactions (compounds C21-24).[11] Analysis of the docking score showed that changing the sulfide to a carbonyl did not significantly affect the docking score: C10 LF dG = -10.165 vs C24 (S) LF dG = -8.526, although more contacts were identified visually (Fig. 5-6B, Table 5.2). This indicates the importance of manually checking the docking of each compound, alongside the assessment of the docking score.

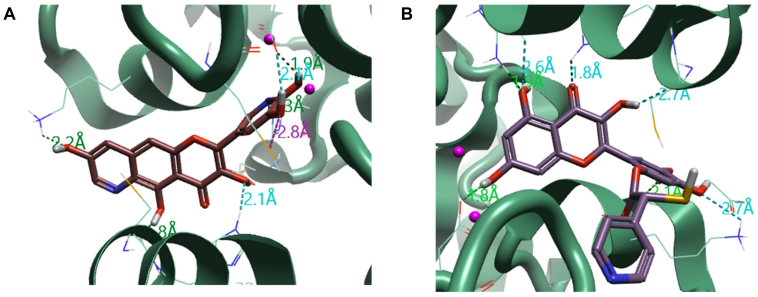

Figure 5-6: (A) B17 (R) containing two pyridine rings which improved the docking score. (B) C24 docked (S) with dotted lines demonstrating the interactions with amino acids: Asp-224, Arg-339, and His-323. Ni^{2+} ions shown as pink spheres. Urease (PDB: 4UBP) shown as green ribbon, selected amino acids as thin sticks and compound docked as thick sticks. Molecules docked and images generated with Cresset ®Flare™ v. 4.0.2.

The natural product, flavonoids, have been identified as urease inhibitors (Section 1.7.2.4).[6] To assess our docking experiments against published *in vitro* and *in silico* data, five flavonoids were docked and their scores compared to the IC_{50} literature results (Section 1.6.2). The published *in silico* data was completed using the crystal structure of urease from *C. ensiformis*.[12] The docking scores from our experiment followed the trend observed with the *in vitro* and *in silico* published data, thus supporting our docking methodology (Fig. 5-7). The flavonoid, chlorogenic acid, appears to have the greatest potency. It was hypothesised that this was due to the extra length of the compound, which increased the likelihood of contacts within the active site. Therefore, in the design of series D, an extra ring was added to quercetin to increase the number of interactions.

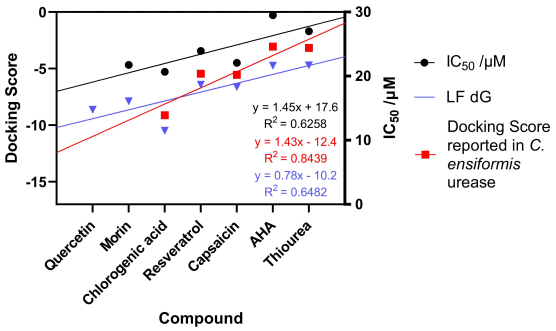

Figure 5-7: LF dG (blue) is the calculated docking score based on the docking results for the flavonoids, acetohydroxamic acid (AHA), and thiourea. The docking score taken from Katrina *et al.,* (red) calculated against urease from *Canavalia ensiformis* (PDB: 3LA4). *In vitro* IC_{50} taken from Xiao *et al.,*(black).[12,6] Graph prepared using GraphPad Prism version 9.4.1. Urease (PDB: 4UBP) was used for docking experiments. Molecules docked with Cresset®Flare™ v. 4.0.2.

From series D, compound Diii2, measured the most negative docking score at -11.171. Interactions within the active site were observed, as well as contacts towards the edge of the protein (Fig. 5-8A). Xiao *et al.,* reported that flavonoids appear to dock more favourably to the active site flap and the results from the docking experiment support this hypothesis.[6] Figure 5-9 demonstrates the distinction between the active site and the active site flap.

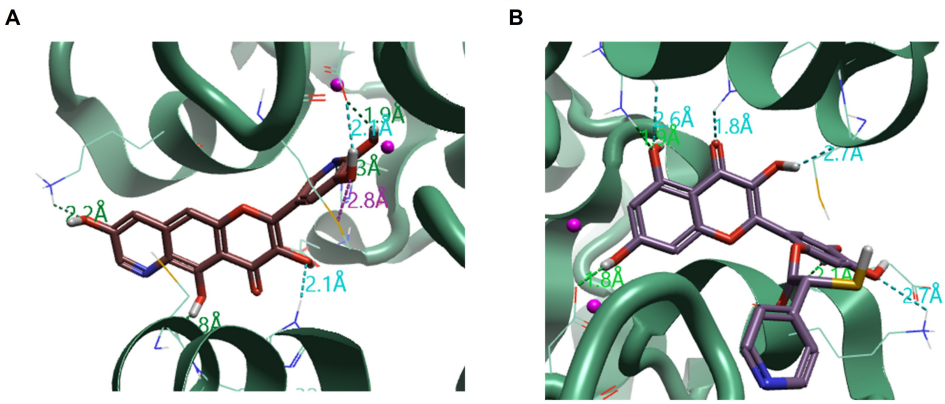

Figure 5-8: (A) Compound from Series D, Diii2, docked into the active site and active site flap. Interactions made with flap: Cys-322 and His323, and within the active site: His-222, Asp-363, and Met-367. (B) Compound from Series E, E5 (R), docked to urease. Contacts made with the active site: Asp-363 and Arg-339, and the active site flap: Cys-322 and His-323. Urease (PDB: 4UBP) was used for docking experiments, shown in green ribbon, selected amino acids as thin sticks and compound docked as think sticks. Molecules docked with Cresset Flare v. 4.0.2. Images generated using Flare™ from Cresset®.

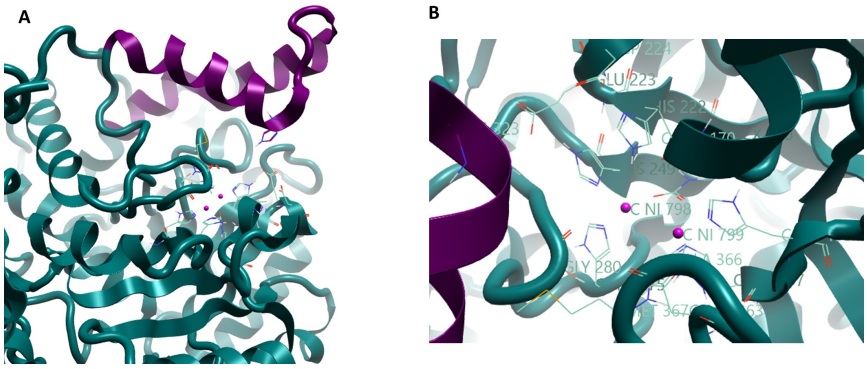

Figure 5-9: (A) Overview of the active site, demonstrating the difference between the active site flap (purple) and the active site which is around the two Nickel ions (pink spheres). The flap is made up of a helix-turn-helix motif. Urease taken from *Sporosarcina pasteurii* (PDB: 4UBP) in teal ribbon. (B) Close up view of the active site, active site amino acids shown as thin stick. those involved in coordinating the Ni ions: carbamylated Lys-220, His-249, His-275, His-137, His-139, and Asp-363. Those involved in catalytic mechanism: Ala-170, His-222, Glu-223, Asp-224, Gly-280, His-323, Ala-366, Met-367. Amino acid assignment taken from Benini *et al.*[13] Images generated using Flare™ from Cresset®.

The results from series C and D concluded that 2-MA could potentially be used as a warhead, with direct interactions within the active site; binding to amino acids involved in catalysis. Whilst the flavonoid-based compound, can act as a tail-end and interact with the active site flap. Therefore, for series E, 2-MA was incorporated on the flavonoid scaffold. Compound E5 (S) resulted in the most negative score of -12.902. Interactions with Cys-322, found in the active site flap, were observed (Fig. 5-8B).[14] Throughout the series the compounds have got bigger and the docking of these larger compounds was slightly restricted by the grid box. If future investigations into these larger compounds were to take place, a larger grid box would need to be designed.

5.4.1.1 Filtering the *in silico* compound screen for SAR.

The compounds were now filtered by physical properties such as, Lipinski's 'rule of five' (Fig. 5-1). The 'rule of five' states that compounds which are drug-like tend to have the following attributes: <5 HBD, <10 HBA, molecular weight <500 Da and logP <5. These are designed around oral delivery, not necessarily diffusion through the Biomodics IPN catheter. However, the properties do crossover and Lipinski's 'rule of five' offers an opportunity to filter the compound list. Diffusion across a membrane depends on solubility and diffusivity, solubility is an important element in oral drug delivery, as well as diffusivity which is important for drugs crossing cell membranes.[15] Therefore, Lipinski's 'rule of five' is a relevant filtering mechanism to use. SAR were identified following filtration. All the top compounds contained a carbonyl group and those from

series C, D, and E contained a catechol moiety. In 18 of the top 20 compounds a pyridine ring was present. Hydrophobic domains were also common, specifically in compounds which scored a high docking score. This agreed with published studies which suggested that hydrophobic behaviour leads to successful urease inhibition.[10] The majority of the top compounds came from series D, flavonoid series. The next step was to assess for accessibility in getting these compounds either by synthesise or purchasing them. Unfortunately, the majority of these compounds are complicated to synthesis and cannot be purchased. This was the first round of drug discovery, which could be an iterative process following Figure 5-1. Therefore, it was decided to obtain the compounds which were simpler in structure, from the thiourea series, and test these out using in *in vitro* tests. The following compounds were purchased from Fluorochem, UK: A5 (N-phenylthiourea), A6 (benzylthiourea), and A11 (N, N'-Bis(3-pyridinylmethyl)thiourea (Bis-TU)).

5.4.2 *In vitro* Experimentation

5.4.2.1 Urease activity assay

The selected compounds: A5, A6, and A11 were tested against purified *C. ensiformis* urease. This allowed the IC_{50} to be determined and compared to control compounds. The following compounds were used as controls: AHA,[16] 2-MA,[1] and quercetin,[6] these are known urease inhibitors. Specifically, AHA which is the only licensed urease inhibitor. Figure 5-10A shows the IC_{50} curves for each of the compounds. All the compounds which were tested were potent against *C. ensiformis* urease and reduced the activity of the enzyme. Newly identifed compound, A11, was 500-fold more potent than AHA, the clinical standard. The three compounds identified in the *in silico* screen: A5, A6, and A11 all outperformed the control compounds (Fig. 5-10A).

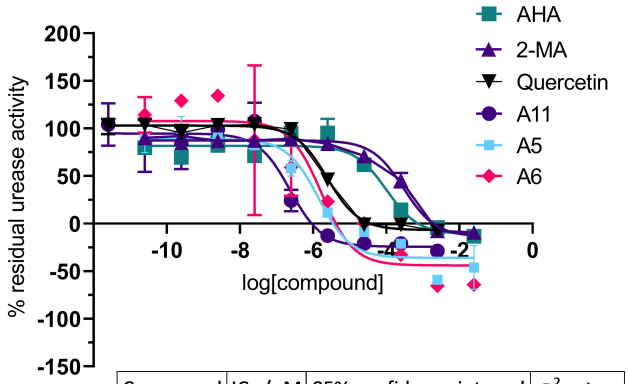

Compound	IC_{50}/µM	95% confidence interval	R^2 value
AHA	101.9	56.23 - 182.2	0.9396
2-MA	299.0	210.2 - 421.6	0.9748
Quercetin	2.413	1.852 - 3.139	0.9855
A11	0.235	0.121 - 0.471	0.9096
A5	1.479	0.618 - 3.108	0.9348
A6	1.705	0.231 - 111.0	0.8253

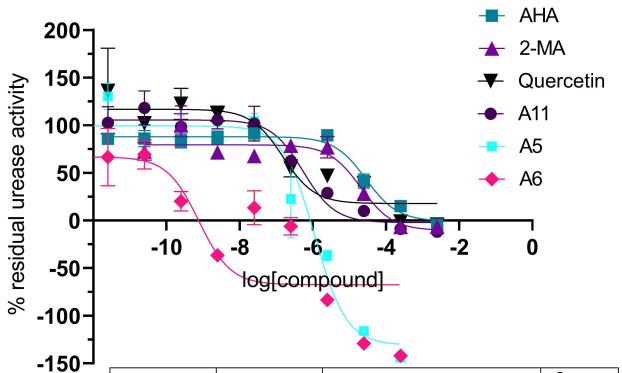

Compound	IC_{50}/µM	95% confidence interval	R^2 value
AHA	28.16	18.15 - 44.41	0.9618
2-MA	20.65	10.72 - 38.87	0.9166
Quercetin	Does not form sigmoidal curve.		
A11	0.562	0.2491 - 1.329	0.9305
A5	1.128	0.4342 - 2.552	0.9395
A6	Does not form sigmoidal curve.		

Figure 5-10: IC_{50} graphs. (A) Urease from *Canavalia ensiformis* measured against the following compounds: Acetohydroxamic acid (AHA), 2- mercaptoacetamide (2-MA), quercetin, A5 (N-phenylthiourea), A6 (benzylthiourea), and A11 (*N,N'*-Bis(3-pyridinylmethyl)thiourea). (B) Urease activity measured from whole cell culture *Proteus mirabilis* against the same compounds in A. IC_{50} calculated using non-linear regression using GraphPad Prism v. 9.4.1. Experiments were completed with three biological repeats. The graphs show the mean of the repeats with error bars representing standard deviation. Graphs generated using GraphPad Prism v. 9.4.1.

Compounds were also tested against whole cell *P. mirabilis*. Urease in *P. mirabilis* is intracellular therefore this assay also tests the ability of the compounds to cross the outer bacterial membrane and access the periplasm.[17] Compounds quercetin and A6 were not effect against *P. mirabilis* and did not form sigmoidal curves (Fig. 5-10B). As these compounds were effective against *C. ensiformis* urease but not whole cell *P. mirabilis*, it was hypothesised that they were unable to cross the outer membrane and access the urease enzyme. A11 demonstrated a 50-fold greater potency compared to AHA. A5 and A11 both outperformed the control compounds. A11 (Bis-TU) was the highest performing compound for the thiourea screen, therefore this was selected for future examinations (Fig. 5-11).

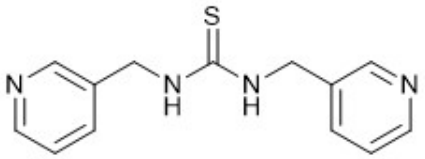

Figure 5-11: Structure of *N,N'*-Bis(3-pyridinylmethyl)thiourea (Bis-TU, A11). Drawn using ChemDraw PerkinElmer, v. 19.0.

5.4.2.2 Minimum Inhibitory Concentration

The urease inhibitors here are designed to knock out the function of urease, the virulence factor (Section: 1.2.1). Therefore, preventing catheter blockage occurring and extending the lifetime of urinary catheters for users. The ability of the compounds to kill common CAUTI causing bacteria: *E. coli* and *P. mirabilis* was assessed, the ranges in which the compounds affected the growth of the bacteria are shown in Table 5.1 (Fig. 5-12). Although killing bacteria would not necessarily be a disadvantage to CAUTI users, the aim of this study was to disarm urease positive bacteria and prevent catheter blockage. As the compounds here were specifically designed to target urease, it was expected that these compounds would not kill bacteria. Additionally, by not killing the bacteria the compounds are not causing a resistance pressure on the bacteria and therefore, it is unlikely the bacteria will develop resistance to the urease inhibitors. High concentrations of AHA and Bis-TU do affect the growth of both species of bacteria: *P. mirabilis* and *E. coli* (Table 5.1, Fig. 5-12). However, they do not appear cytotoxic and instead hinder the growth of the bacteria. Therefore, Bis-TU is unlikely to cause bacterial resistance and is only acting as an anti-virulence strategy.

Table 5.1: Ranges in which for acetohydroxamic acid (AHA) and *N,N'*-Bis(3-pyridinylmethyl)thiourea (Bis-TU) affected the growth of *Proteus mirabilis* and *Escherichia coli*. Neither compound demonstrated full inhibition of growth.

Bacterial Species	**[AHA]/mM**	**[Bis-TU]/mM**
P. mirabilis B4	3.13 - 25.0	1.25 - 5.00
E. coli NSM59	12.5 - 25.0	1.25 - 5.00

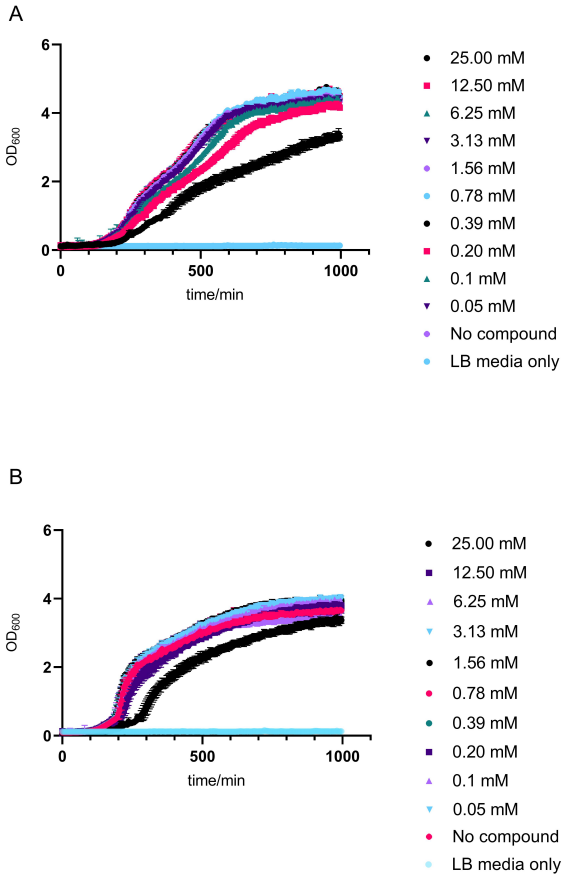

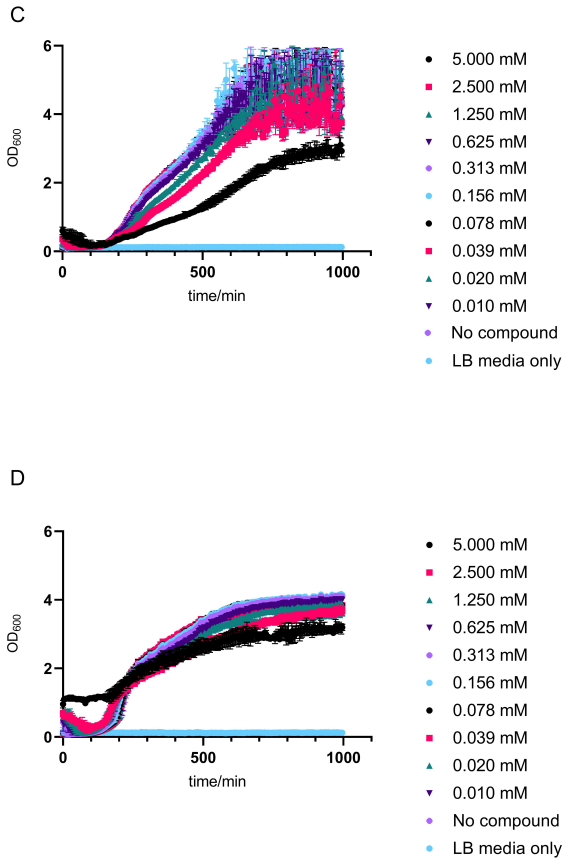

Figure 5-12: Growth curves. (A) *Proteus mirabilis* growth in varying concentrations of acetohydroxamic acid (AHA). (B) *Escherichia coli* grown with AHA. (C) *P. mirabilis* grown with *N,N'*-Bis(3-pyridinylmethyl)thiourea (Bis-TU, A11). (D) *E. coli* grown with Bis-TU. Compounds at the highest concentration contained 2.5% DMSO which was diluted 2-fold as the concentration decreased. Experiments were completed with three biological repeats. The graphs show the mean of the repeats with error bars representing standard deviation. Graphs generated using GraphPad Prism v. 9.4.1.

5.4.2.3 Drug Delivery

As discussed in Section 1.8, Biomodics ApS have designed a catheter that can deliver drugs intravesically via a diffusible catheter balloon. The balloon material, silicone, has been impregnated with a hydrogel which enables the movement of solutes across the membrane. Delivering drugs to the site of action offers multiple advantages: drugs can be delivered directly to the bacteria ensuring a high potent concentration is delivered to the site, additionally drugs which cause side effects when administered orally can be delivered directly to the site without causing systemic toxic effects. For compounds which demonstrate poor solubility, the transfer of drug through the balloon membrane

and water back in both directions enables the solubilisation of the drug within the balloon as the overall concentration is diluted, this could also enable prolonged release. To investigate whether AHA and Bis-TU could be delivered via the Biomodics catheter, diffusion of the compounds was monitored using UV-Vis spectroscopy. Simulated static bladders were generated using AU. Biomodics catheters were compared to standard silicone catheters which are used by long-term catheterised patients (Fig. 5-13). The release rate was calculated and compared to standard silicone catheter release. For both of the compounds tested there was no release of the compounds above the LOD for the standard silicone catheter. Whilst the Biomodics catheter release demonstrated a zero-order kinetic release over the 12 h experiment. Zero-order kinetics is demonstrated by the linear relase of the compounds over 12 hr, this means that the release of the compound over 12 h is not affected by the concentration of the compound in the balloon and instead is determined by the diffusion across the balloon membrane. To conclude, Bis-TU and AHA can be delivered via the Biomodics catheter at a rate independent of drug concentration.

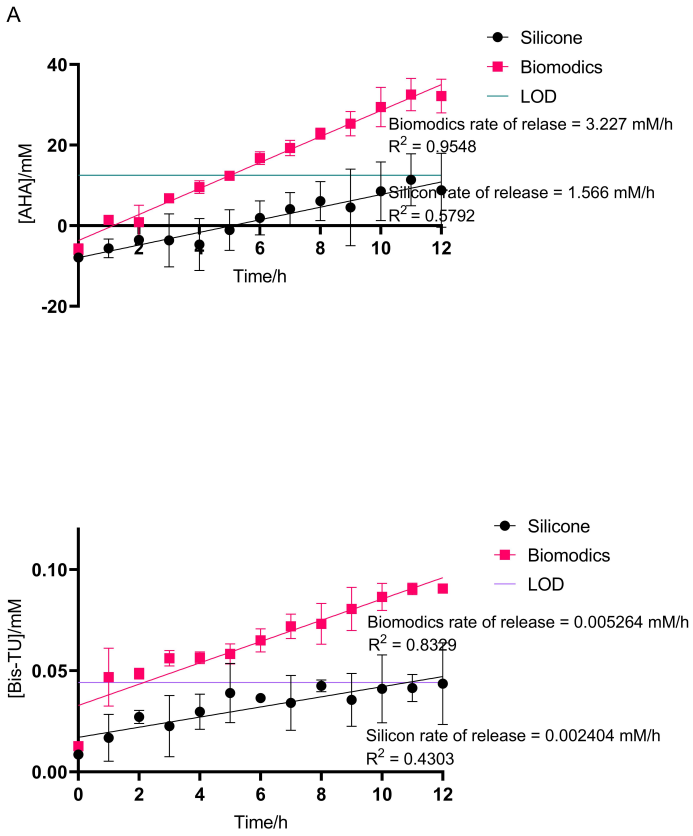

Figure 5-13: Kinetic release studies using a Biomodics IPN catheter. (A) Release of acetohydroxamic acid (AHA). (B) *N,N'*-Bis(3-pyridinylmethyl)thiourea (Bis-TU, A11). Measured across the catheter balloon comparing Biomodics IPN catheters and standard silicone catheters over 12 h. Experiments were completed with three biological repeats. The graphs show the mean of the repeats with error bars representing standard deviation, simple linear regression analysed was used to generate a line of best fit and limit of detection (LOD) is shown. Graphs generated using GraphPad Prism v. 9.4.1.

5.4.2.4 *In vitro* Bladder Models

The *in vitro* bladder model, introduced in Section 2.2.3, are models of a catheterised tract. The model allows the growth of a crystalline biofilm and allows the simulation of urinary catheter blockage.[18,19] The artificial models were infected with high inoculums of bacteria as this represented a late-stage infection. The average inoculation was 3.36×10^7 CFU/mL (standard deviation: 3.6×10^6). Each of the models (3x) were catheterised using a Biomodics IPN catheter, the balloons contained: (1) 20 mM AHA (10% (v/v) DMSO), (2) 20 mM Bis-TU (10% (v/v) DMSO), and (3) control bladder containing saline with 10% (v/v) DMSO. The artificial bladders were allowed to equilibrate over 18 h before inoculation of bacteria. There is approximately a 4-fold dilution of the

compounds during the equilibration process resulting in a concentration of 5 mM at the start of the experiment. The start of the experiment is defined as when the pumps start to move the urine from the 'kidneys' to the bladder. The bladders were inoculated with *P. mirabilis*, left for 1 hour and then the pumps are started. At this point the compounds are continuously diluted owing to the flow of urine into the bladder and out of the catheter, this simulation is comparable to human catheterisation. Throughout the experiment the pH and CFU/mL of *P. mirabilis* is monitored (Fig. 5-14A & B). Bis-TU kept the pH lower than that of the AHA and the control bladders, suggesting that it was inhibiting urease activity (Fig. 5-14A). Whilst the quantity of bacteria within each of the bladders was comparable across all conditions (Fig. 5-14B). The blockage of the catheters, the endpoint of the experiment, was used to compare the compounds and determined whether the compounds could increase the lifetime of the catheter (Fig. 5-14C). Bis-TU significantly outperformed the clinical standard AHA and the control bladder indicating that Bis-TU has anti-ureolytic activity (unpaired t-test, GraphPad Prism 9.4.1, $p = 0.0366$ and $p = 0.426$ respectively.)

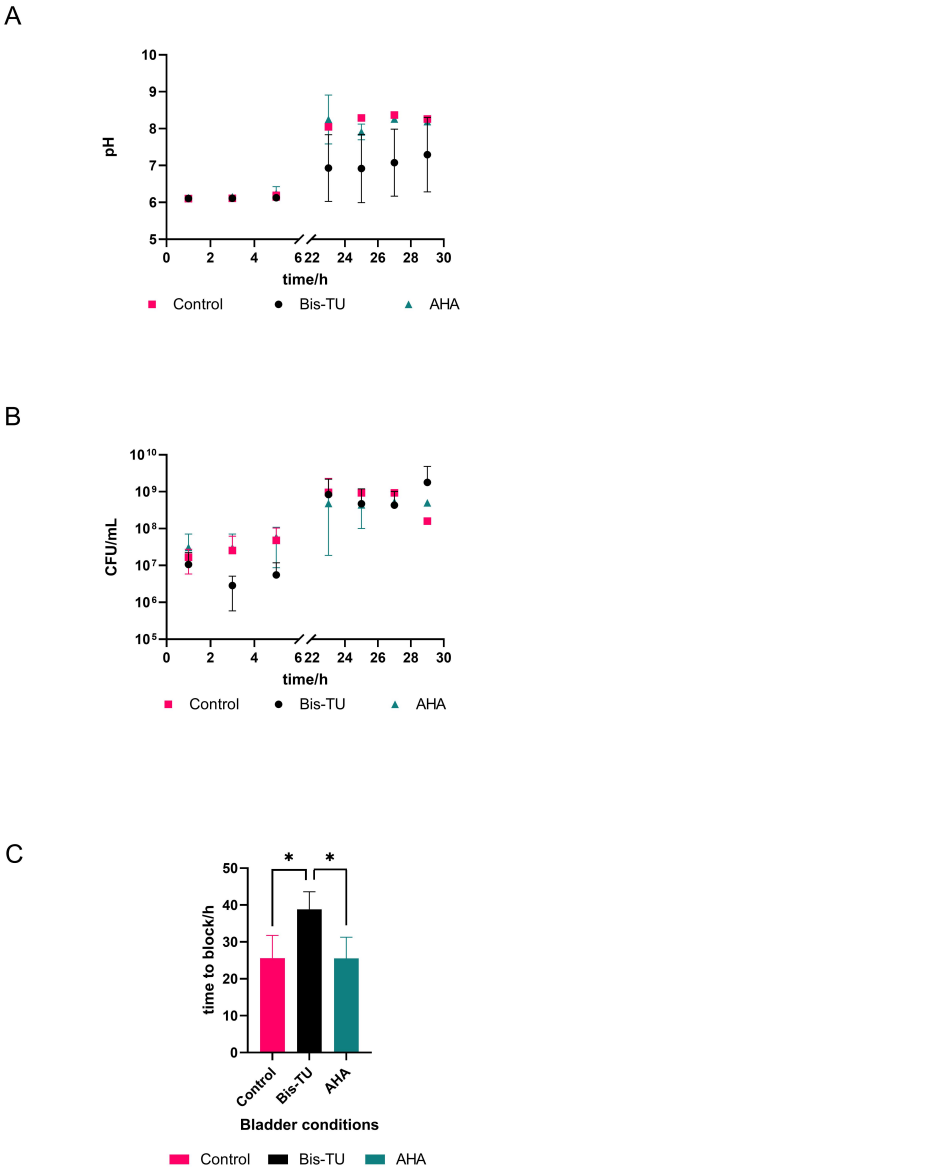

Figure 5-14: Monitoring and endpoint of *in vitro* bladder model experiments. (A) pH monitoring of the internal bladders, comparing bladders treated with: acetohydroxamic acid (AHA), N, N'-Bis(3-pyridinylmethyl)thiourea (Bis-TU, A11), and no treatment (control) (B) Monitoring levels of *P. mirabilis* within the bladders over time. (C) Comparing the blockage time (endpoint) of each of the bladders. Experiments were completed with three biological repeats. The graphs show the mean of the repeats with error bars representing standard deviation, * indicates $p = 0.0366$, and $p = 0.0426$ respectively, calcualted using an unpaired t-test. Graphs generated using GraphPad Prism v. 9.4.1.

5.4.2.5 Cytotoxicity Analysis

Whether AHA or Bis-TU were haemolytic was assessed using an *ex vivo* haemolysis assay. The results showed that neither Bis-TU or AHA appeared to cause haemolytic activity (Fig. 5-15A). MTT assay assesses the survival of liver cells when incubated with AHA and Bis-TU for 24 h. Liver cells are often used to evaluate toxicity of compounds during pharmacological research.[8] At the high concentration of 10 mM both Bis-TU and AHA affected the survival of HepG2 cells. As the concentration decreased the cytotoxicity reduced, AHA appears less cytotoxic however, at concentrations less than 1.25 mM both compounds are comparable. Concentrations of compounds used in the *in vitro* bladder experiments were higher than 1.25 mM, at ≈5 mM. However, by utilizing the Biomodics IPN delivery system, Bis-TU can be delivered to the bladder below the systemic toxic concentration and therefore the toxicity is reduced.

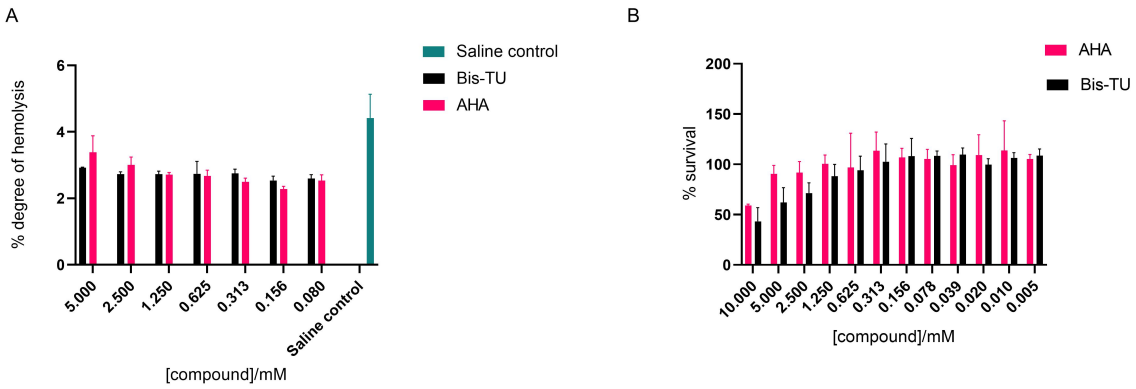

Figure 5-15: Cytotoxicity assessment of acetohydroxamic acid (AHA) and N, N'-Bis(3-pyridinylmethyl)thiourea (Bis-TU, A11). (A) *Ex vivo* haemolysis assay. (B) HepG2 mammalian cell cytotoxicity experiment assessed over 24 h. Experiments were completed with three biological repeats. The graphs show the mean of the repeats with error bars representing standard deviation. Graphs generated using GraphPad Prism v. 9.4.1.

5.5 Conclusion

This aim of this Chapter was to identify a new urease inhibitor using a rational *in silico* drug design method. Here we have identified Bis-TU, a newly identified urease inhibitor which significantly extends the lifetime of a urinary catheter compared to the clinical standard, AHA. The *in silico* drug discovery screen is a cost-effective way to identify new drugs. This methodology is underpinned by the following: (1) strong previous literature which is used to design the screen,[3,10] (2) a high-resolution crystal structure for use during the docking experiments, and (3) a physiologically representative *in vitro*

model. This particular drug-discovery method could be used to treat further diseases. The screening method could also be repeated based on the results of these experiments, an iterative manner can be used to improve the potency of Bis-TU and incorporate the learning from the flavonoid screen. Bis-TU's largest limiting factor is its low solubility; future work could entail the addition of excipents into the balloon which could improve the solubility and be incorporated in the balloon formulation. This would allow effective delivery at higher concentrations of Bis-TU. This Chapter also demonstrates the use of the Biomodics IPN catheter as a local drug delivery mechanism of Bis-TU directly into the bladder.

5.6 Appendix

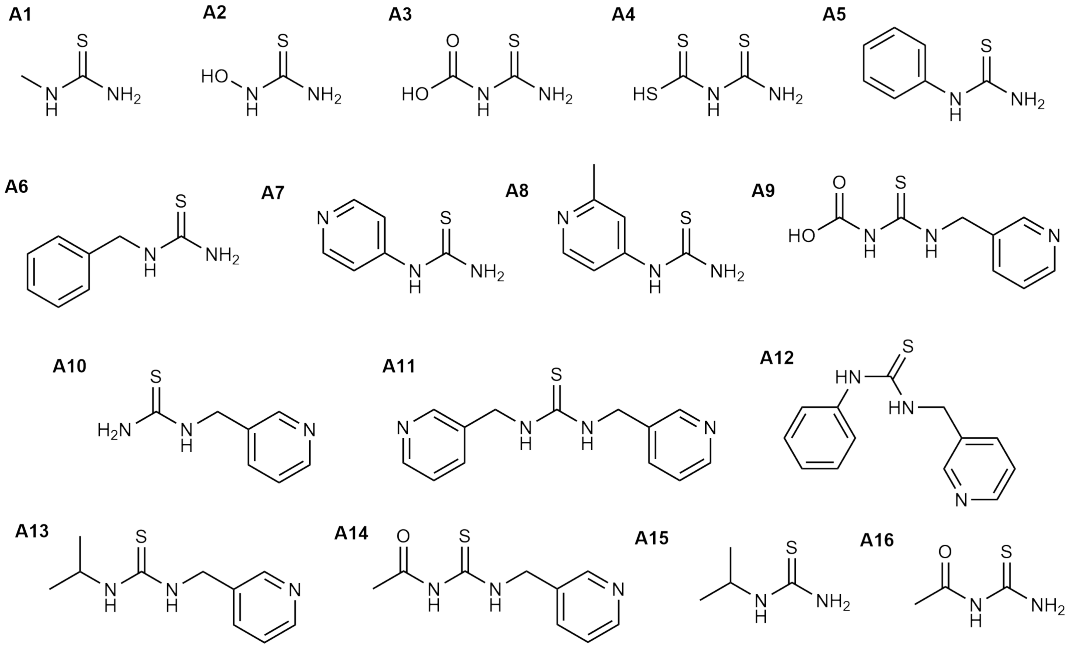

Figure 5-16: Series A

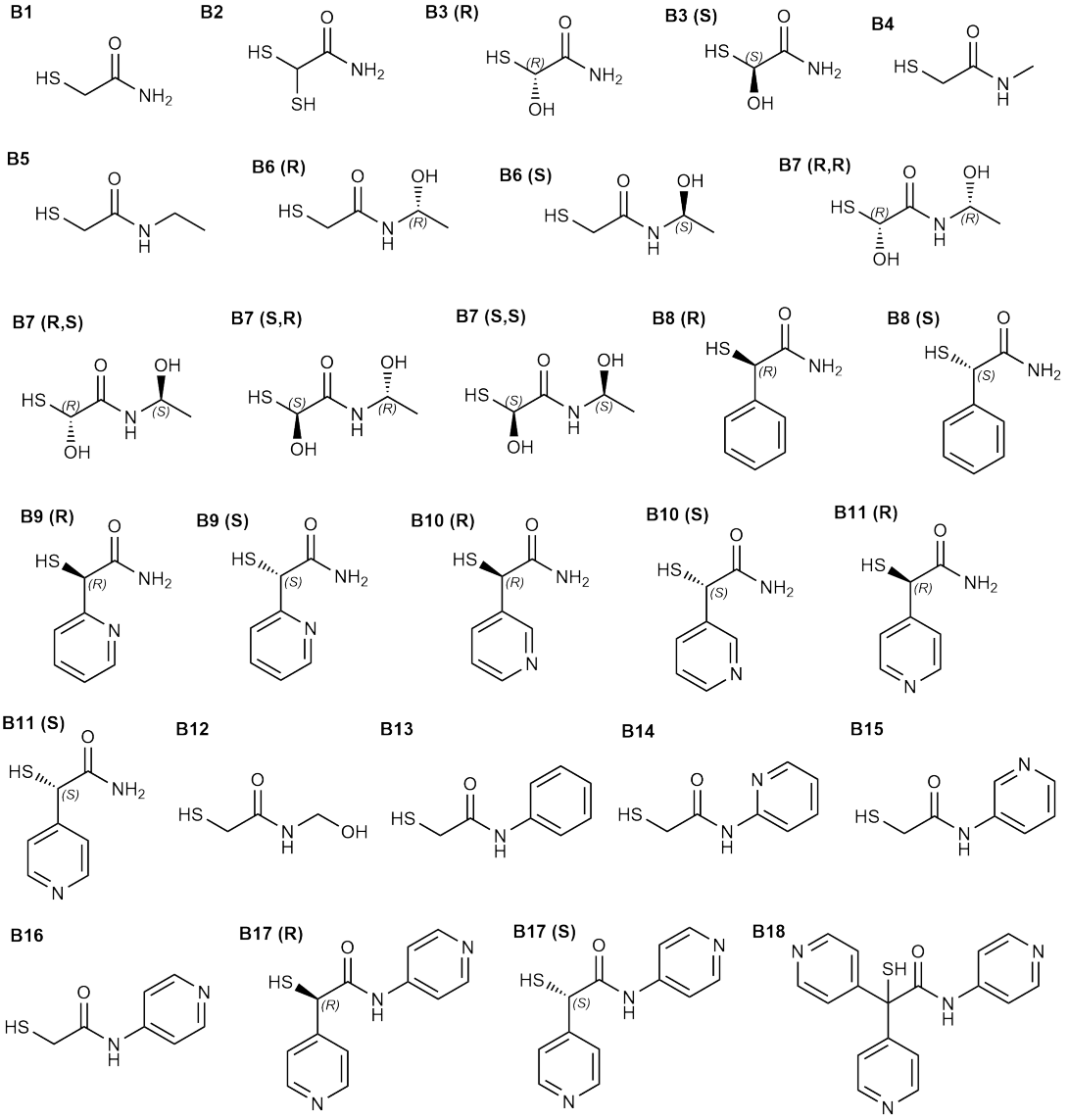

Figure 5-17: Series B

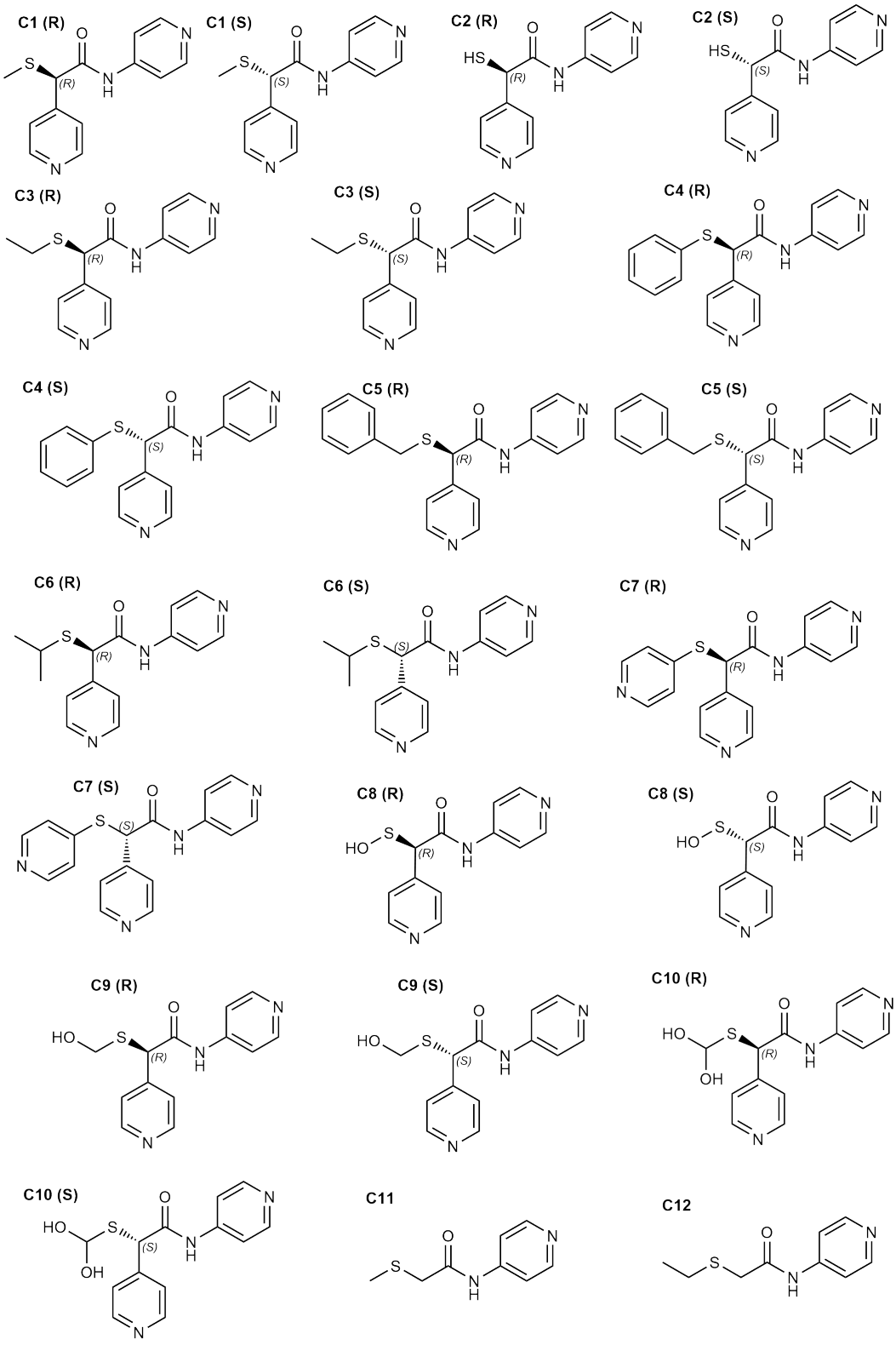

Figure 5-18: Series C

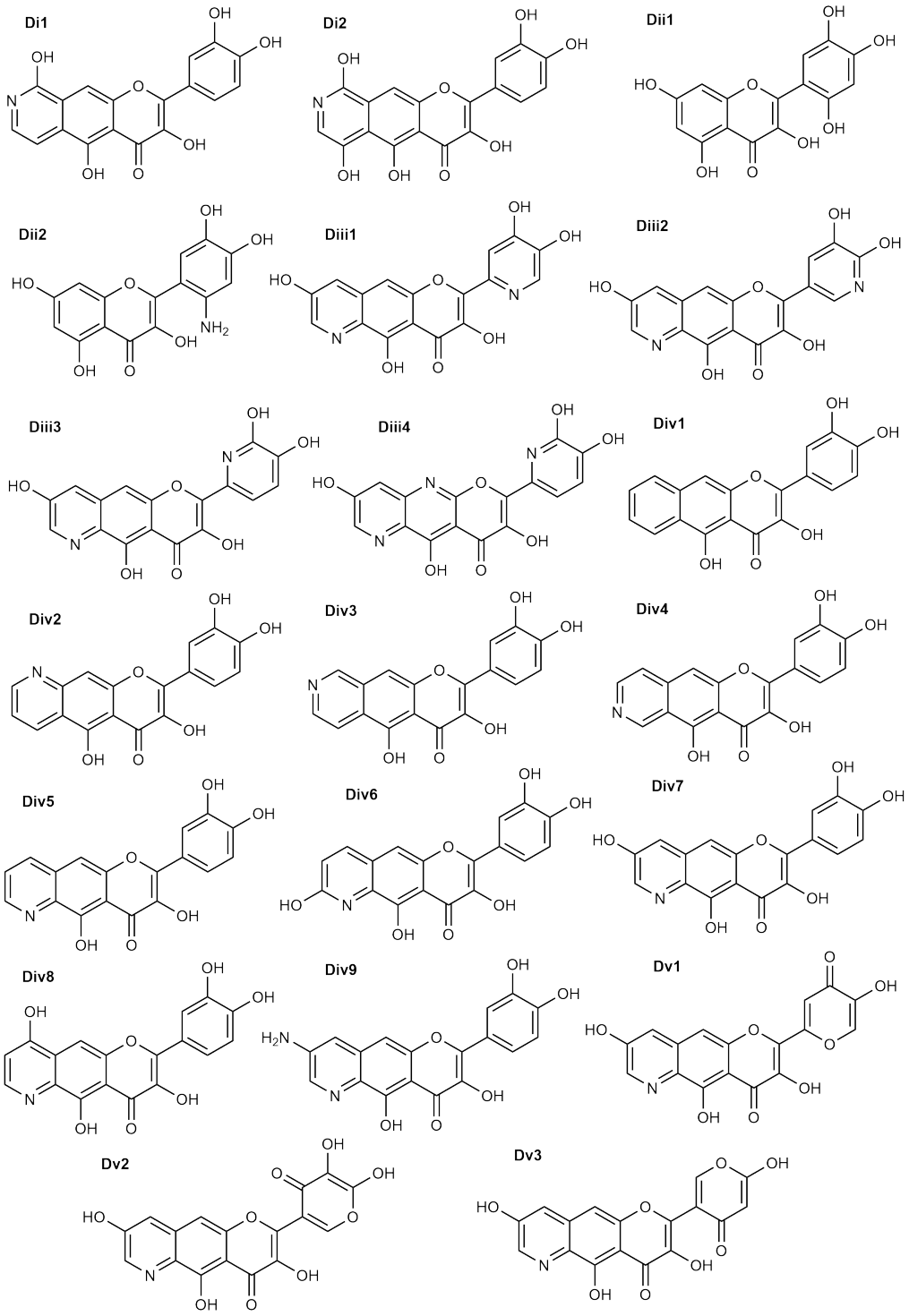

Figure 5-19: Series D

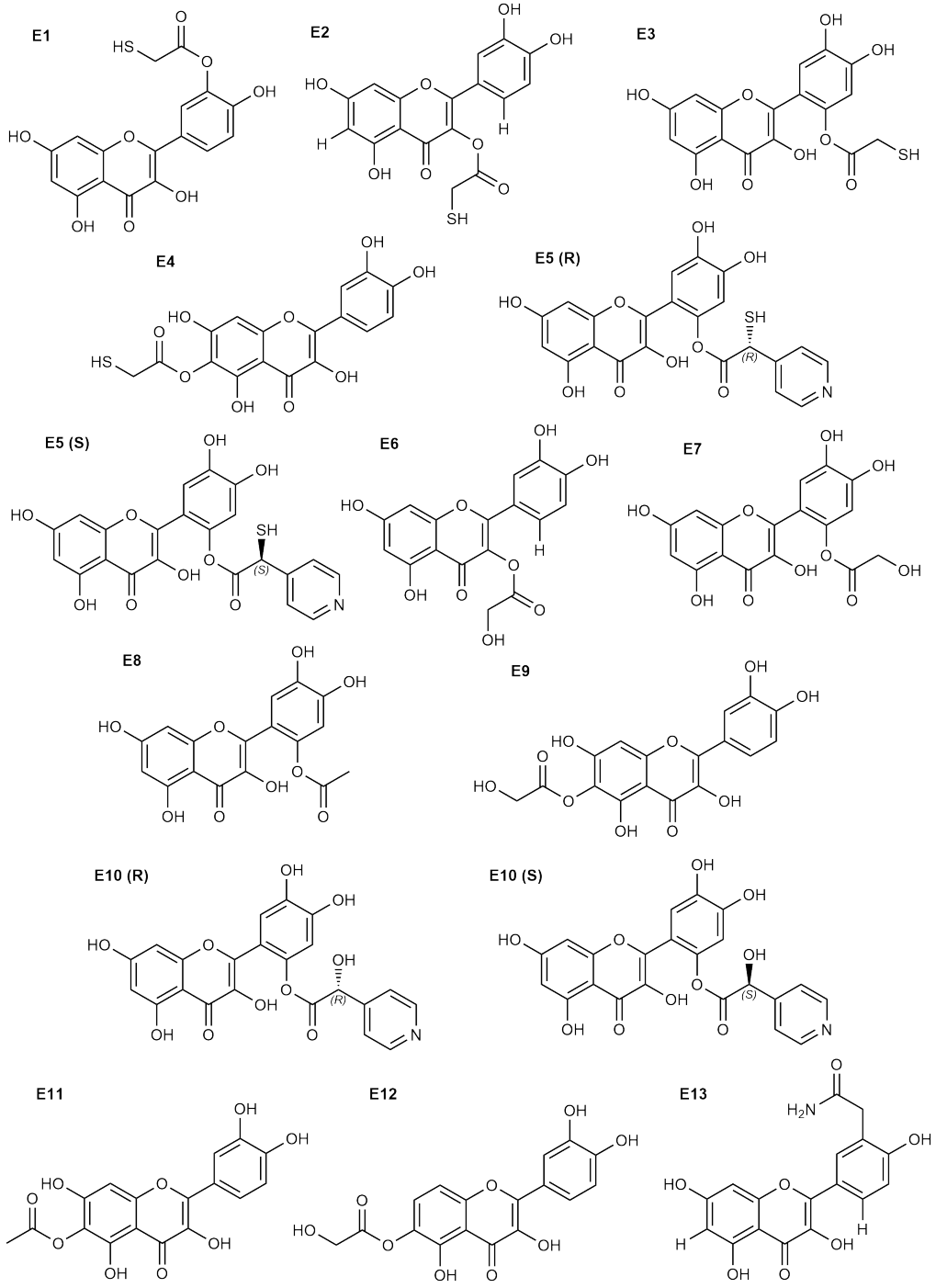

Figure 5-20: Series E

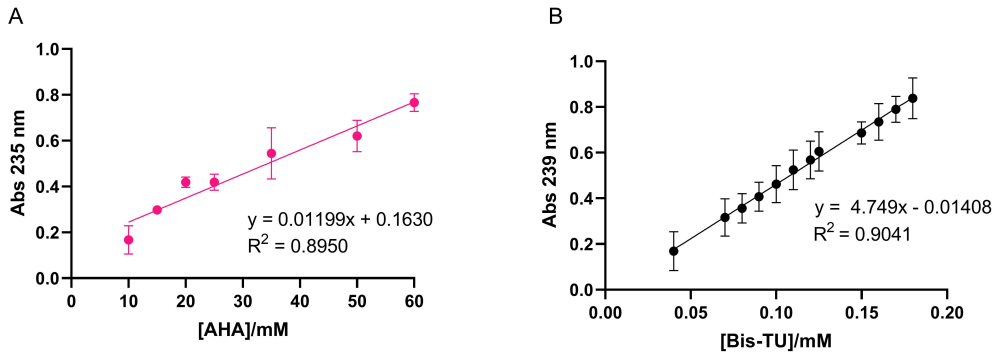

Figure 5-21: Calibration curves for Biomodics kinetic release experiments. (A) Acetohydroxamic acid. (B) *N,N'*-Bis(3-pyridinylmethyl)thiourea. Determined using UV-Vis spectroscopy, experiments were completed with three biological repeats. Simple linear regression was used to determine the equation of the line and assess the fit. The graphs show the mean of the repeats with error bars representing standard deviation. Graphs generated using GraphPad Prism v. 9.4.1.

Table 5.2: The docking score and the number of contacts (contacts <3.5 Å were counted) for each of the compounds designed.

Code	R_1	R_2	R_3	R_4	R_5	R_6	R_7	Docking Score (LF dG)	Number of Contacts
Series A									
A9	COOH	CH_2(pyridin-3-yl)	-	-	-	-	-	-9.652	9
A3	COOH	H	-	-	-	-	-	-9.007	6
A4	CSSH	H	-	-	-	-	-	-8.714	8
A12	benzene	CH_2(pyridin-3-yl)	-	-	-	-	-	- 8.209	4
A11	CH_2(pyridin-3-yl)	CH_2(pyridin-3-yl)	-	-	-	-	-	-7.213	6
A7	pyridin-3-yl	H	-	-	-	-	-	-7.017	7
A13	isopropyl	CH_2(pyridin-3-yl)	-	-	-	-	-	-6.945	5
A6	CH_2(benzene)	H	-	-	-	-	-	-6.581	3
A10	H	CH_2(pyridin-3-yl)	-	-	-	-	-	-6.374	9
A5	benzene	H	-	-	-	-	-	-6.102	3
A16	$COCH_3$	H	-	-	-	-	-	-5.925	5
A8	3-methyl pyridin-4-yl	H	-	-	-	-	-	-5.759	5
A15	isopropyl	H	-	-	-	-	-	-5.671	4
A14	$COCH_3$	CH_2(pyridin-3-yl)	-	-	-	-	-	-5.560	8
A1	Me	H	-	-	-	-	-	-5.419	4
A2	OH	H	-	-	-	-	-	-5.050	5
Thiourea	H	H	-	-	-	-	-	-4.411	4
Series B									
B17 (R)	pyridin-4-yl	pyridin-4-yl	-	-	-	-	-	-9.321	6
B11 (S)	pyridin-4-yl	H	-	-	-	-	-	-8.852	7
B18	2x pyridin-4-yl	pyridin-4-yl	-	-	-	-	-	-8.737	4
B9 (R)	pyridin-2-yl	H	-	-	-	-	-	-8.501	7
B17 (S)	pyridin-4-yl	pyridin-4-yl	-	-	-	-	-	-8.092	5

B10 (R)	pyridin-3-yl	H	-	-	-	-	-	-7.949	8
B6 (R)	H	CH(OH)Me	-	-	-	-	-	-7.730	8
B11 (R)	pyridin-4-yl	H	-	-	-	-	-	-7.675	8
B16	H	pyridin-4-yl	-	-	-	-	-	-7.395	8
B7 (S,R)	OH	CH_2OH	-	-	-	-	-	-7.350	12
B10 (S)	pyridin-3-yl	H	-	-	-	-	-	-7.237	9
B8 (S)	benzene	H	-	-	-	-	-	-7.229	5
B2	SH	H	-	-	-	-	-	-7.194	6
B7 (R,S)	OH	CH_2OH	-	-	-	-	-	-7.152	9
B7 (R,R)	OH	CH_2OH	-	-	-	-	-	-7.128	12
B6 (S)	H	CH(OH)Me	-	-	-	-	-	-6.959	13
B7 (S,S)	OH	CH_2OH	-	-	-	-	-	6.937	15
B9 (S)	pyridin-2-yl	H	-	-	-	-	-	-6.867	11
B13	H	benzene	-	-	-	-	-	-6.483	4
B5	H	Et	-	-	-	-	-	-6.298	4
B12	H	CH_2OH	-	-	-	-	-	-6.288	10
B15	H	pyridin-3-yl	-	-	-	-	-	-6.279	11
B4	H	Me	-	-	-	-	-	-5.871	6
B3 (S)	OH	H	-	-	-	-	-	-5.765	6
B3 (R)	OH	H	-	-	-	-	-	-5.755	8
B1 (2-MA)	H	H	-	-	-	-	-	-5.611	8
B14	H	pyridin-2-yl	-	-	-	-	-	-5.316	8
B8 (R)	benzene	H	-	-	-	-	-	-4.702	5
Series C									
C10 (R)	CH_2OH	pyridin-4-yl	pyridin-4-yl	-	-	-	-	-10.195	11
C7 (R)	pyridin-4-yl	pyridin-4-yl	pyridin-4-yl	-	-	-	-	-9.761	8
C7 (S)	pyridin-4-yl	pyridin-4-yl	pyridin-4-yl	-	-	-	-	-9.617	6
C2 (R)	H	pyridin-4-yl	pyridin-4-yl	-	-	-	-	-9.288	5
C9 (S)	CH_2OH	pyridin-4-yl	pyridin-4-yl	-	-	-	-	-9.209	9
C6 (S)	isopropyl	pyridin-4-yl	pyridin-4-yl	-	-	-	-	-9.158	7
C8 (R)	OH	pyridin-4-yl	pyridin-4-yl	-	-	-	-	-9.088	7
C9 (R)	CH_2OH	pyridin-4-yl	pyridin-4-yl	-	-	-	-	-8.955	7

C6 (R)	isopropyl	pyridin-4-yl	pyridin-4-yl	-	-	-	-	-8.942	5
C8 (S)	OH	pyridin-4-yl	pyridin-4-yl	-	-	-	-	-8.888	9
C3 (R)	Et	pyridin-4-yl	pyridin-4-yl	-	-	-	-	-8.841	7
C2 (S)	H	pyridin-4-yl	pyridin-4-yl	-	-	-	-	-8.692	3
C1 (R)	Me	pyridin-4-yl	pyridin-4-yl	-	-	-	-	-8.594	8
C16	pyridin-4-yl	H	pyridin-4-yl	-	-	-	-	-8.579	3
C24 (S)*	$CH(OH)_2$	pyridin-4-yl	pyridin-4-yl	-	-	-	-	-8.526	14
C5 (S)	CH_2(benzene)	pyridin-4-yl	pyridin-4-yl	-	-	-	-	-8.436	9
C23 (R)*	pyridin-4-yl	pyridin-4-yl	pyridin-4-yl	-	-	-	-	-8.311	7
C4 (S)	benzene	pyridin-4-yl	pyridin-4-yl	-	-	-	-	-8.040	8
C23 (S)*	pyridin-4-yl	pyridin-4-yl	pyridin-4-yl	-	-	-	-	-7.994	8
C10 (S)	$CH(OH)_2$	pyridin-4-yl	pyridin-4-yl	-	-	-	-	-7.974	11
C24 (R)*	$CH(OH)_2$	pyridin-4-yl	pyridin-4-yl	-	-	-	-	-7.970	13
C3 (S)	Et	pyridin-4-yl	pyridin-4-yl	-	-	-	-	-7.627	10
C5 (R)	CH_2(benzene)	pyridin-4-yl	pyridin-4-yl	-	-	-	-	-7.540	8
C14	CH_2(benzene)	H	pyridin-4-yl	-	-	-	-	-7.497	4
C13	benzene	H	pyridin-4-yl	-	-	-	-	-7.470	2
C20	CH_2(benzene)	H	H	-	-	-	-	-7.371	5
C1 (S)	Me	pyridin-4-yl	pyridin-4-yl	-	-	-	-	-7.190	8
C4 (R)	benzene	pyridin-4-yl	pyridin-4-yl	-	-	-	-	-7.077	5
C11	Me	H	pyridin-4-yl	-	-	-	-	-7.014	9
C22 (R)*	CH_2(benzene)	pyridin-4-yl	pyridin-4-yl	-	-	-	-	-6.981	7
C19	benzene	H	H	-	-	-	-	-6.920	6
C15	isopropyl	H	pyridin-4-yl	-	-	-	-	-6.819	8
C12	Et	H	pyridin-4-yl	-	-	-	-	-6.686	5
C22 (S)*	CH_2(benzene)	pyridin-4-yl	pyridin-4-yl	-	-	-	-	-6.409	7
C21*	benzene	pyridin-4-yl	pyridin-4-yl	-	-	-	-	-6.235	6
C18	Et	H	H	-	-	-	-	-6.213	8
C17	Me	H	H	-	-	-	-	-5.901	6
2-MA	H	H	H	-	-	-	-	-5.758	7
Series D									
Diii2	C	C	C	N	-	-	-	-11.171	12
Diii3	C	N	C	C	-	-	-	-10.631	16
Diii1	C	C	N	C	-	-	-	-10.189	14
Diii4	N	N	C	C	-	-	-	-9.865	14

Div7	C	C	C	N	H	OH	H	-9.716	7
Dv2	y	-	-	-	-	-	-	-9.554	10
Dii2	NH_2	-	-	-	-	-	-	-9.197	10
Div6	C	C	C	N	H	H	OH	-9.163	10
Di2	OH	-	-	-	-	-	-	-9.150	11
Div8	C	C	C	N	OH	H	H	-9.110	9
Dv1	x	-	-	-	-	-	-	-9.103	6
Di1	OH	H	-	-	-	-	-	-8.897	10
Dv3	z	-	-	-	-	-	-	-8.836	8
Dii1	OH	-	-	-	-	-	-	-8.722	15
Div9	C	C	C	N	H	NH_2	H	-8.678	9
Div3	C	N	C	C	H	-	H	-8.486	7
Div5	C	C	C	N	H	H	H	-8.313	7
Div4	C	C	N	C	H	H	-	-8.113	8
Div2	N	C	C	C	-	H	H	-8.006	8
Div1	C	C	C	C	H	H	H	-7.880	6
Series E									
E5 (S)	OH	H	OH	OCOCSH(pyridin-4-yl)	OH	-	-	-12.902	11
E5 (R)	OH	H	OH	OCOCSH(pyridin-4-yl)	OH	-	-	-11.943	11
E10 (S)	OH	$OCOCH_3$	OH	OCOCSH(pyridin-4-yl)	OH	-	-	-11.710	11
E3	OH	H	OH	$OCOCH_2SH$	OH	-	-	-11.215	11
E2	OH	H	$OCOCH_2SH$	H	OH	-	-	-11.095	9
E14	OH	H	OH	CH_2CONH_2	OH	-	-	-10.252	10
E7	OH	H	OH	$OCOCH_2OH$	OH	-	-	-10.237	10
E10 (R)	OH	$OCOCH_3$	OH	OCOCSH(pyridin-4-yl)	OH	-	-	-10.145	11
E1	OH	H	OH	H	$OCOCH_2SH$	-	-	-9.648	7
E17	OH	H	OH	CH_2CHO	OH	-	-	-9.611	10
E8	OH	H	OH	$OCOCH_3$	OH	-	-	-9.549	10
E13	OH	H	OH	H	CH_2CONH_2	-	-	-9.157	10
E6	OH	H	$OCOCH_2OH$	H	OH	-	-	-9.097	11
E11	OH	$OCOCH_2OH$	OH	H	OH	-	-	-8.754	8
E12	H	H	OH	H	OH	-	-	-8.601	11

E18	H		CH_2CONH_2	OH	H		OH	-	-	-8.600	11
E9	OH		$OCOCH_2OH$	OH	H		OH	-	-	-8.491	11
E16	OH		CH_2CONH_2	OH	H		OH	-	-	-8.403	9
E4	OH		$OCOCH_2SH$	OH	H		OH	-	-	-7.836	9
E15	OH		H	CH_2CONH_2	H		H	-	-	-7.704	7

5.7 Bibliography

[1] Milo S, Heylen RA, Glancy J, Williams GT, Patenall BL, Hathaway HJ, et al. A small-molecular inhibitor against Proteus mirabilis urease to treat catheter-associated urinary tract infections. Scientific Reports. 2021 dec;11(1):3726. Available from: http://www.nature.com/articles/s41598-021-83257-2.

[2] Kappaun K, Regina A, Regina C, Ligabue-braun R. Ureases: Historical aspects, catalytic, and non-catalytic properties – A review. Journal of Advanced Research. 2018;13:3–17. Available from: https://doi.org/10.1016/j.jare.2018.05.010.

[3] Kafarski P, Talma M. Recent advances in design of new urease inhibitors: A review. Journal of Advanced Research. 2018;13:101–112. Available from: https://www.sciencedirect.com/science/article/pii/S2090123218300171.

[4] Mazzei L, Cianci M, Musiani F, Lente G, Palombo M, Ciurli S. Inactivation of urease by catechol: Kinetics and structure. Journal of Inorganic Biochemistry. 2017;166:182–189. Available from: http://dx.doi.org/10.1016/j.jinorgbio.2016.11.016.

[5] Khan KM, Naz F, Taha M, Khan A, Perveen S, Choudhary MI, et al. Synthesis and in vitro urease inhibitory activity of N,N'- disubstituted thioureas. European Journal of Medicinal Chemistry. 2014;74:314–323. Available from: https://www.sciencedirect.com/science/article/abs/pii/S0223523414000282.

[6] Xiao ZP, Wang XD, Peng ZY, Huang S, Yang P, Li QS, et al. Molecular Docking, Kinetics Study, and Structure-Activity Relationship Analysis of Quercetin and Its Analogous as Helicobacter pylori Urease Inhibitors. Journal of Agricultural and Food Chemistry. 2012;60(42):10572–10577. Available from: https://pubs.acs.org/doi/pdf/10.1021/jf303393n.

[7] Kataria R, Khatkar A. Molecular docking, synthesis, kinetics study, structure – activity relationship and ADMET analysis of morin analogous as Helicobacter pylori urease inhibitors. BMC Chemistry. 2019;13(45):1–17. Available from: https://doi.org/10.1186/s13065-019-0562-2.

[8] Vinken M, Rogiers V, editors. Protocols in In Vitro Hepatocyte Research. vol. 1250. Springer New York; 2015. Available from: https://link.springer.com/book/10.1007/978-1-4939-2074-7.

[9] Carta G, Knox AJS, Lloyd DG. Unbiasing Scoring Functions: A New Normal-

ization and Rescoring Strategy. Journal of Chemical Information and Modeling. 2007;47(4):1564–1571.

[10] Rego YF, Queiroz MP, Brito TO, Carvalho PG, Queiroz VTD, Fátima ÂD, et al. A review on the development of urease inhibitors as antimicrobial agents against pathogenic bacteria. Journal of Advanced Research. 2018;13:69–100. Available from: https://doi.org/10.1016/j.jare.2018.05.003.

[11] Batista GMF, De Castro PP, Dos Santos JA, Skrydstrup T, Amarante GW. Synthetic developments on the preparation of sulfides from thiol-free reagents. Organic Chemistry Frontiers. 2021;8(2):326–368.

[12] Kataria R, Khatkar A. Molecular Docking of Natural Phenolic Compounds for the Screening of Urease Inhibitors. Current Pharmaceutical Biotechnology. 2019;20(5):410–421.

[13] Benini S, Rypniewski WR, Wilson KS, Miletti S, Ciurli S, Mangani S. The complex of Bacillus pasteurii urease with acetohydroxamate anion from X-ray data at 1.55 Å resolution. Journal of Biological Inorganic Chemistry. 2000;5(1):110–118. Available from: https://doi.org/10.1007/s007750050014.

[14] Benini S, Rypniewski WR, Wilson KS, Miletti S, Ciurli S, Mangani S. A new proposal for urease mechanism based on the crystal structures of the native and inhibited enzyme from Bacillus pasteurii: Why urea hydrolysis costs two nickels. Structure. 1999;7(2):205–216.

[15] Dahan A, Miller JM. The solubility-permeability interplay and its implications in formulation design and development for poorly soluble drugs. AAPS Journal. 2012;14(2):244–251.

[16] Burns JR, Gauthier JF. Prevention of Urinary Catheter Incrustations by Aacetohydroxamic Acid. The Journal of Urology. 1984;132(3):455–456. Available from: http://dx.doi.org/10.1016/S0022-5347(17)49689-3.

[17] Mclean RJC, Cheng KJ, Gould WD, Nickel JC, Costerton WJ. Histochemical and biochemical urease localization in the periplasm and outer membrane of two Proteus mirabilis strains. Canadian Journal of Microbiology. 1986;32(10):772–778. Available from: https://doi.org/10.1139/m86-142.

[18] Stickler DJ, Morris NS, C W. Simple Physical Model to Study Formation and Physiology of Biofilms on Urethral Catheters. Methods in Enzymology.

1999;310:494–501. Available from: https://doi.org/10.1016/S0076-6879(99)10037-5.

[19] Nzakizwanayo J, Pelling H, Milo S, Jones BV. An In Vitro Bladder Model for Studying Catheter-Assoicated Urinary Tract Infection and Asssoicated Analysis of Biofilms. Humana Press; 2019. Available from: https://link.springer.com/protocol/10.1007/978-1-4939-9601-8{_}14.

Chapter 6

Nasturtium officinale extract: natural urease inhibitors to treat urease-positive infections

6.1 Introduction

Nasturitium officinale, watercress, has been used in traditional medicine in Azerbaijan, Iran, Mauritius, and Morocco.[1] It has been identified to have the following medicinal properties antioxidant, anticancer, antibacterial, anti-inflammatory, and cardioprotective.[2,3,4,5,6,7] *N. officinale* is often used as a vegatable in salads, it is a semi-aquatic plant from the family Brassicaceae.[8] The leaves and stems of the plant contain polyphenols,[9,7] saponins, isothiocyanates,[10] glucosinolates,[11] palmitic acid, monoterpenoids, sesquiterpenoids, and various vitamins and their derivatives.[1,12]

The potential of natural products as a source or starting point for urease inhibitors is examined in Section: 1.7.2.4. Natural products have historically been a successful starting point for drug discovery. In this Chapter extract taken from *N. officinale* is examined for its use as a urease inhibitor. Generally, it is difficult to market a plant extract as a therapeutic because owing to the varying growing and manufacturing techniques, it is not possible to control the quantity and presence of distinct compounds during every batch (batch-to-batch variability), thus making it difficult to regulate. Consequently, therapeutics often consist of synthesised small compounds, in which the manufacture is standard and can be quality controlled. However, mixtures of compounds such as a plant extract could hold added advantages such as synergy between the compounds and improvements in solubility. For example: flavonoids are insoluble in aqueous solution however, natural surfactants such as palmitic acid occurring within the mixture could allow the solubilisation of compounds, which are normally insoluble at specific concentrations.[13,14] The greatest difficulty in investigating *N. officinale* extract as a therapeutic is the initial identification of the compounds present. During these experiments the identity of compounds believed to be present was provided by the Watercress Research Ltd., collaborators on this project (Appendix 6.1). The list mainly includes compounds categorised as isothiocyanates (ITC) and flavonoids.

Human trials using *N. officinale* extract did not report any adverse side effects or associated toxicity.[15,16,12] Therefore, *N. officinale* extract is a good starting point for investigating potential medicinal properties. A review written by Klimek-Szczykutowicz *et al.,* highlighted that *N. officinale* might hold undiscovered novel therapeutic compounds.[1] The aim of this Chapter is to explore the anti-ureolytic properties of *N. officinale* extract and examine the use of the extract as a treatment against urease-positive infections specifically those associated with CAUTI and *H. pylori*.

6.2 Methods

General methods are described in Chapter 2. The following methods are specific to this Chapter.

6.2.0.1 *Nasturtium officinale* (*N. officinale*) *In silico* Docking Experiment

This work was done in collaboration with Watercress Research Ltd. Unit 24, Exeter SkyPark, Exeter, EX5 2GE, UK. The founders of Watercress Research: Dr Kyle Stewart and Prof. Paul Winyard, assisted in the research carried out. A list of compounds believed to be present in *N. officinale* was provided for the docking experiments and based on previous literature (Appendix 6.1).

Compounds were docked onto the crystal structure of *H. pylori* urease (PDB: 1E9Y). ITC were covalently docked onto cysteine residues, identified on the surface of the protein: C153, C257, and C321. Flavonoids were docked into the active site, which included a grid box around C321 which is present in the active site flap. Ligands were docked using the same settings described in Section 2.2.4.

6.2.1 Investigating Ammonia Scavenging

The ammonia scavenging assay used the Berthelot assay as described in Section 2.2.5. Instead of adding *P. mirabilis* whole cell or *C. ensiformis* urease, ammonium chloride (7 mM in 100 mM sodium phosphate, pH 7.4) was used instead. As the Berthelot assay measures the accumulation of ammonia, here it was used to examine the scavenging of ammonia. The % of ammonia remaining was calculated according to equation 6.1.

$$corrected\,\%\,ammonia\,remaining = \frac{(sample\,well - negative\,control)}{(positive\,control - negative\,control)} \times 100 \tag{6.1}$$

It was hypothesised that the ammonia was being scavenging via the formation of a thioamide bond between ITCs and ammonia. This was investigated by reacting PE-ITC (3.06 mM) with excess ammonia hydroxide (30.6 mM, 35% (v/v)) for 72 h in methanol at room temperature (reaction volume 10 mL). The resulting product was assessed using H^1 nuclear magnetic resonance (NMR) spectroscopy, in CD_3OD solvent using a Bruker 500 MHz spectrometer. The resulting spectra was analysed using TopSpin

4.0.8.

6.3 Results and Discussion

6.3.1 *In silico* docking experiments

H. pylori is a microaerophilic, Gram-negative, spiral bacterium which is able to form an environmental niche within the lining of the stomach.[17] The urease activity is pivotal in enabling *H. pylori* to increase the pH of the surrounding area, thus escaping the bactericidal stomach acid.[18] Barry J. Marshall and Robin Warren won the Nobel Prize in 2005 for the discovery of *H. pylori* in 1982, and deducing that it is the bacterium which causes gastritis and ulceration of the stomach or duodenum; not lifestyle factors or stress which was widely believed as the causative.[19] Marshall even had to conduct 'self-help' experiment on himself, whereby a gastric biopsy was conducted to prove that he did not have a *H. pylori* infection and then he infected himself to prove that *H. pylori* does cause this disease.[19] Urease is an essential survival factor for *H. pylori*, therefore inhibition of urease could be cytotoxic to the bacteria.[17] Emphasis initially was for the treatment of *H. pylori* infection with *N. officinale* extract, owing to the accessibility via oral delivery of the extract, therefore the structure of the *H. pylori* enzyme was used for the *in silico* docking studies. As discussed in Section 1.7, *H. pylori* has a well-conserved amino acid sequence compared to other urease enzymes (Fig. 1-11). However, it does have a slightly different supramolecular structure (Fig. 1-13). Therefore, the compounds identified as urease inhibitors via the *in silico* screen could also be effective against urease from other species because the docking is completed on one monomer where the sequences are well conserved. Although, the compounds could demonstrate different potencies when tested on *P. mirabilis* vs *H. pylori* bacteria. Additionally, it should be noted that urease from *H. pylori* is found both internally within the cytoplasm and on the surface of the bacteria; therefore compounds can be active on urease without crossing the bacterial membrane.[17] To assess the docking of the compounds, the docking score: LF dG and the docking position was taken into account. AHA and Urea were docked initially in the active site to assess the accuracy of the docking experiment (Fig. 6-1).

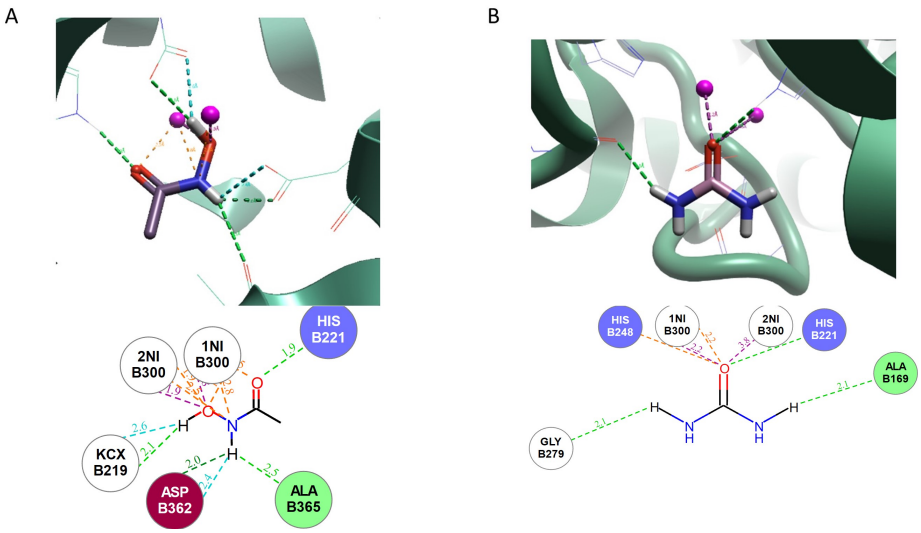

Figure 6-1: Control compounds docked to urease: Acetohydroxamic acid (AHA) and urea, with corresponding interaction maps. (A) AHA bound to the active site from *Helicobacter pylori* urease (PDB: 1E9Y). AHA coordinates with the Ni^{2+} ion and bonds to A365 (2.5 Å), H221 (1.9 Å), K219 (2.2 Å), and D362 (2.0 Å). This is comparable to the crystal structure of urease with AHA bound.[20]. (B) Urea docking into the active site of urease, chelating with Ni^{2+} ions and coordinating with the expected amino acids: A169 (2.1 Å), H221 (2.0 Å), H248 (2.4 Å), and G279 (2.4 Å). Urease shown as a green ribbon, Ni ions as pink spheres, close contacts as a thin line, docked ligand as thick lines. Molecules docked and images generated using Cresset®Flare^{TM} v. 4.0.2.

6.3.1.1 ITC docking

ITCs have previously been identified as urease inhibitors.[1,21,12] The functional group: -N=C=S, is predicted to form covalent bonds with cysteine residues in urease. Therefore, ITCs could act as covalent inhibitors. Section 1.7.2.5 discusses the use of covalent inhibitors; these are rarely observed in the clinic because of their associated toxicity however the compounds could be potent drugs.[22] Macegoniuk *et al.,* identifed butendioic acid as a covalent inhibitor to Cys-322 from *S. pasteurii* urease.[23] The cysteines on the surface of *H. pylori* urease were identified: C153, C257, and C321; as these would be more accessible to the ITCs (Fig. 6-2).

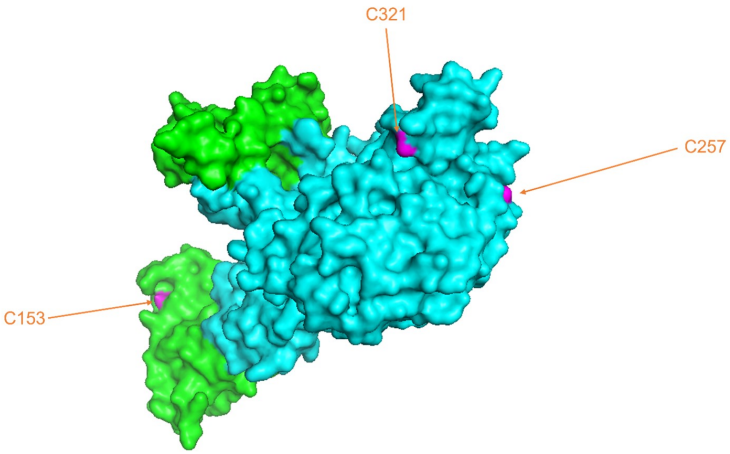

Figure 6-2: Cysteine residues identified on the surface of *Helicobacter pylori* urease: C153, C257, and C321. Chain A is shown in green, chain B in blue, and cysteine residues in magenta. Image generated using Flare^{TM} v. 4.0.2.

The LFdG score for docking to each cysteine residue was compared with a series of ITC molecules (Fig. 6-3). Docking scores are shown in Table 6.2 of the Appendix, the more negative the docking score the higher the prediction of effective binding to the enzyme. The docking to C153 and C321 was generally more favourable than C257 (Fig. 6-3). As the length of the ITC compound increased generally the docking score increased, this was observed over all three cysteines. However, some molecules did not show this trend, for example: methylsulfinyl-ITC bound to C257 (Fig. 6-3B). The docking results associated with C321 were the most interesting results because C321 is associated with the active site flap. Compounds docking here appear to bind down towards the active site. Fahey *et al.,* completed *in vitro* analysis of the ITC compounds and was able to show that 4-(methylsulfinyl)butyl-NCS reduced the activity of *H. pylori* urease to 36% following 30 min of incubation.[21] In the *in silico* experiment this ligand measured an LF dG of -5.874 (Fig. 6-3B). The published *in vitro* analysis of 8-(methylsulfinyl)octyl-NCS, 5-(methylsulfinyl)pentyl-NCS, 2-phenylethyl-NCS did not demonstrate activity against urease, although the *in silico* experiment did show comparable docking scores.[21] This emphasises the importance of *in vitro* experimentation alongside *in silico*. ITC molecules are synethsised by plant cells using the myrosinase enzyme, during the mechanical disruption of the *N. officinale* to produce the extract, ITC compounds are produced by the metabolization of glucosinolates.[24,25] Optimisation of the harvest and processing of *N. officinale*, alongside the use of different mechanical disruption techniques could produce more ITC compounds.[1]

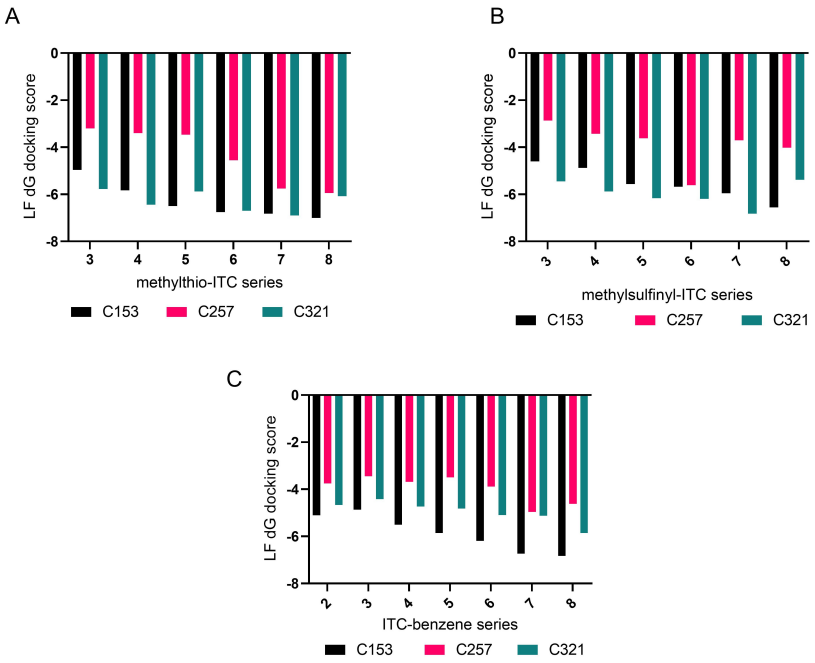

Figure 6-3: Comparison of the docking scores for covalently docked isothiocyanates. (A) methylthio-ITC series. (B) methylsulfinyl-ITC series. (C) ITC-benzene series. Numbers on the x-axis denote the number of carbons in the ITC chain. Docking scores are displayed in Appendix 6.2. Molecules docked and images generated using Cresset®Flare™ v. 4.0.2.

6.3.1.2 Flavonoid Docking

Flavonoids are another group of compounds found within *N. officinale* extract.[9,1,12] Flavonoids have already been computationally docked to urease, Xiao *et al.*, predicted that flavonoids would associate with C321.[26] Flavonoids are much larger molecules compared to ITCs, a large grid box for docking was prepared around C321 based on the work completed by Xiao *et al.*[26] Owing to the larger molecular weight of flavonoids, in comparison to ITCs, the resulting docking scores which tend to be higher this is because there are more contacts identified with the protein but does not necessarily mean the flavonoid would be a better drug.[27] For example, a small compound might make fewer identifiable contacts with the protein but be small enough to fit into the active site and make stronger contacts with the protein. The flavonoids gave higher docking scores than the ITC ligands (Fig. 6-4A). The highest scoring flavonoid was quercetin-3-sophoroside which appears to bind down towards the active site whilst also interacting with the active site flap (Fig. 6-4B).

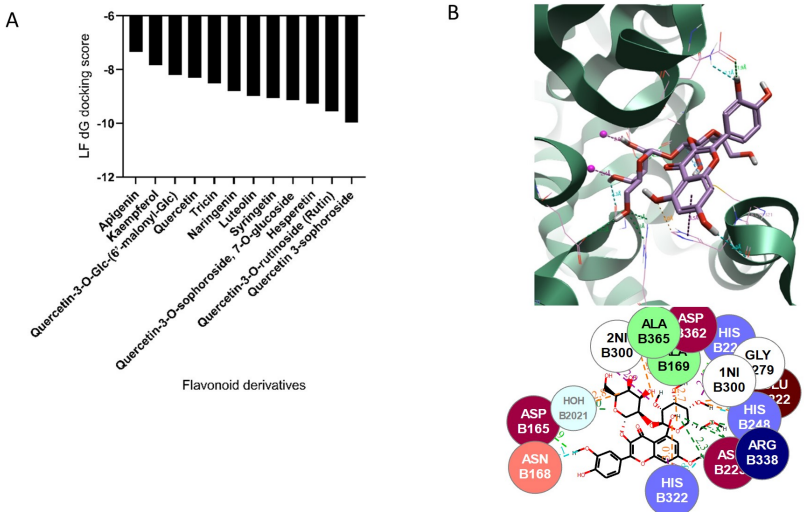

Figure 6-4: *In silico* flavonoid docking results to *Helicobacter pylori* urease with interaction map. (A) Comparing the LF dG docking scores of the flavonoid ligands. (B) The highest scoring flavonoid: quercetin-3-sophoroside bound to urease, forming contacts between the Ni^{2+} ions and the amino acid residues: D165, N168, E222, G279, H221, H322, H248, R338, D362, A169, and A365. Urease shown as a green ribbon, Ni ions as pink spheres, close contact amino acids as a thin line connected with dotted lines, docked ligand as thick lines. Molecules docked and images generated using Cresset®Flare™ v. 4.0.2.

Computational docking by Xiao *et al.,* predicted that quercetin interacted with the active site flap.[26] However, results from this experiment predicted that the phenyl moiety interacts with the active site and there are less interactions with the active site flap (Fig. 6-5). This indicates the variability which can occur with *in silico* docking software and experimentation, and further emphasises the importance of confirming *in silico* results with *in vitro* experimentation.

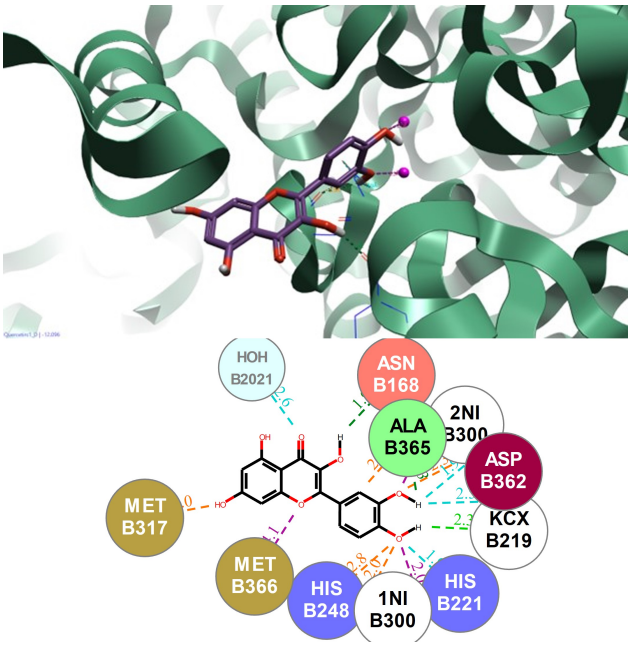

Figure 6-5: Quercetin docked into the active site of urease from *Helicobacter pylori* with interaction map. Quercetin interacting with the Ni^{2+} ions and amino acids: D168, M317, M366, H248, H221, K219, A365, N362, and N168. Urease shown as a green ribbon, Ni ions as pink spheres, close contact amino acids as a thin line connected with dotted lines, docked ligand as thick lines. Molecules docked and images generated using Cresset®Flare™ v. 4.0.2.

6.3.2 Urease Activity Assay

P. mirabilis was used as a model organism to test the ability of *N. officinale* extract to inhibit urease activity. *P. mirabilis* is a well studied, urease-positive, microbe frequently associated with CAUTI and urinary catheter blockage. Although the docking experiments were completed using *H. pylori* urease, as discussed in Section 1.7, there is conservation at a sequence level between the urease enzymes. Although the use for *N. officinale* extract has been discussed as a treatment for *H. pylori* infection, it could additionally be used to treat any urease-positive infection. Urease from *P. mirabilis* is intracellular therefore these experimentations also test the ability of *N. officinale* to cross the bacterial membrane.[28] Previous work shown in Chapter 5 hypothesised that quercetin is unable to cross the bacterial membrane (Fig. 5-10). Compounds such as palmitic acid, found within *N. officinale* extract, could improve the solubility of the flavonoids and therefore allow transport across the bacterial membrane. The inhibitory assay demonstrated that <10% (v/v) of extract is sufficient to inhibit *P. mirabilis* urease (Fig. 6-6).

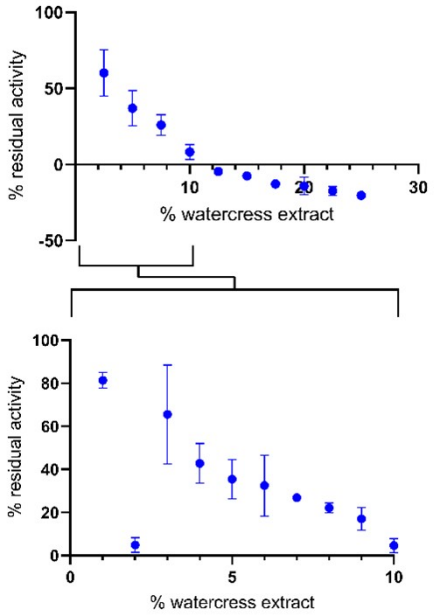

Figure 6-6: Urease activity measuring *Nasturtium officinale* extract's ability to inhibit *Proteus mirabilis* urease. First graph shows % of *N. officinale* between 0-25%, second graph look in more detail at *N. officinale* between 0 - 10%. Experiments show three biological repeats, each experiment consisting of two technical repeats. Graph shows mean values of biological repeats, error bars representing standard deviation. Graphs generated using GraphPad Prism v. 9.4.1.

6.3.3 Testing cytotoxicity of *N. officinale* against *P. mirabilis*

N. officinale is not known to be antibiotic and does not appear cytotoxic against *P. mirabilis* (Fig. 6-7). Therefore *N. officinale* should not present resistance pressures on bacteria. This is advantageous because it will not damage the commensal flora whilst still being an effective anti-virulence inhibitor to urease.

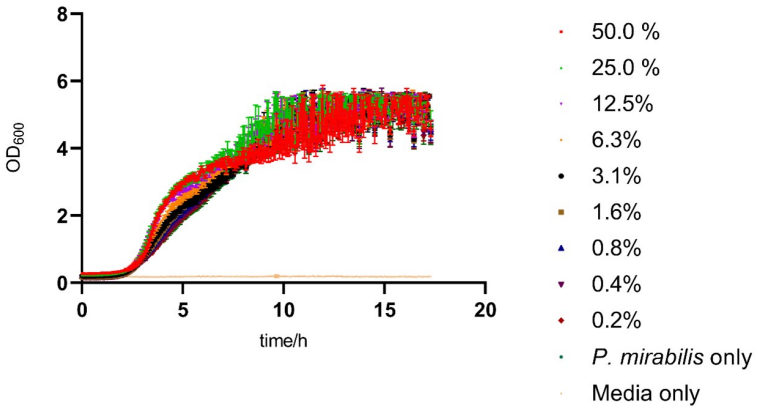

Figure 6-7: Growth curve in the presence of *Nasturtium officinale* extract measured using *Proteus mirabilis*. Experiments show three biological repeats, each experiment consisting of two technical repeats. Graph shows mean values of biological repeats, error bars representing standard deviation. Graphs generated using GraphPad Prism v. 9.4.1.

6.3.4 Ammonia Scavenging

Results from the inhibitory assay showed that a concentration greater than 12% (v/v) demonstrated a negative measurement of percentage residual activity (Fig. 6.3.2). It was hypothesised that another mechanism could be involved, specifically that the *N. officinale* extract had the ability to scavenge the ammonia. A chemical reaction between the ITC molecules and ammonia is well established (Fig. 6-9).[29] To measure whether the extract could scavenge ammonia, the urease activity assay which measures the accumulation of ammonia over time was used in the absence of urease. The allowed the sequestration of the ammonia to be tested. The quantity of ammonium chloride reduced as it was incubated with *N. officinale* extract (Fig. 6-8). A concentration of 20% (v/v) *N. officinale* is sufficient to sequester 7 mM NH_4Cl over the assay reaction time of 30 min, compared to the control (Fig. 6-8). It is predicted that both urease inhibition with the compounds examined in the docking experiments (Section 6.3.1) and ammonia sequestration are involved in the prevention of ammonia production and removal of exisiting ammonia. Ammonia is the pivotal compound which causes the increase in pH which subsequently causes urinary catheter blockage and allows *H. pylori* to establish an infection and buffer the stomach acid.[30,17] The sequestration property of *N. officinale* extract enables the extract to target and treat urease-positive infections by more than one mechanism. Additionally it could be hypothesised, based on work completed in Chapter 5, that the resulting 1-phenethylthiourea could act as a competitive urease inhibitor.

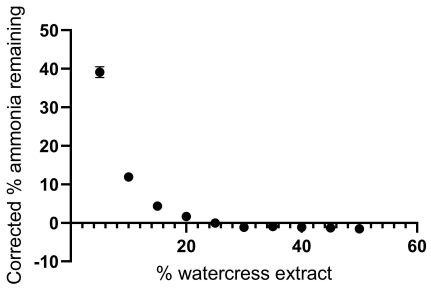

Figure 6-8: Ammonium chloride scavenged by extract from varying concentrations of *Nasturium officinale*. Experiments show three biological repeats, each experiment consisting of two technical repeats. Graph shows mean values of biological repeats, error bars representing standard deviation. Graphs generated using GraphPad Prism v. 9.4.1.

It was predicted that the ITC molecules would react with ammonia and form a thioamide bond, therefore allowing the scavenging of ammonia (Fig. 6-9). To test this theory PE-ITC was used to represent the ITCs within *N. officinale* extract, it was reacted with ammonia hydroxide to test the formation of 1-phenethylthiourea. To show that the thioamide bond had been produced the product, from the reaction, was analysed by H^1-NMR (Fig. 6-10). Despite this not being completed using *N. officinale* extract PE-ITC is a known compounds within the extract and therefore, it is likely the formation of the thioamide bond occurs via this mechanism.[12,31]

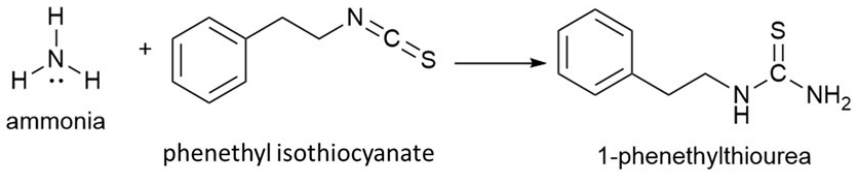

Figure 6-9: Mechanism for ammonia sequestration by isothiocyanate molecules. Phenethyl isothiocyanate reacts with ammonia to form 1-phenethylthiourea. Schematic drawn using ChemDraw v.19.0.1.28.

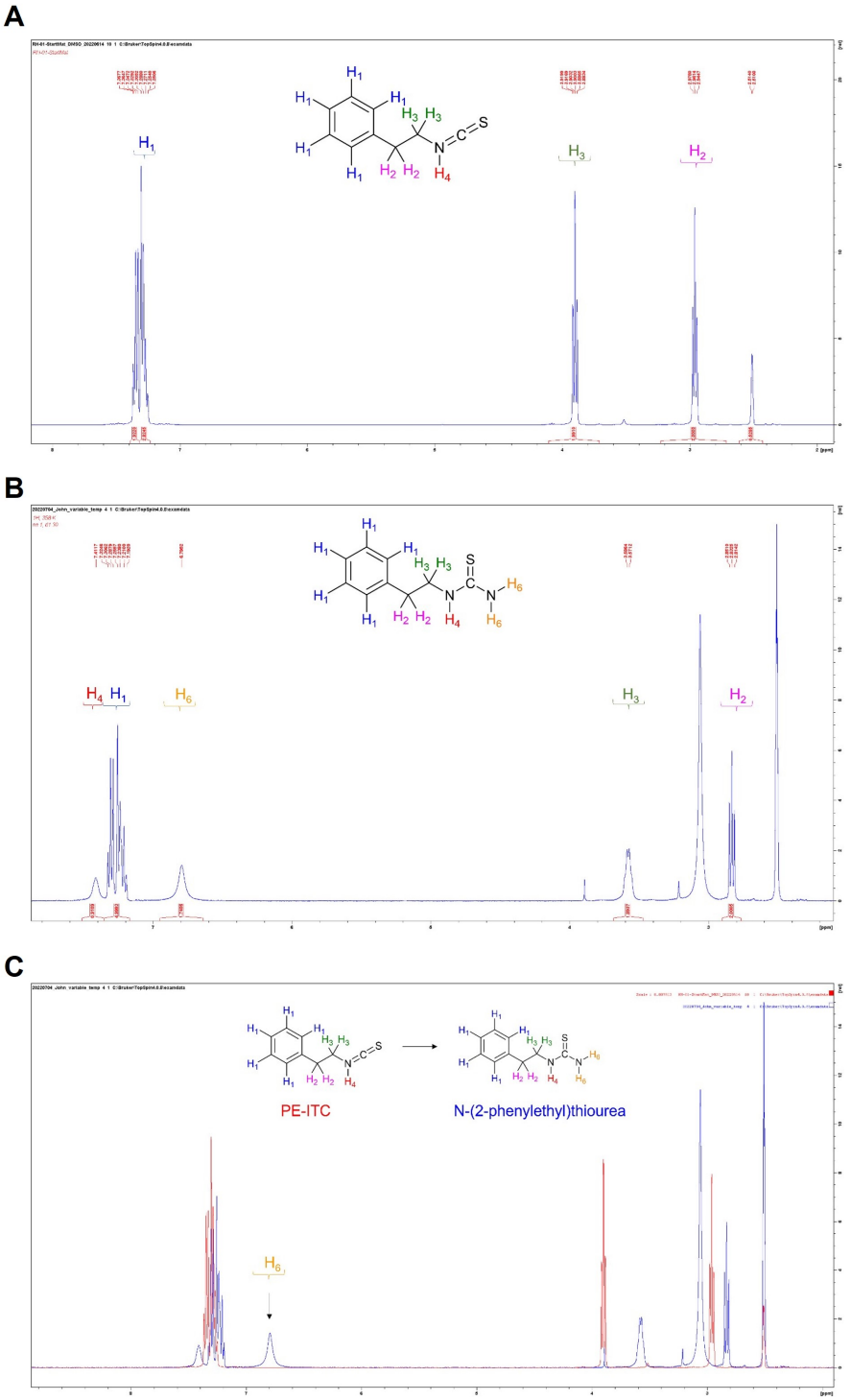

Figure 6-10: H^1-NMR spectra demonstating the formation of the thioamide bond. (A) spectra of phenethyl-isothiocyanate (PE-ITC). (B) Spectra of 1-phenethylthiourea. (C) overlay of each spectra: PE-ITC (red) and 1-phenethylthiourea(blue). NMR spectra acquired using Bruker 500 MHz spectrometer in CD_3OD and processed by TopSpin 4.0.8.

6.4 Conclusion

N. officinale is a mixture of various compounds including lipids, fatty acids, ITCs, and flavonoids. It is predicted that there is synergistic relationships between these compounds which enable solubility for compounds such as flavonoids. Here the compounds present have been computationally docked against the urease from *H. pylori*. *In vitro* experimentation has demonstrated the extracts ability to inhibit urease and sequester ammonia; as shown with PE-ITC and the formation of the thioamide bond. The use of *N. officinale* extract for use in healthcare is relatively an unexplored area, here two mechanisms of activity against the pathogenic affect of urease are demonstrated. Additionally, alternative manufacturing processes and growing conditions could be optimised to ensure the production of advantageous compounds during the plant's growth. Therefore, the extract offers interesting biological properties which could be utilized in the treatment of CAUTI, and *H. pylori* infections.

6.5 Appendix

Table 6.1: Compounds believed to be present in *N. officinale* extract.

Ligand	Predicted targeted Binding site
Isothiocyanates (ITCs)[21,1,12]	
3(methylsulfinyl)propyl-ITC	Covalent docking C153,C257, and C321
4(methylsulfinyl)butyl-ITC	Covalent docking C153,C257, and C321
5(methylsulfinyl)pentyl-ITC	Covalent docking C153,C257, and C321
6(methylsulfinyl)hexyl-ITC	Covalent docking C153,C257, and C321
7(methylsulfinyl)heptyl-ITC	Covalent docking C153,C257, and C321
8(methylsulfinyl)oxtyl-ITC	Covalent docking C153,C257, and C321
3(mehtylthio)propyl-ITC	Covalent docking C153,C257, and C321
4(mthylthio)butyl-ITC	Covalent docking C153,C257, and C321
5(methylthio)pentyl-ITC	Covalent docking C153,C257, and C321
6(methylthio)hexyl-ITC	Covalent docking C153,C257, and C321
7(methylthio)heptyl-ITC	Covalent docking C153,C257, and C321
8(methylthio)octyl-ITC	Covalent docking C153,C257, and C321
(2-isothiocyanethyl)benzene	Covalent docking C153,C257, and C321
(3-isothiocyanatopropyl)benzene	Covalent docking C153,C257, and C321
(4-isothiocyantobutyl)benzene	Covalent docking C153,C257, and C321
(5-isothiocyantopentyl)benzene	Covalent docking C153,C257, and C321
(6-isothiocyantohexyl)benzene	Covalent docking C153,C257, and C321
(7-isothiocyantoheptyl)benzene	Covalent docking C153,C257, and C321
(8-isothiocyantooctyl)benzene	Covalent docking C153,C257, and C321
Flavonoids[9,1,12]	
Quercetin	Active site
Quercetin-3-O-sophoroside	Active site and flap
Quercetin-3-sophoroside, glucoside	Active site and flap
Quercetin-3-O-Glc-(6'-malonyl-Glc)	Active site
Quercetin-3-O-rutinoside (rutin)	Active site and flap
Kaempferol	Active site
Luteolin	Active site and flap
Syringetin	Active site
Tricin	Active site
Naringenin	Active site
Hesperetin	Active site and flap
Apigenin	Active site

Table 6.2: Docking scores of compounds against *Helicobacter pylori* urease.

Isothiocyanates			
	Cystein docking score		
Ligand	**C153**	**C257**	**C321**
3(methylsulfinyl)propyl-ITC	-4.602	-2.869	-5.452
4(methylsulfinyl)butyl-ITC	-4.876	-3.429	-5.874
5(methylsulfinyl)pentyl-ITC	-5.561	3.619	-6.164
6(methylsulfinyl)hexyl-ITC	-5.683	-5.615	-6.194
7(methylsulfinyl)heptyl-ITC	-5.955	-3.702	-6.822
8(methylsulfinyl)oxtyl-ITC	-6.558	-4.014	-5.381
3(mehtylthio)propyl-ITC	-2.167	-3.196	-5.773
4(mthylthio)butyl-ITC	-5.833	-3.403	-6.441
5(methylthio)pentyl-ITC	-6.497	-3.469	-5.876
6(methylthio)hexyl-ITC	-6.760	-4.556	-6.694
7(methylthio)heptyl-ITC	-6.822	-5.750	-6.897
8(methylthio)octyl-ITC	-7.006	-5.952	-6.078
(2-isothiocyanethyl)benzene	-5.111	-3.749	-4.670
(3-isothiocyanatopropyl)benzene	-4.862	-3.450	-4.423
(4-isothiocyantobutyl)benzene	-5.511	-3.682	-4.733
(5-isothiocyantopentyl)benzene	-5.862	-3.499	-5.097
(6-isothiocyantohexyl)benzene	-6.196	-3.893	-5.097
(7-isothiocyantoheptyl)benzene	-6.738	-4.964	-5.125
(8-isothiocyantooctyl)benzene	-6.831	-4.624	-5.858
Flavonoids			
Quercetin	-8.299		
Quercetin-3-O-sophoroside	-9.979		
Quercetin-3-sophoroside, glucoside	-9.131		
Quercetin-3-O-Glc-(6'-malonyl-Glc)	-8.204		
Quercetin-3-O-rutinoside (rutin)	-9.559		
Kaempferol	-7.840		
Luteolin	-8.972		
Syringetin	-9.060		
Tricin	-8.517		
Naringenin	-8.807		
Hesperetin	-9.280		
Apigenin	-7.352		

6.6 Bibliography

[1] Klimek-Szczykutowicz M, Szopa A, Ekiert H. Chemical composition, traditional and professional use in medicine, application in environmental protection, position in food and cosmetics industries, and biotechnological studies of Nasturtium officinale (watercress) – a review. Fitoterapia. 2018;129:283–292. Available from: https://doi.org/10.1016/j.fitote.2018.05.031.

[2] Bahramikia S, Yazdanparast R. Effect of hydroalcoholic extracts of Nasturtium officinale leaves on lipid profile in high-fat diet rats. Journal of Ethnopharmacology. 2008;115(1):116–121.

[3] Chai TT, Ooh KF, Quah Y, Wong FC. Edible freshwater macrophytes: a source of anticancer and antioxidative natural products—a mini-review. Phytochemistry Reviews. 2015;14(3):443–457. Available from: http://dx.doi.org/10.1007/s11101-015-9399-z.

[4] Shahani S, Behzadfar F, Jahani D, Ghasemi M, Shaki F. Antioxidant and anti-inflammatory effects of Nasturtium officinale involved in attenuation of gentamicin-induced nephrotoxicity. Toxicology Mechanisms and Methods. 2017;27(2):107–114.

[5] Yehuda H, Soroka Y, Zlotkin-Frušić M, Gilhar A, Milner Y, Tamir S. Isothiocyanates inhibit psoriasis-related proinflammatory factors in human skin. Inflammation Research. 2012;61(7):735–742.

[6] Zafar R, Zahoor M, Shah AB, Majid F. Determination of antioxidants and antibacterial activities, total phenolic, polyphenol and pigment contents in Nasturtium officinale. Pharmacologyonline. 2017;1(June 2018):11–18.

[7] Zeb A. Phenolic profile and antioxidant potential of wild watercress (Nasturtium officinale L.). SpringerPlus. 2015;4(1):1–7.

[8] Al-Snafi AE. A review on Nasturtium officinale: A potential medicinal plant. IOSR Journal Of Pharmacy. 2020;10(9):33–43. Available from: www.iosrphr.org.

[9] Boligon AA, Janovik V, Boligon AA, Pivetta CR, Pereira RP, Rocha JBTD, et al. HPLC Analysis of Polyphenolic Compounds and Antioxidant Activity in Nasturtium officinale. International Journal of Food Properties. 2013;16(1):61–69. Available from: https://doi.org/10.1080/10942912.2010.528111.

[10] Fusari CM, Beretta HV, Locatelli DA, Nazareno MA, Camargo AB. Seasonal

isothiocyanates variation and market availability of Brassicaceae species consumed in Mendoza. Revista de la Facultad de Ciencias Agrarias. 2019;51(2):403–408.

[11] Jeon J, Bong SJ, Park JS, Park YK, Arasu MV, Al-Dhabi NA, et al. De novo transcriptome analysis and glucosinolate profiling in watercress (Nasturtium officinale R. Br.). BMC Genomics. 2017;18(1):1–14.

[12] Panahi Kokhdan E, Khodabandehloo H, Ghahremani H, Doustimotlagh AH. A Narrative Review on Therapeutic Potentials of Watercress in Human Disorders. Evidence-based Complementary and Alternative Medicine. 2021;2021. Available from: https://doi.org/10.1155/2021/5516450.

[13] Tarahovsky YS, Kim YA, Yagolnik EA, Muzafarov EN. Biochimica et Biophysica Acta Flavonoid – membrane interactions : Involvement of fl avonoid – metal complexes in raft signaling. BBA - Biomembranes. 2014;1838(5):1235–1246. Available from: http://dx.doi.org/10.1016/j.bbamem.2014.01.021.

[14] Zhao J, Yang J, Xie Y. Improvement strategies for the oral bioavailability of poorly water-soluble flavonoids: An overview. International Journal of Pharmaceutics. 2019;570(June):118642. Available from: https://doi.org/10.1016/j.ijpharm.2019.118642.

[15] Fogarty MC, Hughes CM, Burke G, Brown JC, Davison GW. Acute and chronic watercress supplementation attenuates exercise-induced peripheral mononuclear cell DNA damage and lipid peroxidation. British Journal of Nutrition. 2013;109(2):293–301.

[16] Gill CIR, Haldar S, Boyd LA, Bennett R, Whiteford J, Butler M, et al. Watercress supplementation in diet reduces lymphocyte DNA damage and alters blood antioxidant status in healthy adults. American Journal of Clinical Nutrition. 2007;85(2):504–510.

[17] Baj J, Forma A, Sitarz M, Portincasa P, Garruti G, Krasowska D. Helicobacter pylori Virulence Factors — Mechanisms of Bacterial Pathogenicity in the Gastric Microenvironment. Cells. 2021;10(27):1–37.

[18] Abadi ATB. Strategies used by Helicobacter pylori to establish persistent infection. World Journal of Gastroenterology. 2017;23(16):2870–2882.

[19] Ahmed N. 23 years of the discovery of Helicobacter pylori: Is the debate over? Annals of Clinical Microbiology and Antimicrobials. 2005;4:3–5.

[20] Ha Nc, Oh St, Sung JY, Cha KA, Lee MH, Oh Bh. Supramolecular assembly and acid resistance of Helicobacter pylori urease. Nature Structural Biology. 2001;8(6):505–509. Available from: https://www.nature.com/articles/nsb0601{_}505.

[21] Fahey JW, Stephenson KK, Wade KL, Talalay P. Urease from Helicobacter pylori is inactivated by sulforaphane and other isothiocyanates. Biochemical and Biophysical Research Communications. 2013;435(1):1–7. Available from: http://dx.doi.org/10.1016/j.bbrc.2013.03.126.

[22] Kafarski P, Talma M. Recent advances in design of new urease inhibitors: A review. Journal of Advanced Research. 2018;13:101–112. Available from: https://www.sciencedirect.com/science/article/pii/S2090123218300171.

[23] Macegoniuk K, Kowalczyk R, Rudzińska A, Psurski M, Wietrzyk J, Berlicki Ł. Potent covalent inhibitors of bacterial urease identified by activity-reactivity profiling. Bioorganic and Medicinal Chemistry Letters. 2017;27(6):1346–1350. Available from: https://doi.org/10.1016/j.bmcl.2017.02.022.

[24] Angelino D, Jeffery E. Glucosinolate hydrolysis and bioavailability of resulting isothiocyanates: Focus on glucoraphanin. Journal of Functional Foods. 2014;7(1):67–76. Available from: http://dx.doi.org/10.1016/j.jff.2013.09.029.

[25] Mitsiogianni M, Amery T, Franco R, Zoumpourlis V, Pappa A, Panayiotidis MI. From chemo-prevention to epigenetic regulation: The role of isothiocyanates in skin cancer prevention. Pharmacology and Therapeutics. 2018;190:187–201. Available from: https://doi.org/10.1016/j.pharmthera.2018.06.001.

[26] Xiao ZP, Wang XD, Peng ZY, Huang S, Yang P, Li QS, et al. Molecular Docking, Kinetics Study, and Structure-Activity Relationship Analysis of Quercetin and Its Analogous as Helicobacter pylori Urease Inhibitors. Journal of Agricultural and Food Chemistry. 2012;60(42):10572–10577. Available from: https://pubs.acs.org/doi/pdf/10.1021/jf303393n.

[27] Carta G, Knox AJS, Lloyd DG. Unbiasing Scoring Functions: A New Normalization and Rescoring Strategy. Journal of Chemical Information and Modeling. 2007;47(4):1564–1571.

[28] Mclean RJC, Cheng KJ, Gould WD, Nickel JC, Costerton WJ. Histochemical and biochemical urease localization in the periplasm and outer membrane of two

Proteus mirabilis strains. Canadian Journal of Microbiology. 1986;32(10):772–778. Available from: https://doi.org/10.1139/m86-142.

[29] Agerbirk N, De Nicola GR, Olsen CE, Müller C, Iori R. Derivatization of isothiocyanates and their reactive adducts for chromatographic analysis. Phytochemistry. 2015;118:109–115. Available from: http://dx.doi.org/10.1016/j.phytochem.2015.06.004.

[30] Stickler DJ, Feneley RCL. The encrustation and blockage of long-term indwelling bladder catheters: A way forward in prevention and control. Spinal Cord. 2010;48(11):784–790. Available from: https://doi.org/10.1038/sc.2010.32.

[31] Rose P, Yen KW, Choon NO, Whiteman M. β-Phenylethyl and 8-methylsulphinyloctyl isothiocyanates, constituents of watercress, suppress LPS induced production of nitric oxide and prostaglandin E2 in RAW 264.7 macrophages. Nitric Oxide - Biology and Chemistry. 2005;12(4):237–243.

Chapter 7

Conclusions and Future Directions

7.1 Conclusions

The overall aims of this Thesis were to investigate new methods in identifying and preventing urease activity and their associated pathologies. The first half of the research focused on the optimisation and testing of a diagnostic lozenge for patients suffering with CAUTI. This sensor had the ability to predict the occurrence of urinary catheter blockage in long-term users. *In vitro* experimentation showed that the newly optimised lozenge design was able to provide a warning time of 6.7 h prior to catheter blockage. Thus, allowing users to heed the warning and either flush or replace their catheter. The lozenge can be sterilised using ethylene oxide and is stable in healthy urine (Chapter 3).

The sensor was then assessed in a pilot clinical trial. The trial was designed to test the sensor externally to the participant. The primary endpoint was the link between sensor detection and subsequent catheter blockage, assessed by a three-week follow up phone call. Despite the low-sample numbers and limitations of the trial, the lozenge demonstrated predictability and functionality in detecting catheter blockage and a urine pH increase. Microbial analysis of the bacteria within the urine of these users was assessed and demonstrated a polymicrobial, diverse nature of the bacteria causing CAUTI (Chapter 4).

The second half of the research was focused on the development of a drug to treat urease-positive CAUTI. Using a rational drug design method, ligands were designed and computationally docked to urease. Predictions in the ability of compounds to bind to urease was assessed and three compounds were tested *in vitro*. This process identified a new urease inhibitor, Bis-TU, which significantly extended the lifetime of the urinary catheter compared to AHA (clinical standard) in an *in vitro* model of a catheterised tract. Bis-TU was delivered through the Biomodics catheter, utilizing the diffusible balloon technology. This enable the drugs to be delivered directly to the bladder. Bis-TU demonstrates low-toxicity in haemolytic and HepG2 assays. The methodology presented in this chapter could be used to identify new urease inhibitors which are highly potent and possess ideal drug delivery characteristics (Chapter 5).

In the final Chapter, the natural products within *N. officinale* extract were examined for their anti-ureolytic properties. Compounds expected to be present within the extract were identified and docked against urease. The extract was examined for its ability to inhibit urease *in vitro*. An additional ammonia scavenging property was identified whereby the ITCs could sequester ammonia by forming a thioamide bond. It is hypothesised that the cocktail of compounds are acting on urease by multiple

mechanisms. Future analysis of *N. officinale* extract is required to identify the true components. Different varieties, or manufacturing processing techniques could lead to different composition of compounds and thus needs examination (Chapter 6).

7.2 Future Directions

The work presented here has many potential directions and routes. Regarding the development of the diagnostic sensor the next steps are GMP manufacture, followed by a Phase I medical device trial where the sensor would be tested by participants using long-term catheters. The methodology from Chapter 5 could be used to improve the *N. officinale* extract identifying key compounds which are involved in urease inhibition (Chapter 6). Identifying key compounds which could allow for a mixture of compounds to be synthesised to treat urease-positive infections. The synthesis of the compounds would allow for them to be marketed as a therapeutic treatment.